AD-A171 624 FUNDAMENTAL STUDIES ON THE ALUMINUM-LITHIUM-BERYLLIUM ALLOY SYSTEM(U) LOCKHEED MISSILES AND SPACE CO INC PALO ALTO CA RESEARCH AND D.. J WADSWORTH ET AL. AUG 86 1/2

UNCLASSIFIED LMSC-D067295 N00014-84-C-0032 F/G 11/6 NL

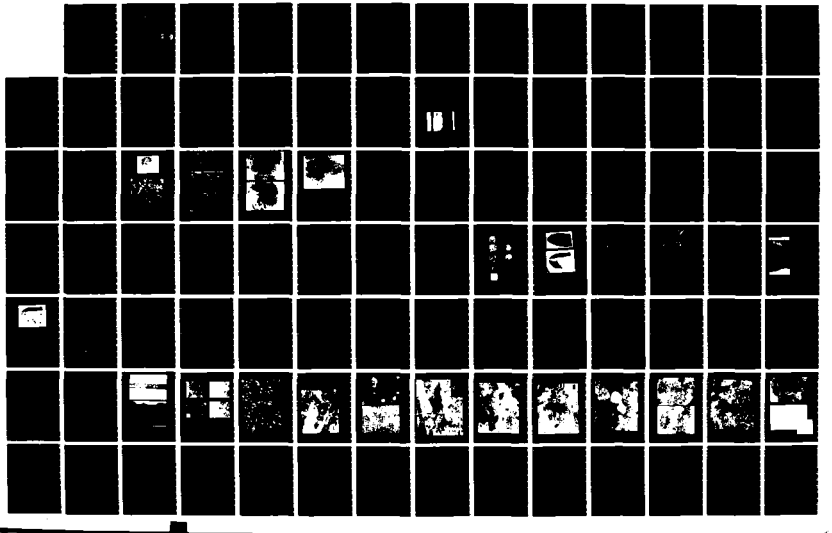

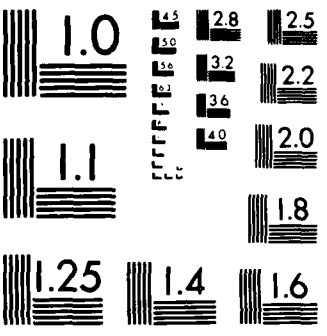
1.0
1.1
1.25
1.4
1.6
1.8
2.0
2.2
2.5
2.8
3.2
3.6
4.0
4.5
5.0
5.6
6.3

(12)

LMSC-D067295

FUNDAMENTAL STUDIES ON THE ALUMINUM-LITHIUM-BERYLLIUM ALLOY SYSTEM

Jeffrey Wadsworth, T.G. Nieh, et al.
Research & Development Division
Lockheed Missiles & Space Company, Inc.
3251 Hanover Street
Palo Alto, California 94304

August 1986

Final Technical Report for Period February 1984 to August 1986
Contract N00014-84-C-0032

Approved for Public Release; Distribution unlimited

Sponsored by:
OFFICE OF NAVAL RESEARCH
Arlington, Virgina 22217-5000

FUNDAMENTAL STUDIES ON THE ALUMINUM-LITHIUM-BERYLLIUM ALLOY SYSTEM

Jeffrey Wadsworth, T.G. Nieh, et al.
Research & Development Division
Lockheed Missiles & Space Company, Inc.
3251 Hanover Street
Palo Alto, California 94304

August 1986

Final Technical Report for Period February 1984 to August 1986
Contract N00014-84-C-0032

Approved for Public Release; Distribution unlimited

Sponsored by:
OFFICE OF NAVAL RESEARCH
Arlington, Virgina 22217-5000

FOREWORD

This Final Technical Report was prepared by Lockheed Missiles and Space Company, Inc., Research and Development Division, Palo Alto, California, under ONR Contract N00014-84-C-0032. The work was sponsored by the Office of Naval Research, Arlington, Virginia, with Dr. D.A. Polk as Program Manager.

This report covers the period February 1984 to August 1986 for the program to investigate fundamental aspects of the Al-Li-Be alloy system.

Dr. J. Wadsworth, the Principal Investigator on the first year and a half of the program, and Dr. T.G. Nieh, the Principal Investigator on the second year of the program, were assisted by Dr. A.E. Vidoz, Mr. R.E. Lewis, Dr. A. Joshi, Mr. D.D. Crooks, and Ms. C.A. Henshall of the Lockheed Palo Alto Research Laboratory, Dr. A.R. Pelton of Ames Research Laboratory, Ames, IA, and Dr. W.C. Oliver of Oak Ridge National Laboratory, Tennessee.

TABLE OF CONTENTS

FUNDAMENTAL STUDIES OF THE ALUMINUM-LITHIUM-BERYLLIUM ALLOY SYSTEM

SUMMARY

Recent developments in aluminum alloys for aerospace applications have emphasized low-density alloys and in large part this emphasis has been on Al-Li based alloys. This is because Li effectively reduces the density of aluminum and, at the same time, improves the modulus. Furthermore, by the addition of other elements such as Cu, Mg, and Zr, high strength Al-Li-based alloys can be produced. The element Be also significantly decreases the density and increases the modulus of Al. Aluminum has a very limited solid solubility for Be, however, and upon conventional casting, massive segregation of coarse, primary, Be particles occurs. This segregation leads to unacceptable mechanical properties in cast Al-Be based alloys.

The development of fine-structured Al-Li-Be alloys remains an interesting prospect for further decreasing the density and increasing the modulus of Al. This is because, for developing low density Al-Li alloys, there is an upper useful bound of about 3 wt% Li in Al. Beyond this level, the undesirable delta phase (AlLi) can precipitate and lead to poor ductility. If the Be additions to Al-3 wt% Li alloys can be finely dispersed, such alloys will have a range of properties that will compete with the most advanced Al alloys and Al-based metal matrix composites for

applications in which weight savings (governed by low density or high modulus to density ratios) are important.

The most obvious way to create a fine dispersion of Be in Al is by rapid solidification processing (RSP). In the present study, an examination of the microstructures and properties of Al-Li-Be ternary alloys prepared by arc-melting and casting is described, as well as by the RSP methods of splat quenching and melt spinning.

In the initial study, a microstructural investigation was carried out on a series of small castings of arc-melted Al-Li-Be alloys. The alloy compositions included amounts of Li up to 3 wt% and Be up to 10 wt%. Optical metallographic examination revealed gross macrosegregation in the as-cast, highly-alloyed, compositions. On the microstructural level, the structure consists of primary Be particles in a matrix of aluminum-lithium containing eutectic structure at the cell walls. A detailed Auger electron spectroscopy examination was carried out on a section of an Al-3Li-10Be arc-cast alloy to determine the precise compositional variations. This approach was demonstrated to be a necessary prerequisite for selection of material for RSP by techniques such as splat quenching.

The first attempts to produce RSP structures in Al-Li-Be alloys by splat quenching produced mixed results. The preliminary results indicate that under conditions of RSP, fine dispersions of Be can be introduced into Al alloys containing Li but the

distribution of the Be particles is not uniform. The presence of the Be dispersoids does not appear to influence the precipitation behavior of δ'. It is clear that there are severely segregated regions even in these splat quenched Al-Li-Be alloys. Detailed investigations of such splat quenched Al-Li-Be based alloys must therefore be carried out with caution. Nominal compositions ascribed to alloys may well deviate considerably from the local compositions studied, for example, in thin TEM sections of splats.

The next RSP investigation involved Al-3Li-2Be and Al-3Li-10Be (by wt%) alloys produced using rapid solidification processing via melt spinning. The microstructures of the alloys were investigated in the as-melt-spun condition, after consolidation and heat treatment to peak hardness, and after tensile testing in the heat treated condition. In particular, changes in the size and distribution of primary Be particles and Al_3Li precipitates are described. The mechanical properties of the alloys in the heat treated condition are also presented. For example, the Al-3Li-10Be alloy shows nearly a 40% improvement in the specific modulus over conventional aluminum alloys, exhibits a tensile strength of 520 MPa and a tensile elongation of 4%.

From a microstructural viewpoint, in the melt spun condition, the alloys contain fine δ' particles (5-10 nm in diameter), some large α-Be particles (>100 nm), and a segregated dispersion of fine α-Be particles (5-50 nm) located on cell boundaries. After

consolidation, and heat treatment, rather inhomogeneous structures were observed. Coarsening of the δ' and coarsening and agglomeration of the α-Be particles is evident and precipitate (δ') free zones are observed at grain boundaries.

One of the problems facing RSP alloys in general is their consolidation. Surface oxides and hydroxides on melt spun ribbon, as well as organic contamination, can have a profound influence on particulate agglomeration behavior and the contingent mechanical and chemical properties of the final compact. Hence, a thorough understanding of the ribbon surface species including oxides is desirable in the understanding of these subsequent material properties and microstructure. The composition and thickness of surface oxides of rapid solidification processed ribbons or particulates is strongly influenced by the alloying elements, as well as a wide range of processing variables. It is well established that PM Al alloys face special problems because of the tenacious Al_2O_3 surface film that inevitably forms on pure Al powder or particulate. In the case of Al-Li-Be alloys, the problem is further complicated because Al, Li, and Be all form very stable equilibrium oxides. In the present work, an initial study to determine the nature of the oxides in RSP Al-Li-Be alloys produced by melt spinning techniques is reported.

The Al-Li-Be alloys might be expected to show high temperature strengthening due to the fine Be dispersions produced by rapid solidification. An evaluation and characterization of the high

temperature properties of Al-Be binaries and Al-Li-Be ternaries was carried out. A rapidly-solidified, Al-2Li-10Be alloy was produced. The mechanical properties of the alloy at temperatures between 121 and 232°C have been characterized. In this temperature range, the material behaves like a conventional oxide-dispersion strengthened alloy; namely, it exhibits a high stress exponent (n=12) and an activation energy of 126kJ/mol, which is close to the activation energy for self diffusion in Al. Despite the fact that the material is stronger than Al (and Al-Be binary alloys), it is still much weaker, even on a density-compensated basis, than most of the high-temperature Al alloys.

Rapidly solidified Al-Be binary alloys(10%, 20%,and 40% Be by weight) have also been produced by melt spinning techniques. The microstructure, as well as the elevated temperature mechanical properties, have been characterized over a range of strain rates. Despite the fact that the materials exhibited duplex microstructures, resulting from high-temperature processing, they also show behavior typical of dipersion strengthened alloys. The mechanical properties at elevated temperature can be accurately described by the equation $\dot{\varepsilon} = A\,(\sigma/E)^{12} \exp(-126(kJ/mol)/RT)$, where $\dot{\varepsilon}$ is the true strain rate, σ is the stress, E is the modulus, A is a material constant, R is the gas constrant and T is the absolute temperature. A direct comparison of the deformation properties was made amongst the binary Al-Be compositions, an Al baseline, and some high temperature Al alloys. The Al-Be alloys do not exhibit good high temperature

resistance, by comparison with other high-temperature Al alloys, e.g. the Al-Fe-Ce alloy. This is concluded to be a result of particle coarsening and agglomeration during processing and testing.

In a final study, an investigation of the heat treat response of RSP Al-Li-Be ribbons was carried out. Microstructural evolution in the heat-treated ribbons was analyzed using a number of techniques including Differential Scanning Calorimetry(DSC), hardness measurements, and Transmission Electron Microscopy(TEM). It was found that the general aging characteristics of the ternary Al-Be-Li alloys were very similar to binary Al-Li alloys. Although δ' precipitates were present in the as-spun ribbon, uniform δ' distribution was not observed until aging temperatures of about 180 ^{o}C. Heat treatment of the ribbon at higher temperatures, e.g. 300 ^{o}C, resulted in δ' to δ transformation. In the Al-Be-Li ternary, the α-Be particles were present in the Al-Li matrix as independent dispersoids and had little effect on the aging response of the Al-Li matrix. The size distribution of the α-Be particles was nonuniform. Upon heat treatment at temperatures higher than 300 ^{o}C, the α-Be particles tended to coarsen and the growth behavior of these particles followed a classical Ostwald coarsening mechanism.

List of Publications

1. "Surface Oxides on Melt Spun Ribbons of an Al-Li-Be Alloy," A. Joshi, J. Wadsworth, and A.E. Vidoz, Scripta Metallurgica, Vol. 20, (1986), p. 529.

2. "Microsegregated Microstructures in Al-Li-Be Alloys Prepared by Splat Quenching," J. Wadsworth, A.R. Pelton, and A.E. Vidoz, International Journal of Material Science and Engineering, Vol. 78, No.2, (1986), p. 115.

3. "Microstructural Evaluation of Arc-Melted Al-Li-Be alloys," J. Wadsworth, A. Joshi, D.D. Crooks, and A.E. Vidoz, Journal of Materials Science, In Press, 1986.

4. "Microstructural Evaluation of Rapidly Solidified Al-Li-Be Alloys," J. Wadsworth, A.R. Pelton, D.D. Crooks, R.E. Lewis, A.E. Vidoz, Journal of Materials Science, In Press, 1986.

5. "High Temperature Properties of Rapidly Solidified Al-Be Alloys," T.G. Nieh, C.A. Henshall, J. Wadsworth, Submitted for Publication, 1986.

6. "Mechanical Properties of a Rapidly Solidified Al-10%Be-2%Li Alloy at Elevated Temperature," T.G. Nieh, Submitted for Publication, 1986.

7. "Characterization of the Aging Response of Melt-Spun Al-Be-Li Alloy Ribbon," T.G. Nieh, W.C. Oliver, J. Wadsworth, Submitted for Publication, 1986.

APPENDIX A

SURFACE OXIDES ON MELT SPUN RIBBONS OF AN Al-Li-Be ALLOY

A. Joshi, J. Wadsworth and A.E. Vidoz
Department of Metallurgy
Lockheed Palo Alto Research Laboratory
3251 Hanover Street, Palo Alto CA 94304

Introduction

In recent years considerable effort has been expended in the development of advanced aluminum alloys. Part of this work, in recognition of the overriding importance of low density in weight savings in aerospace structures (1), is the development of low density and high modulus aluminum alloys based on the Al-Li system (2,3). Although these alloys are predominantly manufactured using ingot metallurgy techniques, successful rapid solidification processed (RSP) alloys, consolidated using powder or particulate metallurgy (PM) techniques have also been produced (4,5).

In order to reduce further the density of aluminum alloys, it is necessary to consider other alloying elements. This is because beyond a level of about 3 wt.% Li, deleterious effects of Li can be observed on the ductility and toughness of Al-li alloys. It is important to recognize that the selection of other elements is restricted to those that not only decrease density, but also do not decrease Young's modulus. Beryllium is the only other element, besides Li, that significantly decreases the density of Al whilst increasing Young's modulus of Al. Because of the limited solubility of Be in Al at room temperature, (<0.03 wt. %)(6), the production of Al-Li-Be alloys requires RSP techniques. Under conventional solidification techniques massive segregation of the Be-rich phase results in poor mechanical properties(7).

One of the problems facing RSP alloys is their consolidation. Surface oxides and hydroxides on melt spun ribbon, as well as organic contamination, can have a profound influence on particulate agglomeration behavior and the contingent mechanical and chemical properties of the final compact. Hence, a thorough understanding of the ribbon surface species including oxides is desirable in the understanding of subsequent material properties and microstructure. The composition and thickness of surface oxides of rapid solidification processed ribbons or particulates is strongly influenced by the alloying elements, the rate of cooling from the melt and the partial pressures of H_2O and reactive gases such as O_2 during their preparation and storage(8). Also, handling and storage procedures including the vacuum/ambient quality can alter the amounts and nature of organic contamination(8). It is well established that PM Al alloys face special problems because of the tenacious Al_2O_3 surface film that inevitably forms on pure Al powder or particulate(8). In the case of Al-Li-Be alloys, the problem is further complicated because Al, Li, and Be all form very stable equilibrium oxides. In the present paper, an initial study to determine the nature of the oxides in RSP Al-Li-Be alloys produced by melt spinning techniques is reported.

Experimental

Al-Li-Be ternary alloys were prepared by arc melting high purity ingot stock Al, high-purity, battery-grade Li and electrolytic

induction melted Be stock. The arc melted buttons were converted to melt spun ribbon of approximate dimensions 1 mm in width and less than 0.1 mm thickness. Melt spinning was carried out using an apparatus and techniques described elsewhere (7). Two Al-Li-Be alloys, Al-3wt%Li-2wt%Be and Al-3wt%Li-10wt%Be, were selected for study.

Melt spun ribbons of Al-3Li-2Be and Al-3Li-10Be were selected for investigations of the nature of surface oxides. The specimens were subjected to surface analysis in the as-spun condition and also after being subsequently oxidized at 500°C for 20 minutes in room air (in order to determine the tendency for formation of equilibrium surface oxides). The technique of Auger Electron Spectroscopy (AES) was utilized for all the surface analyses as it offered (i) the desired surface sensitivity (<0.5-2nm), (ii) sensitivity for light elements including Li, Be, and O, (iii) chemical state information to determine whether the elements are present as oxides, (iv) high lateral resolution and (v) capability of depth profiling using inert gas ion sputtering. All the studies were conducted in a Perkin Elmer model PHI 560 ESCA/SAM system.

Results and Discussion

Optical photomicrographs of a melt spun Al-3Li-10Be alloy are shown in Fig.1. As may be seen, a rather uniform, fine microstructure is observed after rapid solidification. Samples of this type of ribbon were used for analysis of surface chemistry.

AES survey spectra obtained from the surfaces of various ribbons showed enrichment of C, O, Li and Be at the surface. The composition-depth profiles obtained by Ar ion sputtering indicated that C is generally localized in the top 10-30 nm followed by a Li and Be rich oxide layer.

Aluminum was found to be present in the entire oxide, but in much lower proportions than in the bulk. In some of the specimens, particularly those ribbons subsequently oxidized at 500°C for 20 minutes in air, a Li-rich oxide was present at the surface followed by a well-defined layer of Be-rich oxide. The total oxide thicknesses varied in the range of 10-50nm for the as-spun ribbons while the thicknesses varied in the 2.5 to 3 μm range for the oxidized specimens. Examples of the depth profiles of the as-spun and oxidized specimens are shown in Figs. 2 and 3, respectively. The layering of the Li- and Be-rich oxides upon oxidation at 500°C is demonstrated in Fig. 3. The atomic concentration estimates (the ordinate in these plots) should be used only on a relative basis since they were derived using elemental sensitivity factors and are therefore subject to large errors.

The data clearly indicates preferential oxidation of Li and Be in the alloy. An examination of the free energies of formation of the metal oxides, shown in Fig. 4, suggests that BeO is the most stable oxide followed by Li_2O and Al_2O_3. The experimental evidence of ready formation of LiO_x at the surface, and its ease

of formation relative to Al_2O_3, suggests that kinetic factors play an important role in formation of these surface oxides. Formation of lithium rich oxides at the surface indicates that rapid diffusion of Li, relative to Be, through the oxide layer is an important factor. Purely thermodynamic factors would not explain the formation of the observed layered oxide structures.

Formation of surface oxides during melt spinning and atomization is a general phenomenon in Al alloys. In Al-3Cu-2Li-1Mg-0.2Zr (nominal weight percent) alloys (8), oxide films enriched in Li and Mg were observed at melt spun flake and atomized powder particulate surfaces. The thicknesses of these oxides were estimated to be in the 150-500Å range, considerably greater than those in several non-Li containing compositions(8). Melt spun flake specimens exhibited oxide thicknesses that were different at the top surface from the roll-facing surface (as evident in Fig. 1, the top and bottom surfaces can be identified from topological examination). As with the Al-Li-Be ribbon specimens, the top-surface oxide was thicker by approximately a factor of two compared to the roll-facing side. Oxide thicknesses were also slightly higher on the top surfaces of large melt spun flakes compared to the smaller (and thinner) ones. Thus, for a given alloy, the oxide thickness appears to be a strong function of cooling rate. It is believed that high cooling rates available at the roll-facing surfaces of the ribbon result in the formation of a rather thin oxide film. This behavior is similar to that observed on atomized powder particulates in which the finest powders exhibit the thinnest oxide films(8).

The above results demonstrate that high cooling rates, in addition to the alloy composition and ambient conditions, significantly affect the nature and thickness of particulate surface oxides. The role of surface oxides on the agglomeration behavior during consolidation of comminuted particulates, and their effect on microstructure and mechanical properties of processed material is an important area of current technological study.

Acknowledgement

This work was supported by the Office of Naval Research under Contract N00014-84-C-0032.

References

1. J.C. Ekvall, J.E. Rhodes, and G.C. Wald, ASTM STP 761, Amer. Soc. for Testing and Materials, Phildelphia, PA, 1982, p. 328.
2. E.A. Starke, Jr., and T.H. Sanders, Jr., eds., "Aluminum-Lithium Alloys," Proc. First Int. Al-Li Conf., AIME, Warrendale, PA (1981).
3. E.A. Starke, Jr., and T.H. Sanders, Jr., eds., "Aluminum-Lithium Alloys II," Proc. Second Int. Al-Li Conf., AIME, Warrendale, PA (1983).

4. R.E. Lewis, I.G. Palmer, J.C. Ekvall, I.F. Sakata, and W.E. Quist, Proc. Third Conf. on Rapid Solidification Processing: Principles and Technology, Gaithersburg, MD, Dec. 6-8, 1982, p. 615.

5. I.G. Palmer, R.E. Lewis, and D.D. Crooks, Proc. Second Int. Conf. on Rapid Solidification Processing, Mar. 1980, R. Mehrabian, B.H. Kear, and M. Cohen, eds., Claitors Publishing Div., Baton Rouge, LA, 1980, p. 342.

6. Aluminum, Vol. 1, Properties, Physical Metallurgy and Phase Diagrams, K.R. Van Horn, ed., ASM, Metals Park, OH, 1968.

7. A.E. Vidoz, D.D. Crooks, R.E. Lewis, I.G. Palmer, and J. Wadsworth, Rapidly Solidified Powder Aluminum Alloys, ASTM STP No. 890, Amer. Soc. for Testing and Materials, Philadelphia, PA, 1985, to be published.

8. A. Joshi and R.E. Lewis, Lockheed Palo Alto Research Laboratory, Unpublished Research, 1985.

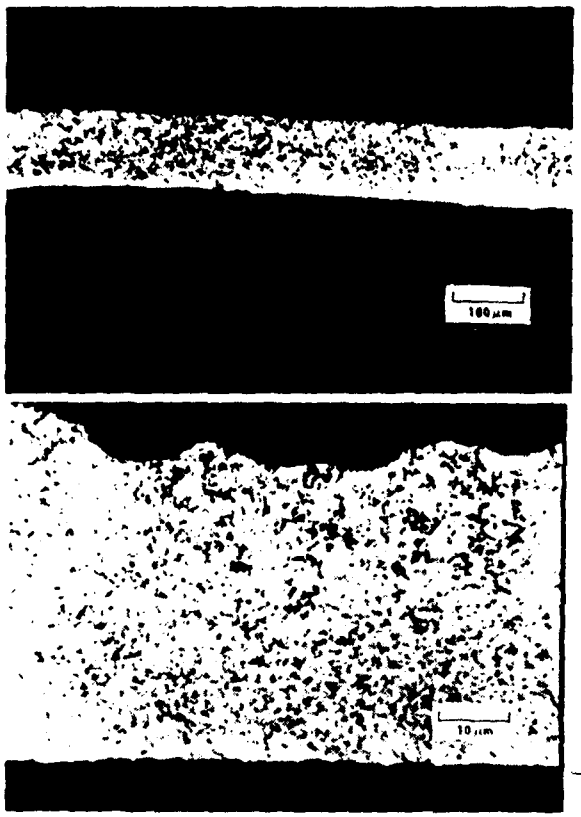

Fig. A1. Optical photomicrographs of *thickness section of melt-spun* Al-3Li-10Be

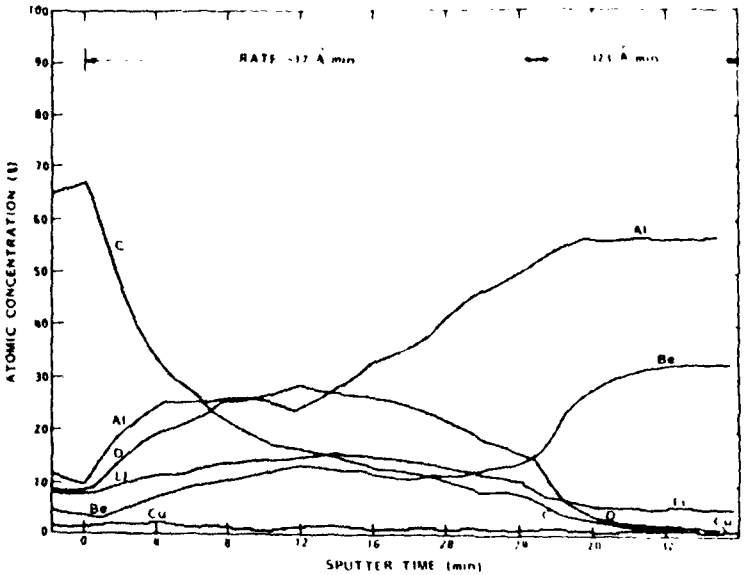

Fig. A2. AES depth profile of Al-10wt%Be-3wt%Li ribbon in as-spun condition, roll facing surface.

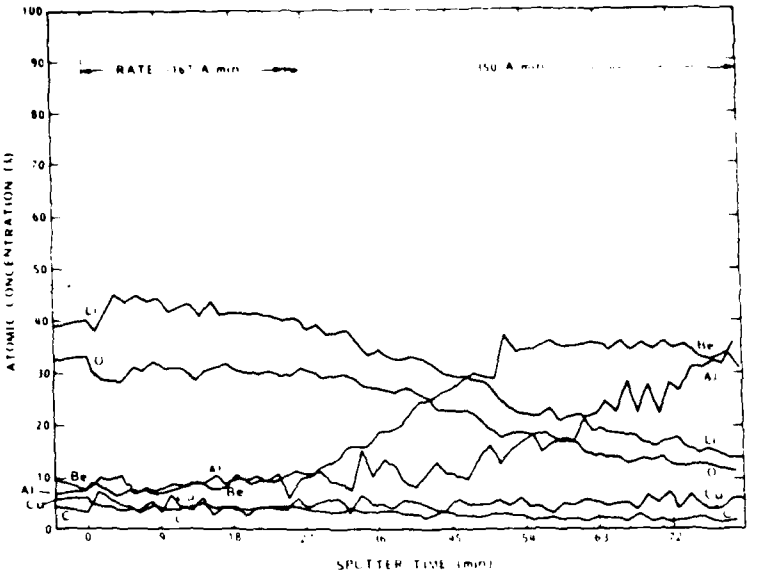

Fig. A3. AES depth profile of a similar surface as in Figure 2 after oxidation at 500°C for 20 minutes in air.

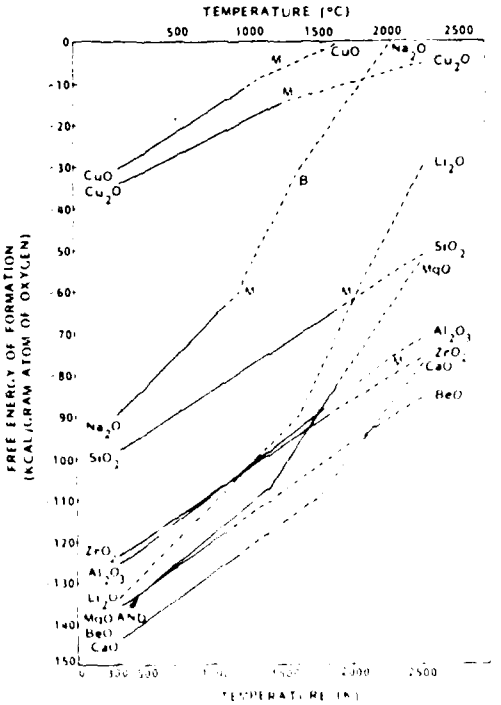

Fig. A4. Free Energies of formation of common oxides of interest (relative to Al-Li alloys).

APPENDIX B

MICROSEGREGATED MICROSTRUCTURES IN Al-Li-Be ALLOYS PREPARED BY SPLAT QUENCHING

J. Wadsworth, A.R. Pelton*, and A.E. Vidoz

Lockheed Palo Alto Research Laboratory
Metallurgy Department
3251 Hanover Street
Palo Alto CA 94304

*Ames Laboratory
Metallurgy Building
Ames IA 50011

Recent developments in aluminum alloys for aerospace applications have emphasized the development of low-density alloys. In large part, the development has centered on Al-Li based alloys.[1-3] This is because Li effectively reduces the density of aluminum, and at the same time improves the modulus. Furthermore, by the addition of other elements such as Cu, Mg, and Zr, high strength Al-Li alloys can be produced.[1-3] The element Be also decreases the density of Al and increases the modulus.[4] Aluminum has a very limited solid solubility for Be, however, and upon conventional casting, massive segregation of the Be into coarse primary Be particles occurs.[4]

The development of fine-structured Al-Li-Be alloys remains an interesting prospect for further decreasing the density and increasing the modulus of Al. There is an upper useful bound of about 3 wt% Li in Al. Beyond this level, the undesirable delta phase can precipitate upon solution treatment and aging and can lead to poor ductility.[1-3] If the Be additions to Al-3 wt% Li alloys could be finely dispersed, such alloys would have a range of properties that would compete with the most advanced Al alloys and Al-based metal matrix composites for applications in which weight savings are important.[4]

The most obvious way to create a fine dispersion of Be in Al is by rapid solidification processing (RSP). In the present study, an initial examination is described of the microstructures of Al-Li-Be ternary alloys prepared by splat quenching.

Ternary Al-Li-Be alloys, containing up to 3 wt% Li and 10 wt% Be were prepared by casting arc melted alloys using a procedure described elsewhere.[5] A detailed examination of the microstructure of these castings has been carried out using optical metallography and Auger electron spectroscopy.[5] The results of this study have emphasized the importance of selecting areas from arc cast buttons of known composition. This is because severe macrosegregation occurs in cast Al-Li-Be alloys and nominal compositions (based on alloy additions to the melt) are insufficient for manufacturing splats of known chemistry. As a result of carefully analyzing the arc-melted alloys, material for splat quenching experiments was cut from the castings. Three compositions were examined. These compositions were Al-3Li-2Be, Al-3Li-5Be, and Al-3Li-10Be by wt%. The accuracy of the Li and Be concentration is within about 20%.[5]

Rapid solidification experiments were carried out using splat quenching. For the splat quenching experiments, small cubes (50-100 mg) were removed from the castings and splat quenched, after melting with an arc, in a hammer-anvil apparatus. In this device, a spring loaded Cu hammer, triggered with a solenoid release, is used to create a splat from the small molten pool. The typical cooling rates for such a process are typically in the 10^5 to 10^6°C s^{-1} range.

Three of the Al-Li-Be alloys, Al-3Li-2Be, Al-3Li-5Be and Al-3Li-10Be, were prepared by splat quenching. A typical splat quenched sample is shown in Figure 1(a). The splat technique results in a nonuniform thickness from the center to the edge of the splat and, as a result, the microstructure varies considerably within a given splat. This is illustrated in Figure 1(b) for the AL-3Li-10Be alloy. Nonetheless, it is possible to compare the microstructures of the three alloys and this comparison is shown in Figure 2. It is observed that the incidence of coarse, primary Be particles (the dark phase) is evident at the high Be concentrations even in these samples produced by splat quenching.

A transmission electron microscopy study was carried out on material cut from the thin fine-structured sections of splat quenched Al-3Li-2Be and Al-3Li-10Be alloys. It was observed that alloys from both compositions contained mainly cellular microstructures. The cell walls were defined by dislocations and were associated with α-Be particles. In general, the δ′ particles were uniformly distributed, although there was some evidence of denuded zones adjacent to both low and high angle boundaries.

The α-Be particle volume fraction is quantitatively observed to follow the expected trend, i.e., the volume fraction in the Al-3Li-10Be sample was greater than that in the Al-3Li-2Be sample. In both cases the α-Be particles were less than 100 nm in size and generally in the range from 5 to 50 nm. The smaller particles were usually confined to cell boundaries or grain

boundaries. The large particles ($\geq$ 100 nm) were randomly dispersed throughout the alloys. As may have been anticipated from the optical metallographic results of Figure 1, the microstructure is observed to be somewhat nonuniform even within a particular sample. For example, a given grain would be observed to contain a larger volume fraction of α-Be than an adjacent grain. This is presumably a consequence of nonuniformities in both liquid and solid quench rates.

A bright field/dark field (BF/DF) pair of photomicrographs in Figure 3 illustrates the distribution of δ′ in the Al-3Li-10Be splat quenched alloy. Of particular interest are the regions observed in these photomicrographs that are apparently devoid of the δ′ precipitate. The α-Be particles can be observed on the high angle boundary on the right hand side of the photomicrographs. A region from within Figure 3 is shown at high magnification in Figure 4. In addition to the large α-Be particles in the cell interior, and fine α-Be particles in the cell wall, the individual δ′ particles can be resolved in the matrix.

The preliminary results described above indicate that under conditions of rapid solidification processing, fine dispersions of Be can be introduced into Al alloys containing Li but the distribution of the Be particles is not uniform. The presence of the Be dispersoids does not appear to influence the precipitation behavior of δ′. It is clear that there are severely segregated regions apparent even in splat quenched Al-Li-Be alloys.

Detailed investigations of such Al-Be based alloys must therefore be carried out with caution. Nominal compositions ascribed to alloys may well deviate considerably from the local compositions studied, for example, in thin TEM sections.

This work was supported by the Office of Naval Research, Contract #N00014-84-C-0032. The authors wish to thank Mr. R.E. Lewis for his valuable contributions and Mr. D.D. Crooks for carrying out the splat quenching experiments.

(1) E.A. STARKE, Jr., and T.H. SANDERS, Jr., Eds., "Aluminum-Lithium Alloys," Proceedings of the 1st International Aluminum-Lithium Conference, Stone Mountain, Georgia, 1980 (AIME, Warrendale, PA (1981)).

(2) E.A. STARKE, Jr., and T.H. SANDERS, Jr., Eds, "Aluminum-Lithium Alloys II," Proceedings of the 2nd International Aluminum-Lithium Conference, Monterey, California, 1983 (AIME, Warrendale, PA (1983)).

(3) "Aluminum-Lithium Alloys III," Proceedings of the 3rd International Aluminum-Lithium Conference, Oxford, 1985, In Press.

(4) A.E. VIDOZ, D.D. CROOKS, R.E. LEWIS, I.G. PALMER, and J. WADSWORTH, Proceedings of the Conference on Rapidly Solidified Powder Aluminum Alloys, American Society for Testing and Materials, Special Technical Publication #980 (American Society for Testing and Materials, Philadelphia, PA, 1985), In Press.

(5) J. WADSWORTH, A.R. PELTON, D.D. CROOKS, and A.E. VIDOZ, Journal of Materials Science, submitted for publication, 1985.

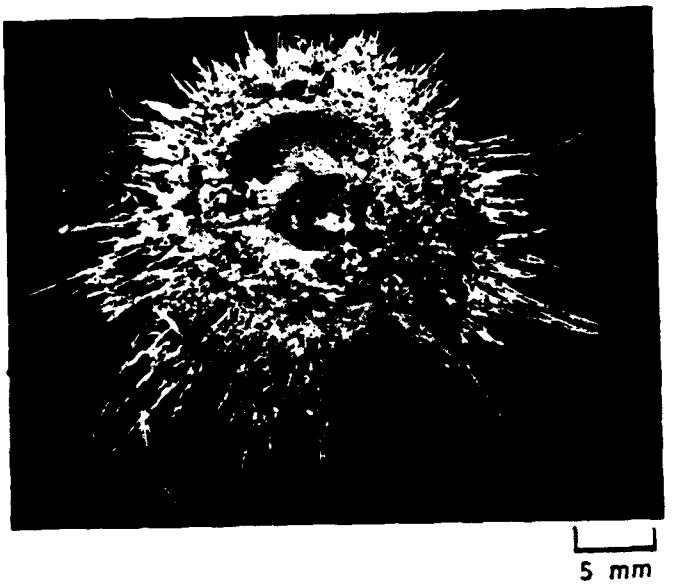

Fig. B1 (a) Splat quenched sample.
(b) Microstructural variation within a splat quenched Al-3Li-10Be alloy.

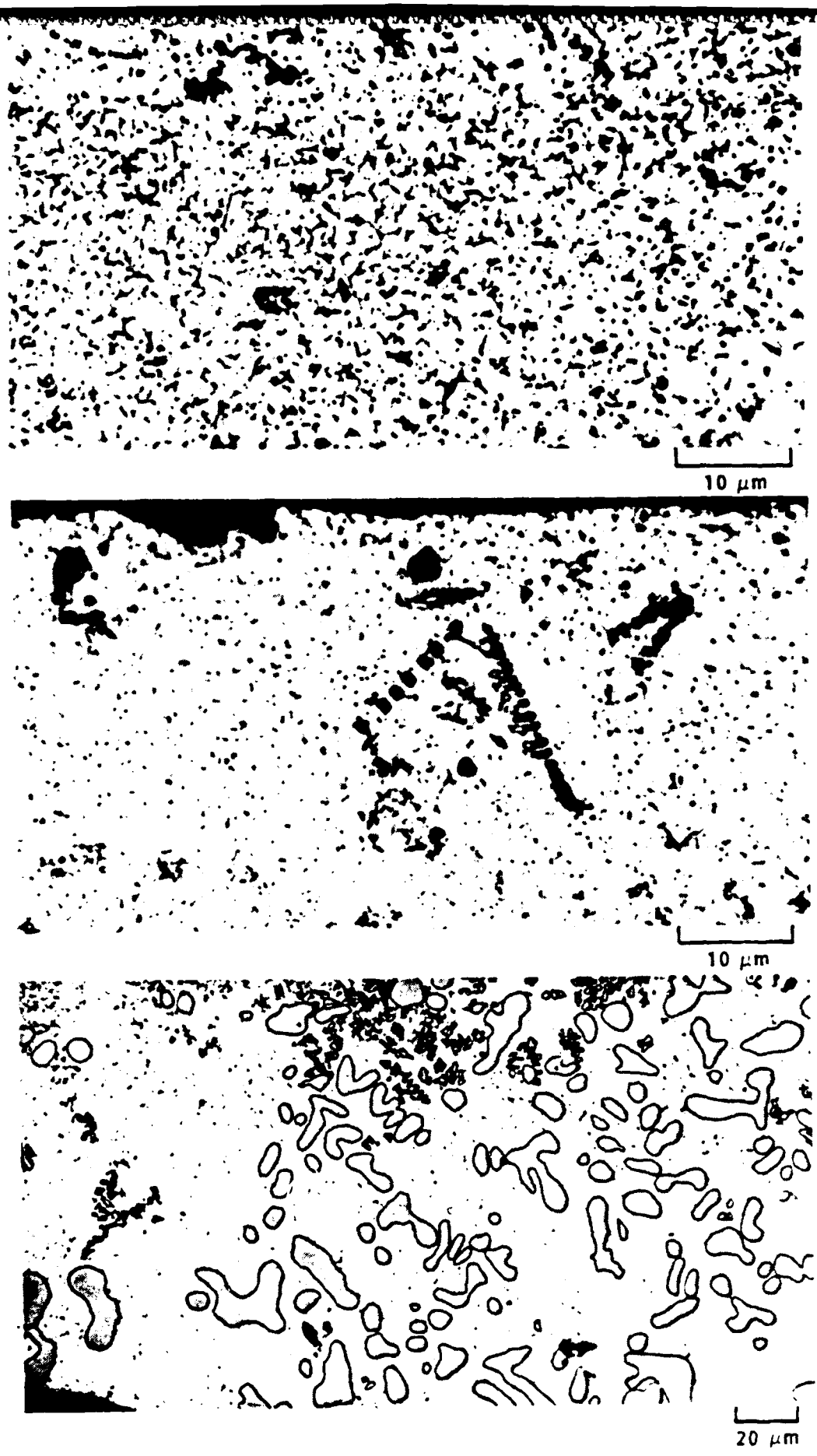

Fig. B2. Microstructures of the splat quenched Al-3Li-2Be (top), AL-3Li-5Be (center), and Al-3Li-10Be (bottom) alloys.

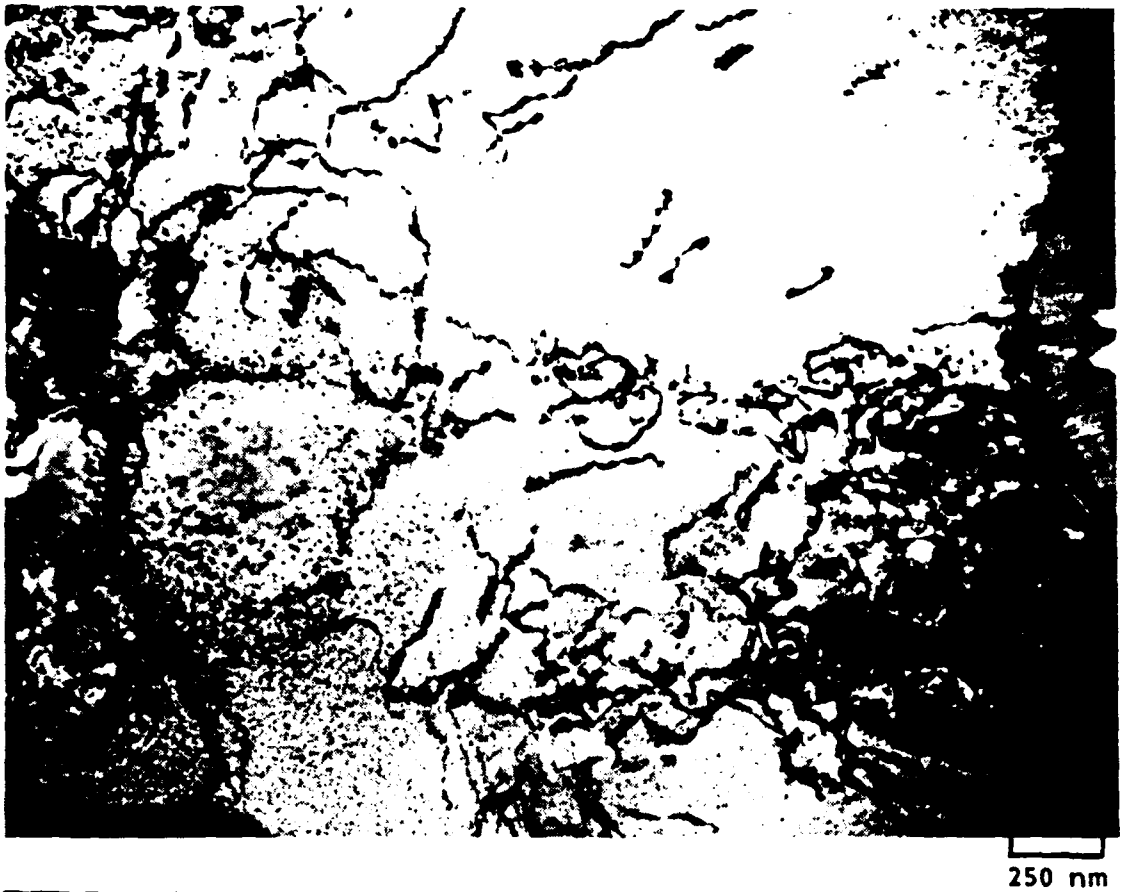

Fig. B3. Bright field/dark field pair of TEMS illustrating the distribution of δ'within the Al-3Li-10Be splat quenched alloy.

Fig. B4. TEM of Al-3Li-10Be splat quenched alloy showing the α-Be particles predominantly at cell walls.

APPENDIX C

MICROSTRUCTURAL EVALUATION OF ARC-MELTED Al-Li-Be ALLOYS

J. Wadsworth, A Joshi, D.D. Crooks, and A.E. Vidoz

Lockheed Palo Alto Research Laboratory
Metallurgy Department
3251 Hanover Street
Palo Alto, CA 94304

Abstract

A microstructural investigation has been carried out on a series of small castings of arc-melted Al-Li-Be alloys. The alloy compositions included amounts of Li up to 3 wt% and Be up to 10 wt%. Optical metallographic examination has revealed gross macrosegregation in the highly alloyed compositions. On the microstructural level, the structure consists of primary Be particles in a matrix of primary aluminum containing eutectic structure at the cell walls. A detailed Auger electron spectroscopy examination has been carried out on a section of an Al-3Li-10Be arc-cast alloy to determine the precise compositional variations. This approach is demonstrated to be a necessary prerequisite for selection of material for rapid solidification processing by techniques such as splat quenching.

INTRODUCTION

In recent years one of the major areas of research in advanced aluminum alloys has been directed toward the development of low-density alloys. The major emphasis of this research has been in alloys based on the Al-Li system; indeed, interest in these alloys is sufficiently great that three international conferences on this subject have been held since 1980 [1-3]. The reason that the Al-Li system is central to the above development is based on the recognition that Li is both the most efficient density-decreasing and elastic modulus-increasing of all metallic

elements when added to Al. In determining potential weight savings in aerospace structures it is now well accepted that low density is an overriding consideration but that increased modulus is also important [4]. There appear to be only three elements which when added to Al both decrease the density and increase the modulus; Li, Be and Si (there is some uncertainty about the influence of B on the modulus of Al although it is known to decrease the density of Al). Of these three elements, only Li and Be significantly offer the simultaneous benefits of decreased density and increased modulus.

The combination of Li and Be in Al alloys has not been attemped because of the limited solubility of Be in Al (less than 0.03 wt% [5]) as shown in Figure 1. In binary alloys of Al and Be the low solubility of Be leads to massive segregation of the Be-rich phase upon soldification under normal ingot production and poor mechanical properties result. Another disadvantage of Be is the well-known toxicity of its oxide which necessitates precautions in the handling and machining of Be metal or Be-based alloys.

Despite the above disadvantages, these are significant advantages to be gained from the development of fine-structured Al-Be or Al-Li-Be alloys. This is because in order to take further advantage of density decreases in Al-Li alloys, it is not possible simply to continue to increase the Li content. Beyond a level of about 3 wt% Li in Al-Li alloys, deleterious effects of Li are observed on toughness and ductility [1-3]. As a result of this restriction, Al-Li-Be alloys become attractive if the Be can be dispersed in a very fine form.

Rapid soldification processing (RSP) is a unique and potentially practical method for the development of high modulus and high strength microstructures in Al-Li alloys containing more than about 0.03 wt% Be. Rapid solidification would eliminate segregation of Be and greatly refine the microstructure of the alloy. Although Be has only a small solubility in Al at low temperature, at increased temperature, Figure 1, it shows an increasing liquid solubility reaching about 10 wt% at 1025°C. The successful development of Al-Li-Be alloys would result in ultra-low density, high modulus and high strength Al alloys, competing with the most promising metal-matrix and non-metal matrix composites with respect to weight savings in advanced aerospace structures. The potential for weight savings in such structures is significantly higher for Al-Li-Be alloys than for any other Al alloy system, including metal matrix composites. In a preliminary study f Al-Li-Be alloys [6] using the S-3A Naval Patrol Aircraft as a structural example [4,7], the weight savings were calculated for two illustrative Al-Li-Be compositions: Al-3Li-3Be and Al-3Li-10Be. The results, together with similar calculations (made using experimental data [8-10] for other advanced aluminum alloys, as well as for metal matrix composites [11], have clearly demonstrated the important potential benefits of the Al-Li-Be alloys. For example, by comparison with Al-7075, an Al-3Li-10Be alloy exhibited a 26% weight savings and an Al-3Li-3Be alloy a 20% weight savings. The Al-Li-Be alloys are therefore a group of alloys which could have applications in aerospace structural components resulting in major increases in range, payload and service life.

During the course of initial attempts by the present authors to make RSP Al-Li-Be alloys, it was discovered that the segregation effects in the as-cast starting material required special attention. This was necessary because it is important to understand precisely the composition of the starting material from which RSP particulate or ribbon is to be manufactured. This is especially true if small quantities are to be made, for example, by splat quenching methods. In the present paper, detailed metallographic examinations of such starting materials from Al-3 wt% Li + 2, 5 and 10 wt% Be alloys are described.

Experimental Procedures

The materials used for manufacturing the Al-Li-Be ternary alloys were: pure Al (99.95%) from high purity ingot stock; high purity battery-grade Li containing less than 1000 ppm of Na (and typically less than 300 ppm of Na), and electrolytic induction melted Be stock (99.6%) with the main impurities being 0, Fe, and Al. The Al was cleaned by chemically etching in a mixture of HNO_3 and HF, the Li was handled in a low humidity (1%) room, and the Be was cleaned by chemical etching in dilute H_2SO_4.

In order to make Al-Li-Be ternaries, master alloys of Al-Be were prepared by arc melting. The arc melting was carried out in a small depression in a water cooled Cu hearth in a chamber containing an Ar atmosphere. A getter button of pure Ti was melted prior to melting the small (20g) charges of Al and Be, in

order to reduce the partial pressures of N_2 and O_2 in argon. The small castings of Al-Be thus produced were remelted several times (inverting the solidified ingot on each occasion) to promote homogeneity. These master alloys were chemically cleaned prior to the addition of Li which was made by placing the elemental Li underneath the Al-Be arc melted buttons, and slowly melting the Li by conduction from the top side of the buttons (at which point the arc was located). This procedure avoided evaporative losses of Li and permitted its diffusion into the master alloy prior to the mass becoming molten. This molten pool was puddled for several minutes, allowed to solidify and then the button was remelted three times.

A number of analyses on these arc melted buttons was carried out, primarily by optical metallography and Auger electron spectroscopy. Because of the severe segregation that was observed using optical metallography, it was necessary to determine the precise compositions at locations within the button. This was carried out using Auger electron spectroscopy.

RESULTS AND DISCUSSIONS

Typical castings produced by arc-melting, of a range of Al-Li-Be alloys, are shown in Figure 2. Generally, a rather thick oxide surface was observed on each alloy. Upon sectioning, it was revealed that macrosegregation was apparent in each of the castings, but much more severely so in the case of the highly

alloyed compositions. Examples of the coarse macrostructures of two of the alloys are given in Figure 3. As may be seen, the Al-3Li-10Be alloy showed an especially segregated structure; it was subsequently determined that the upper part of the casting (the light area of Figure 3 (b)) was rich in Li. A small degree of porosity was also evident in some of the castings. Three castings (Al-3Li-2Be, Al-3Li-5Be, and Al-3Li-10Be) were investigated using optical microscopy and one was investigated (Al-3Li-10Be) for compositional details using Auger electron spectroscopy.

Because of the degree of macrosegregation (the struture varied considerably depending upon the precise location within the casting), it is difficult to present representative microstructures of each alloy. However, examples from the approximate mid-sections of each of the three arc-cast compositions are illustrated in Figures 4(a) (b), and (c) at increasing magnifications for the Al-3Li-2Be, Al-3Li-5Be, and Al-3Li-10Be alloys. The microstructures of the alloys show an increasing amount of primary Be phase as the total Be content is increased. The matrix of the alloys, as clearly evident in the high magnification photomicrographs of Figure 4 (c), shows the relatively fine eutectic structure. It is important to emphasize the inhomogeneity of these castings, and a detailed examination of the Al-3Li-10Be alloy was carried out. Optical photomicrographs are shown in Figure 5 from within one of the castings (the Al-3Li-10Be composition). Despite the variation in structure within individual castings, some general observations

can be made from Figures 4 and 5. As for the case of Al-Be binary alloys, the Be in the Al-Li-Be alloys is extremely insoluble and precipitates upon cooling from the melt in coarse, microsegregated form in a variety of irregular shapes and sizes. This is the predominant phase visible in Figures 4 and 5. This primary Be has a large size range from about 2 to 70 μm. Within these segregated regions, a cellular eutectic structure exists and at the cell walls are found both the Be-phase as well as, presumably, the Li-containing phases (aasumed to be δ' or δ). This type of microstructure is most undersirable from the viewpoint of mechnanical properties because the large Be particles result in brittle behavior. Refinement of such microstructures provides the driving force to produce these compositions of Al-Li-Be alloys by RSP. Furthermore, because of the uncertainty of the compositional ranges within these castings, it was not possible to simply cut pieces for splat quenching experiments and assume nominal compositions. A detailed Auger analysis was therefore carried out to measure the composition fluctuations in a polished half-section of the Al-3Li-10Be alloy ingot in order to locate pre-cisely regions for further study.

Compositional Variations in Al-3Li-10Be Arc Melted Button

A common procedure in preparation of alloy splats involves making a master alloy button (or casting) of a nominal composition and then using a small portion of it (e.g., a cube of side 2.5 mm) to remelt and rapidly solidify by splatting. A source of

composition fluctuation in splats arises from any inhomogeneity present in the master alloy button. The composition of the alloy can also change during each melting step due to evaporation losses and oxidation. These losses can be particularly high or Li and Be, leaving the splat deficient in these elements. Thus, an assurance of homogeneity in the master alloy, and careful melting practice to avoid oxidation and evaporation losses, are important factors in achieving alloy splats of the desired composition. Thise section of the study was aimed at understanding the nature of macrosegregation present in the master alloy and is considered an essential step in preparing splats with preselected compositions.

The alloy with a nominal comosition of Al-3Li-10Be was selected for this macrosegregation study. This alloy had the greatest Be and Li concentrations and was determined to exhibit the greatest degree of inhomogeneity among the various alloys. The macrosegregation study was conducted on a polished thin slice, shown in Figure 6, which was cut from the master alloy button.

The technique of Auger Electron Spectroscopy (AES) was used in evaluation of the lateral compositional inhomogeneity of the alloy. A Perkin-Elmer model PHI 560 ESCA/SAM system was used which has a minimum electron beam diameter of 1 μm. In practice, the Scanning Auger Microprobe (SAM) electron beam was rastered to cover large areas of 400 μm x 400 μm. AES spectra and selected energy region multiplexes were obtained from various regions of the alloy slice and quantitative estimates made using elemental

sensitivity factors. It should be pointed out that these quantitative estimates may have a $\pm$ 30% relative error for most elements and possibly larger errors for lithium concentrations. The errors in Li estimates are larger due to its peak occuring in the very low energy range (36-43 eV), which is also dominated by true secondary electrons. The large errors also arise due to changes in chemical states, e.g., when the elements are present in their oxide forms or mixed states. Attempts at better quantification are currently being made utilizing x-ray photoelectron spectroscopy (XPS) for large area (5mm diameter) surface analysis and Inductively Coupled Plasma (ICP) for high accuracy bulk analysis. Surface analysis efforts using AES does offer a combination of attributes for the present study that include: (i) light element sensitivity (Li, Be, etc.) with the exception of H and He, (ii) high lateral resolution as low as 1 μm, (iii) surface sensitivity (2-5 nm region of the surface), (iv) depth profiling capability in conjunction with ion sputtering and, (v) chemical state information such as needed in distinguishing oxide states from elemental states.

AES estimates of Al, Be, Li, and oxygen concentrations were obtained from the areas shown in Figure 6. These data were obtained after sputter cleaning of surfaces to remove atmospheric oxides and contamination. The top portion of the button, represented by the light area of Figure 6, had a mottled appearance. An AES spectrum (Figure 7) obtained from area 4 within this region indicated high concentrations of Li, determined to be present in the form of an oxide (based upon its

peak position). The estimated atomic concentrations from various locations marked in Figure 6 are shown in Table 1. The data clearly indicates substantial variations in Li and Be concentrations at the various locations. It is generally found that Li is richer near the top surface of the button and in a form combined with oxygen. On the other hand, Be is enriched near the bottom of the button in concentrations estimated to be as high as 70 atomic percent. The absolute quantities described above may be in error, but the relative comparison of data from different areas leads to the conclusion the large scale macrosegregation occurs during the preparation of these master alloy buttons. Hence, caution must be exercised in selecting portions for splat alloy preparation and additional precautions must be taken to assure homogeneity.

Table 1 also shows compositional information obtained from light and dark microscopic phases present in the sample. These data, 1(a) through (c), obtained from the general area 1, indicate that little or no variation in Li concentration occurs in these microscopic regions. On the other hand, the Al/Be ratio varied substantially suggesting precipitation of Be-rich and Be-deficient phases within.

SUMMARY

A series of small castings of Al-Li-Be alloys has been prepared by arc melting. The compositions of the alloys contain up to 3 wt% Li and 10 wt% Be. Despite attempts to homogenize the alloys

by remelting techniques, severe macrosegregation is observed in all alloys but particularly so in the heavily alloyed compositions. The alloy microstructures consist of coarse primary Be particles in an Al matrix containing a relatively fine eutectic structure at cell walls. A detailed Auger electron spectroscopy analysis of a section of the most heavily alloyed casting (Al-3 wt% Li-10 wt% Be) has been carried out to determine a detailed understanding of the compositional variations in the alloy. This procedure is considered to be essential in order to select material of known composition for study by rapid solidification processes such as splat quenching.

ACKNOWLEDGMENTS

This work was supported by the Office of Naval Research, Contract #N00014-84-C-0032. The authors wish to thank Mr. R. E. Lewis for his valuable contributions.

REFERENCES

[1] E. A. STARKE, JR., and T. H. SANDERS, JR., Eds., "Aluminum-Lithium Alloys", Proceedings of the 1st International Aluminum-Lithium Conference, Stone Mountain, Georgia, 1980 (AIME, Warrendale, PA (1981)).

[2] E. A. STARKE, JR., and T. H. SANDERS, JR., Eds., "Aluminum-Lithium Alloys II", Proceedings of the 2nd International Aluminum-Lithium Conference, Monterey, Califorinia, 1983 (AIME, Warrendale, PA (1983)).

[3] G. BAKER, et. al., Eds., "Aluminum-Lithium Alloys III", Proceedings of the 3rd International Aluminum-Lithium Conference, Oxford, 1985, (Institute of Metals, London, 1986), p 199.

[4] J. C. EKVALL, J. E. RHODES, and G. C. WALD, American Society for Testing and Materials, Special Technical Publication #761 (Amer. Soc. for Testing and Materials, Philadelphia, PA 1982), p. 328.

[5] "Aluminum, Vol. 1, Properties, Physical Metallurgy and Phase Diagrams", Edited by K. R. Van Horn (American Society for Metals, 1968).

[6] A. E. VIDOZ, D. D. CROOKS, R. E. LEWIS, I. G. PALMER, and J. WADSWORTH, Proceedings of the Conference on Rapidly Solidified Powder Aluminum Alloys, American Society for Testing and Materials, Special Technical Publication #890 (American Society for Testing and Materials, Philadelphia, PA 1986), p 237.

[7] R. E. LEWIS, I. G. PALMER, J. C. EKVALL, I. F. SAKATA, and W. E. QUIST, "Proceedings of the 3rd Conference on Rapid Solidification Processing: Principles and Technology, Gaithersburg, MD, 1982 (National Bureau of Standards, Washington, 1983) p. 615.

[8] I. G. PALMER, R. E. LEWIS, and D. D. CROOKS, Proceedings of the 2nd International Conference on Rapid Solidification Processing, 1980, edited by R. Mehrabian, B. H. Kear, and M. Cohen (Claitors Publishing Div., Baton Rouge, LA, 1980), p. 342.

[9] E. A. STARKE, JR., T. A. SANDERS, JR., and I. G. PALMER, J. Metals, 33, (1966) p. 24.

[10] H. G. PARRIS, F. R. BILLMAN, W. S. CEBULAK and J. I. PETIT, Proceedings of the 2nd International Conference on Rapid Solidification Processing, Mar. 1980, edited by R. Mehrabian, B. H. Kear, and M. Cohen (Claitors Publishing Div., Baton Rouge, LA, 1980), p. 331.

[11] H. RACK, private communication, ARCO Metals Co., SILAG Operation, Greer, South Carolina, 1983

TABLE 1

AES COMPOSITIONAL ESTIMATES FROM VARIOUS LOCATIONS SHOWN IN FIGURE 6

	ATOMIC %				
AREA/LOCATION*	Al	Be	Li	O	COMMENTS
1	53	34	13	-	
2	45	41	13	1	
3	43	46	10	1	
4	38	36	17	10	
5	41	53	5	1	
6	23	70	3	4	
7	21	68	9	2	
8	25	68	4	2	
9	38	44	16	2	
1(a)*	76	10	13	1	Dark Phase
1(b)*	35	53	11	-	Light Phase
1(c)*	26	63	11	-	Light Phase
Bulk Concentration	68	23	9	-	

*1(a) through 1(c) represent 20 μm x 20 μm areas. All others are 400 μm x 400 μm areas.

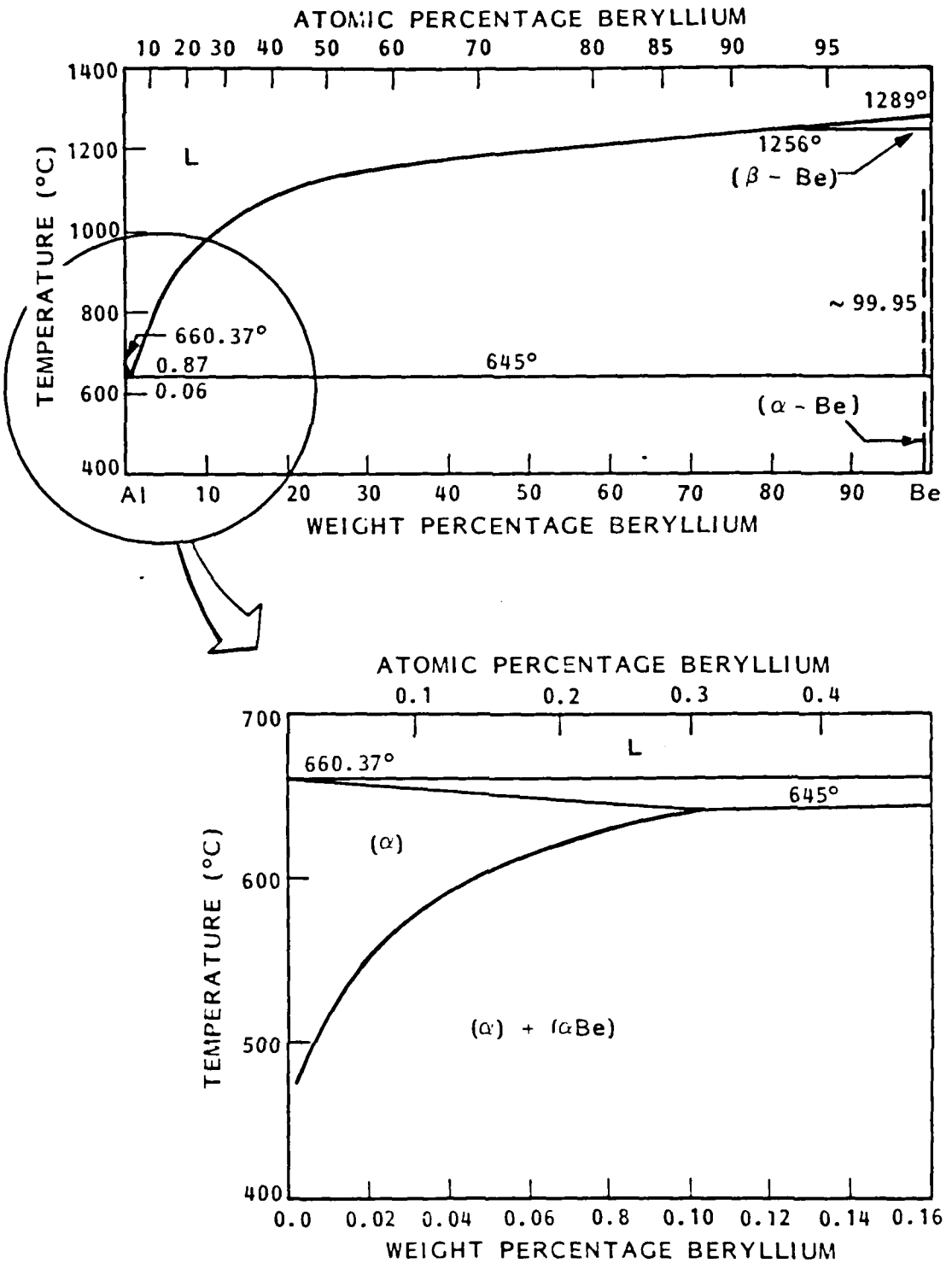

Fig. C1. The aluminum-beryllium equilibrium phase diagram.

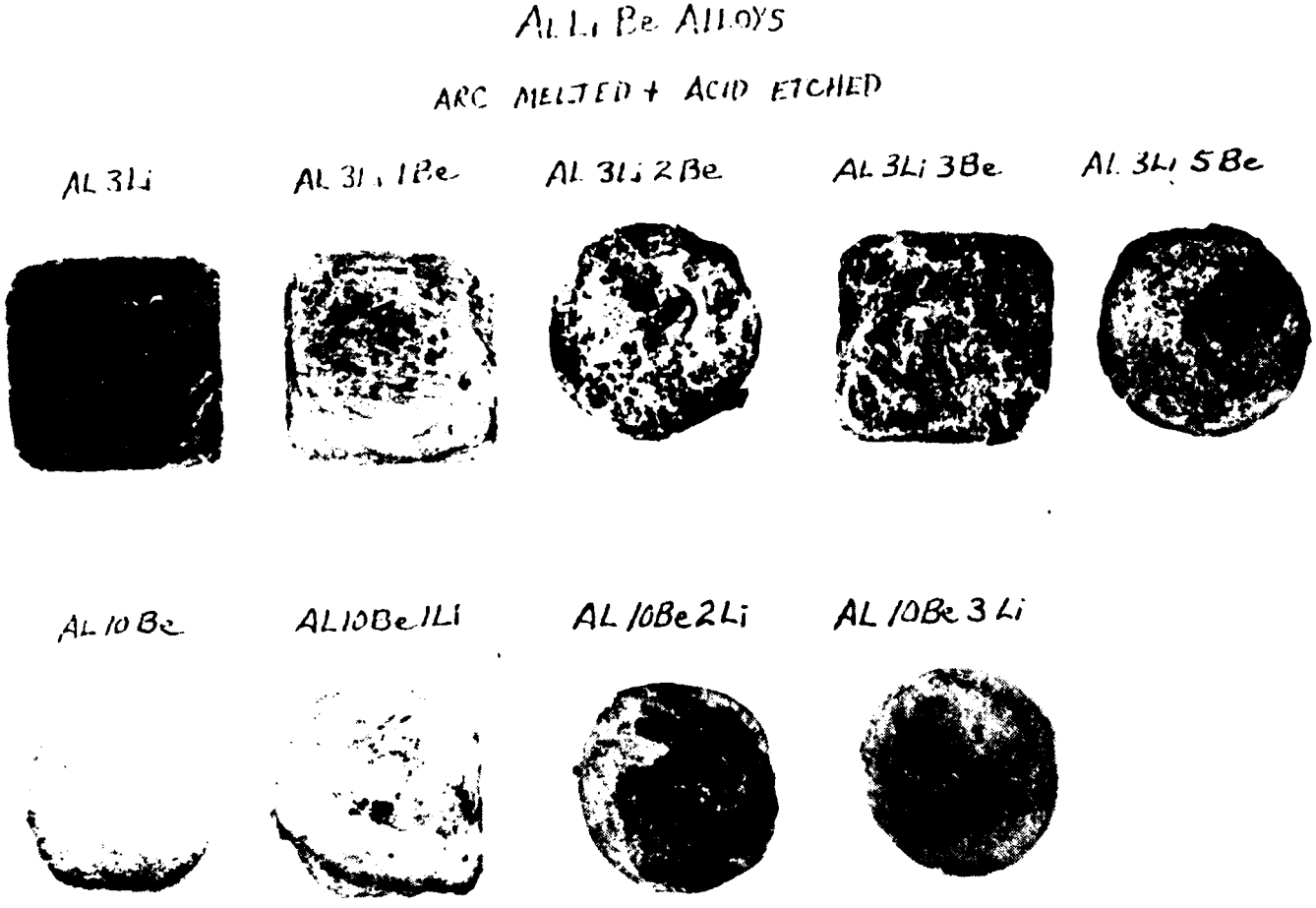

Fig. C2. Arc-melted castings of Al-Li, Al-Be and Al-Li-Be alloys.

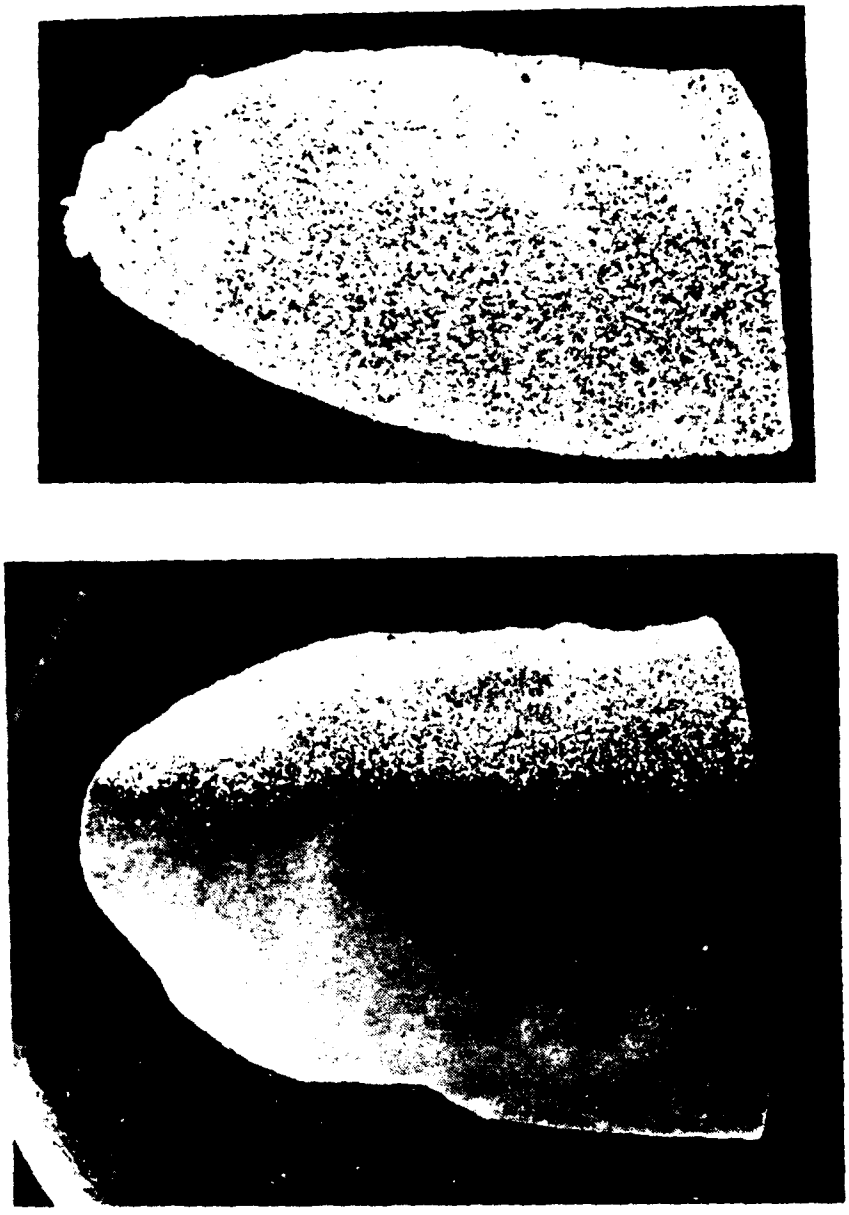

Fig. C3. Sections of the arc-melted castings of Al-3Li-2Be (top) and Al-3Li-10Be (bottom) alloys.

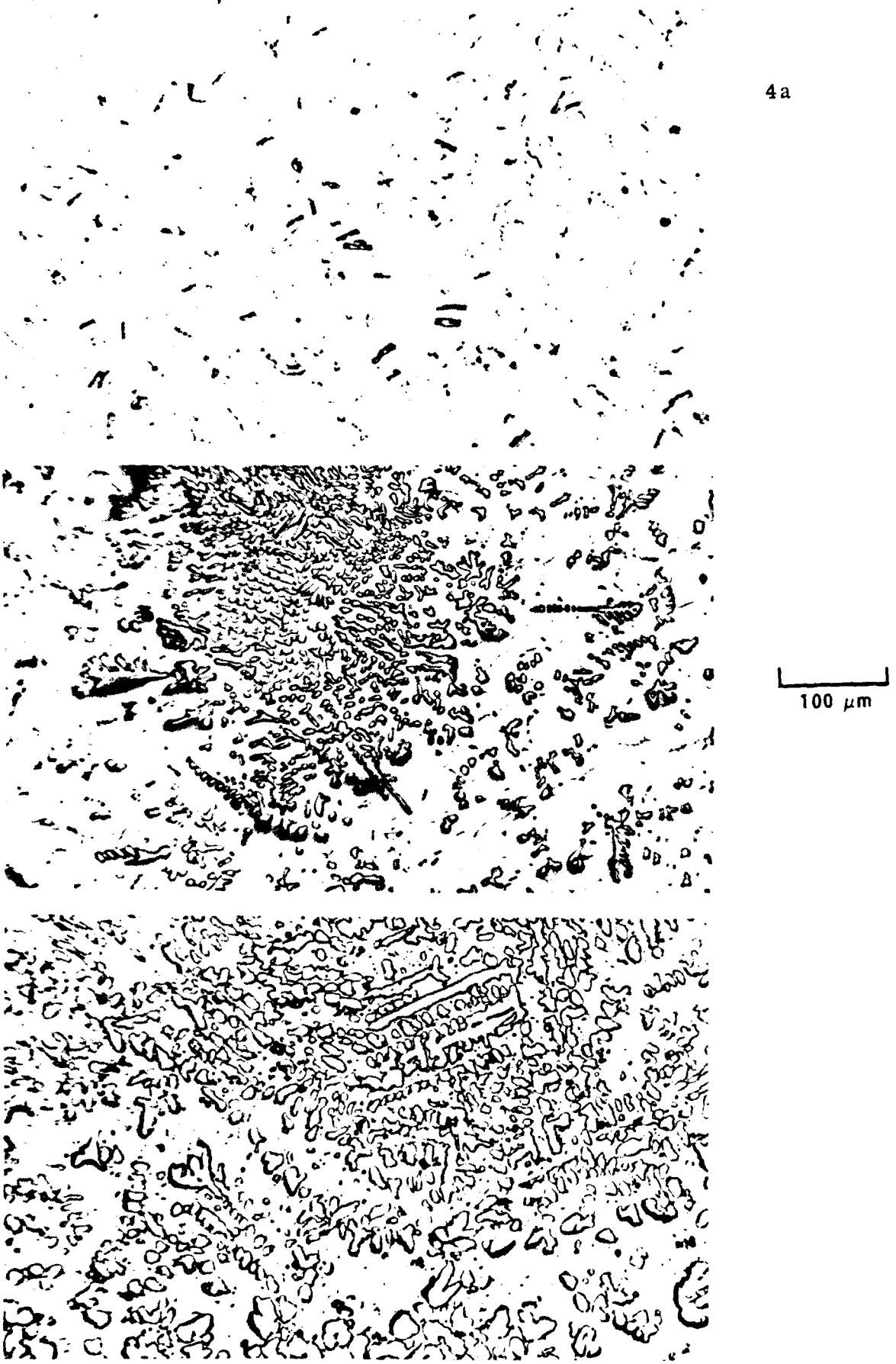

Fig. C4. Optical photomicrographs at (a) low, (b) medium, and (c) high magnification for the Al-3Li-2Be (top), Al-3Li-5Be (center) and Al-3Li-10Be (bottom) alloys in the arc-melted condition.

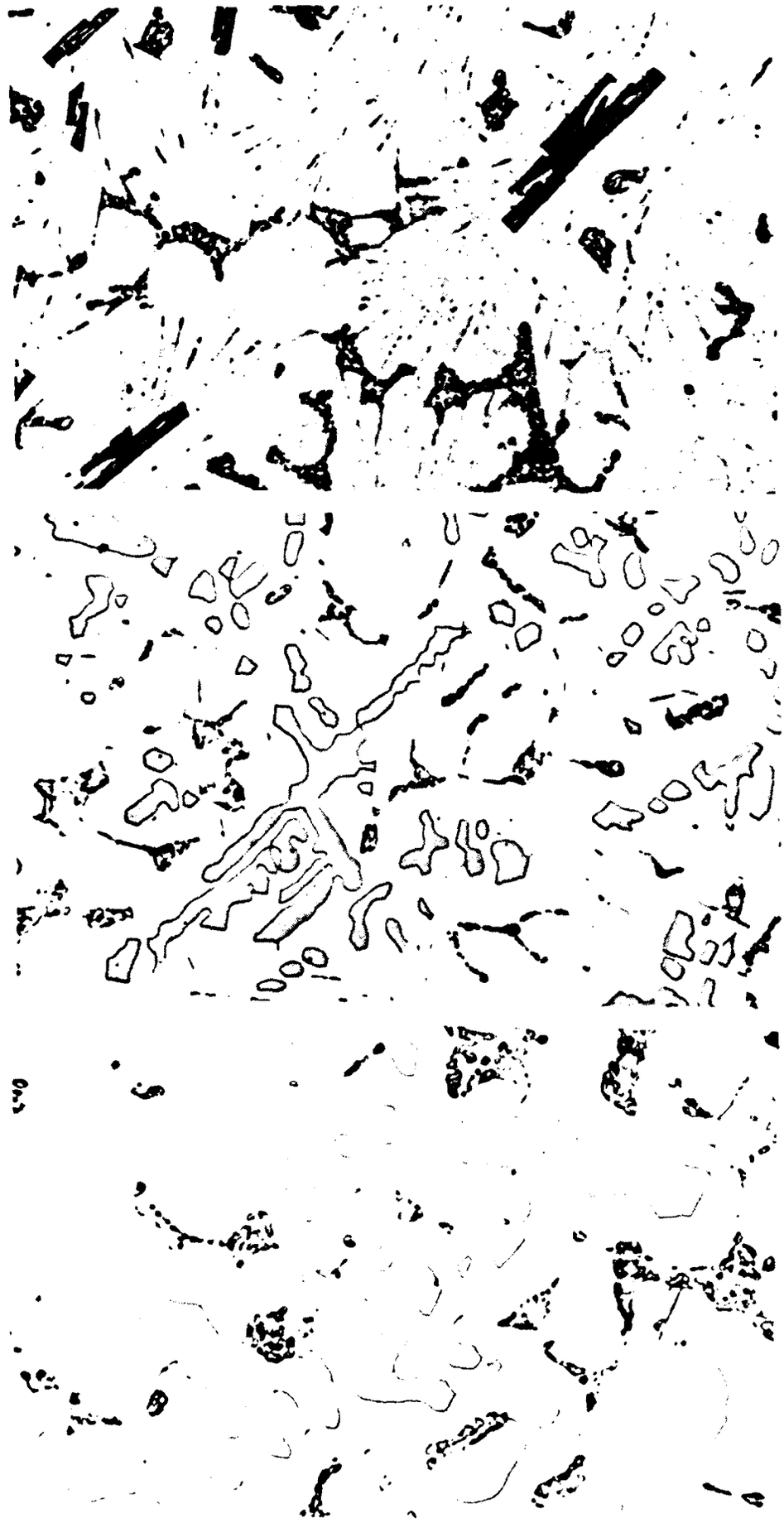

4b


4c
10 μm

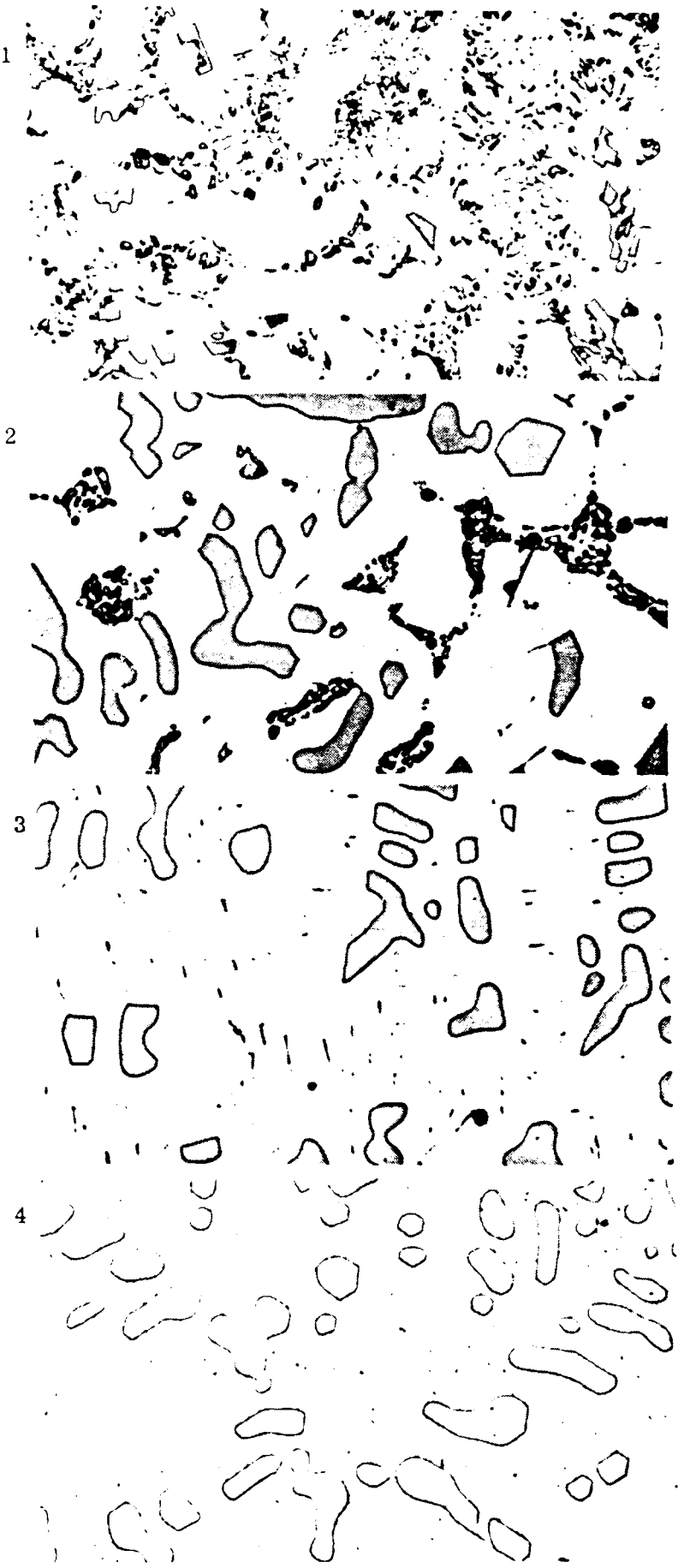

Fig. C5. Variations of microstructure within the arc-melted Al-3Li-10Be alloy.

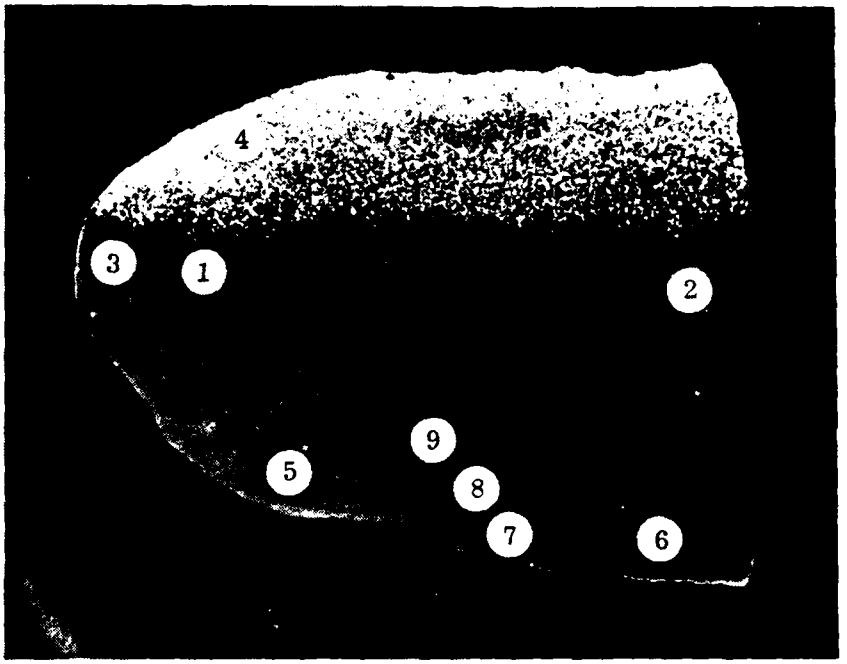

Fig C6. Cast slice of Al-3Li-10Be alloy showing the areas studied by Auger analysis.

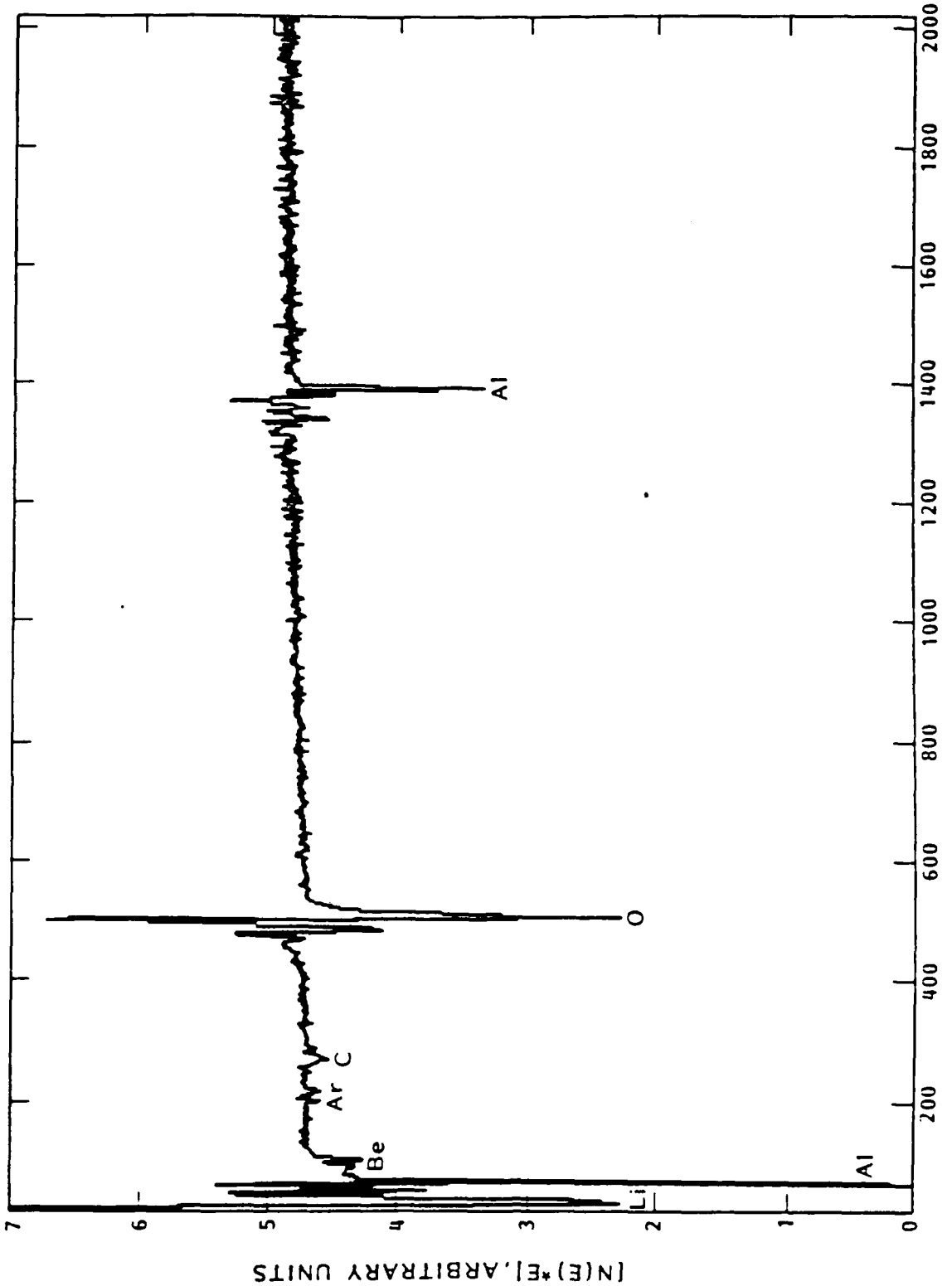

Fig. C7. AES spectrum from area 4 of Fig. C6.

APPENDIX D

MICROSTRUCTURAL EVALUATION OF RAPIDLY SOLIDIFIED Al-Li-Be ALLOYS

J. Wadsworth, A. R. Pelton*, D. D. Crooks,
R. E. Lewis, A. E. Vidoz

Lockheed Palo Alto Research Laboratory
Metallurgy Department
3251 Hanover Street
Palo Alto, CA 94304

*Ames Research Laboratory
Ames, IA 50011

ABSTRACT

Aluminum-Lithium-Beryllium alloys are a group of low-density, high modulus materials that potentially have technological importance in aerospace structures. In this paper, a series of such alloys has been produced using rapid solidification processing via melt spinning. The microstructures of the alloys have been investigated in the as-melt-spun condition, after consolidation and heat treatment to peak hardness, and after tensile testing in the heat treated condition. In particular, changes in the size and distribution of primary Be particles and Al_3Li precipitates are described after consolidation and processing. The mechanical properties of the alloys in the heat treated condition are also presented.

INTRODUCTION

The rationale for the development of ternary Al-Li-Be alloys has been presented recently by Lockheed scientists [1,2]. It was shown that such alloys could have important applications for aerospace structures because of their high potential weight savings. The weight savings originate from the fact that both Li and Be decrease the density of Al and at the same time increase the elastic modulus. In fact, Li and Be are the only elements that have both of these effects when added to Al. Recent studies of the various factors influencing weight savings in aerospace structures clearly emphasize the dominant importance of reduced density[2].

The production of wrought Al-Li-Be alloys by conventional ingot casting having useful engineering properties is not possible [1,2]. This is because Be segregates in a coarse distribution, upon freezing, and this results in poor ductility and toughness. Because of the extremely limited room temperature solubility of Be in Al or Al in Be, alloys based on the Al-Be system constitute an important case for the application of a Rapid Solidification Processing (RSP) technique. At low temperature, altough Be has only a small solid solubility in Al, 0.03 wt. %, at increased temperatures (Figure 1 of Reference 2), it shows an increasing liquid solubility, reaching approximately 10 percent by weight at 1025°C. Therefore, it is possible to obtain by rapid solidification a microstructure in which the aluminum solid solution contains a high concentration of fine discrete particles (dispersoids) of Be. A dispersion of these particles can have at least three important effects upon the mechanical properties of the aluminum alloys: 1) a decrease in density, 2) an increase of the elastic modulus, and 3) an increase in strength. In order to achieve a significant room temperature strength contribution from the Be dispersoids, it would be necessary to avoid excessive coarsening of them during metallurgical processing. However, it has been shown [4,6] that Al-Be binary alloys (containing up to 10 wt.% Be) produced by RSP have a fine dispersion of alpha Be particles. Upon subsequent heat treatment the particles coarsen somewhat but remain with average sizes smaller than 100 nm.

In RSP Al alloys containing both Li and Be, two different precipitates form independently (1). The Al_3Li (δ') phase precipitates as fine, coherent spheroids which will provide a significant contribution to strength[7,8]. The α-Be precipitates as a dispersoid within the Al matrix. It is anticipated that this α-Be could contribute to the mechanical properties of the alloy by adding a dispersion strengthening component to the yield strength, and also by providing a mechanism to disperse dislocation glide, which will allow the Al_3Li phase to contribute more of its full potential to the alloy strength. It has been shown that very fine dispersoids provide a beneficial effect on improving the dispersion of slip in Al-Li alloys[8]. Because the Al_3Li (δ') coherent precipitates are small (2 to 100 nm, depending upon aging conditions) and their misfit with the aluminum lattice is small (less than 0.1 percent), they are readily sheared by dislocations and slip can occur by planar glide in Al-Li alloys containing more than about 1 wt.% Li. Both the limited ductility and low fracture toughness of various Al-Li alloys have been broadly attributed to this planar glide mechanism[8]. There are no known intermetallic compounds between Li and Be[9] and so it is reasonable to expect that these elements will co-exist in an alloy without the formation of undesirable phases. The purpose of this paper is to describe recent work on Al-Li-Be ternary alloys containing about 3 wt.% Li and up to 20 wt.% Be. The structure and properties of alloys after rapid solidification processing will be described.

EXPERIMENTAL

Two alloys (Al-3Li-2Be and Al-3Li-10Be by wt.%) were converted to melt spun ribbon using equipment designed and built at the Lockheed Palo Alto Research Laboratory[1]. Ribbon of approximate dimensions 1 to 2 mm in width and 20 to 70 μm thickness was produced. The ribbon was examined using optical and transmission electron microscopy. For consolidation, the ribbon was comminuted, cold compacted to 50% to 60% density, vacuum hot pressed and extruded[1]. Subsequent heat treatments were carried out in air.

Thinning of the Al-Li-Be alloys for TEM was carried out in an electrolyte of 5% perchloric acid, 35% 2-butoxyethanol, and 60% methanol at 10^{o}C with an applied potential of 15V and a resultant current of 75 mA. The samples were examined with a JEOL 100CX TEM-STEM at 120 kV.

RESULTS AND DISCUSSION

a) Melt Spun Ribbon

Melt spun ribbon of Al-3Li-2Be alloy and Al-3Li-10Be alloy was successfully prepared by melt spinning. Optical photomicrographs of melt spun ribbon of the Al-3Li-10Be alloy are shown in Figure 1. As may be seen, relatively uniform fine microstructures are observed using optical microscopy. These fine structures can be

compared with those produced by splat quenching of the same alloy[10] and it is evident that the melt spinning operation produces a more uniform, finer structure than does the splat quenching.

In order to examine the microstructures of the ribbons more closely, a TEM examination was carried out.

Figure 2.I is a bright field/weak-beam dark field pair showing a typical microstructure of an as-quenched Al-3Li-2Be alloy. The prominent features of this structure are indicated on the micrographs, and include coherent Al_3Li δ' precipitates (A), and large and small α-Be particles (B); some regions of cellular structure are also observed. This nonuniform microstructure is similar to that of splat-quenched Al-Be alloys[10]. The δ' particles are approximately 5-10 nm in diameter, which is similar in size to δ' observed an as-quenched Al-Li base alloys produced by powder metallurgy or ingot metallurgy techniques. The volume fraction of large (>100 nm) α-Be particles is relatively low (<0.10) and these particles are usually confined to grain boundary regions.

The striking feature evident in the micrographs in Figure 2.II is the segregated cellular structure of the as-quenched Al-3Li-10Be ribbon. There is an enrichment of small α-Be particles concentrated at the cell walls. Although it is not obvious from this figure, the volume fraction of large α-Be particles is

greater in the Al-3Li-10Be alloy than in the Al-3Li-2Be alloy. The inserted <001> zone axis pattern clearly shows the <100>-type reflections from δ' (identical patterns were obtained from Al-3Li-2Be). These precipitates have the typical cube-cube orientation relationship with the matrix (i.e., $[100]_{\delta'}//[100]_{Al}$, $(001)_{\delta'}//(001)_{Al}$).

The selected-area diffraction technique was not sensitive enough to reveal the crystal structure of the α-Be particles; therefore, microdiffraction techniques were employed for this purpose. Analyses of particles of about 200 nm were carried out using convergent beam microdiffraction patterns formed by focusing a 100 nm probe (convergence angle ≈ 1.5 mrad) on the precipitate. The reflection from the precipitates confirmed that they are primary α-Be and are randomly oriented within the grains indicating that they formed prior to the solidification of the Al matrix. This is also commonly observed in splat quenched hypereutectic Al-Be alloys[11].

Similar microstructures have been observed recently in rapidly-solidified Al-Be binaries[5,12]. Van Aken and Fraser[5] ascribe the morphology and distribution of the α-Be particles to a monotectic reaction. Their proposed solidification scheme requires liquid phase separation within a metastable miscibility gap. Tanner, Jacobsen and Gronsky[12] have suggested that α-Be precipitation is due to a simple eutectic reaction similar to the Cu-O and Fe-MnS systems. More detailed experimentation is

necessary to determine the exact nature of the phase transformation.

b) Consolidated and Heat Treated Ribbon

Ribbons of both the Al-3Li-Be and Al-3Li-10Be alloys were converted into extruded bar using techniques previously described[1]. Tensile samples were fabricated from these bars, heat treated to an approximately peak strength condition and then tensile tested.

It was shown previously that both Al-3Li-2Be and Al-3Li-10Be alloys exhibited age hardening responses upon aging at 190°C after quenching from 538°C[1]. The hardening response is representative of the precipitation of Al_3Li (δ')[7,8]. For example, in the as-quenched condition the R_B hardness is 16.5; after aging at 190°C for 22 hrs the R_B hardness is 74[1]. Similar results were observed for an Al-3.6Li-9.8Be alloy[1]. This alloys also was tensile tested and has a modulus of 93.4 GPa, a yield strength of 427 MPa, ultimate tensile strength of 500 MPa and 5.6% elongation. The relatively low strain to failure was traced to inhomogenieties that appear as coarse particles on the fracture surface.

In the following section a transmission electron microscopy study of these alloys in the peak strength condition is presented. Following that section, a study of the alloys after tensile testing is described. In both cases, transmission electron

microscopy samples were taken from samples such that the thin foil lay parallel to the original extrusion direction. In general, coarsening of the α-Be particles from a size of less than 100 nm in the as-quenched melt spun ribbon to the size range of 100 to 500 nm in the final product was observed to have taken place as a result of consolidation.

i) Al-3Li-2Be

Rather inhomogeneous structures were observed in these samples. For example, in Figures 3 and 4, TEM collages from adjacent regions within the same sample are shown. In Figure 3 there is no elongated grain structure as is evident in Figure 4. (As will be seen, such regions do not occur in the Al-3Li-10Be alloy, possibly due to the presence of a much greater volume fraction of α-Be particles.) Furthermore, in both Figures 3 and 4 there appears to be intense deformation zones (the black areas in Figure 3 are regions of high defect density) associated with the α-Be particles. A high magnification bright field/dark field (BF/DF) pair (using a δ′ reflection) is shown in Figure 5. The δ-Be particles do not appear using this reflection but their location can be inferred by the absence or low density of δ′ in these regions. The δ′ particles are about 20-50 nm in size (by comparison, particles of 5-10 nm are observed in the as-quenched melt spun ribbon).

ii) Al-3Li-10Be

In this alloy, the grains were generally observed to be elongated with large angle grain boundaries along the longitudinal axis and generally small angle boundaries perpendicular to them. An example is shown in the TEM collage of Figure 6. The large volume fraction of α-Be particles is also evident. These particles are both on grain boundaries and within grains and have, in some cases, particular orientation relationships with the matrix, e.g., $(10\bar{1}0)_{Be}//(002)_{Al}$. A region from within the overview microstructure of Figure 6 is shown in Figures 7 and 8, at low and high magnifications, respectively. In addition to the large α-Be particles (left side of Figure 7), some agglomeration of the smaller Be particles has occurred during the consolidation processing. This is clearly seen in Figure 8 in a region adjacent to a boundary.

c) Consolidated, Heat Treated and Tensile Tested Condition

The above samples were also examined in the gage length of tensile coupons after mechanical testing. As expected, the major difference between the samples in the as heat treated condition and those in the heat trated and strained condition is the increased dislocation density. The visibility of the dislocations, of course, depends on the diffraction conditions of the particular region. There was not any clear indication of

interactions between the dislocations and particles (α-Be or δ') in the samples examined in this study.

For the Al-3Li-2Be alloy in the aged condition, the grains are not elongated. There are large grains with isolated regions containing smaller subgrains as shown in Figure 9 and there are large depleted zones at the grain boundaries (i.e., regions devoid of δ' particles). Again, the α-Be has mainly precipitated at the grain boundaries of these smaller grains, and is dispersed throughout the larger grains. The precipitate free zones are particularly evident in the BF/WBDF pair of Figure 10 (using a δ' reflection). At present, there is no clear reason why there are the δ'-depleted zones within the grains. Some of these regions could be sites for α-Be dispersoids but not all of them can be.

For the case of the Al-3Li-10Be alloy in the peak aged and tensile tested condition, there are many Be particles as shown in Figure 11. The large α-Be particle in Figure 12 is of particular interest. The small precipitates on the α-Be particle could be small α-Be particles. This type of precipitate has previously been observed by Van Aken and Fraser[5] and by Tanner[6] in Al-Be binary alloys. The convergent beam electron diffraction pattern in Figure 12 is typical for this precipitate.

SUMMARY

Two low-density, high modulus aluminum-lithium-beryllium alloys (Al-3Li-2Be and Al-3Li-10Be by wt.%) have been produced by rapid

solidification via melt spinning. The alloys have been consolidated, heat treated to maximum strength and tensile tested. The mechanical properties of the alloys in the heat treated condition have been described. The microstructures of the alloys in each of the above conditions have been investigated using transmission electron microscopy. In the melt spun condition, the alloys contain fine δ′ particles (5-10 nm in diameter), some large α-Be particles (>100 nm), and a segregated dispersion of fine α-Be particles (5-50 nm) located on cell boundaries. After consolidation, and heat treatment, rather inhomogeneous structures were observed. Coarsening of the δ′ and coarsening and agglomeration of the α-Be particles is evident and precipitate free zones are observed at grain boundaries.

ACKNOWLEDGMENTS

This work was supported by the Lockheed Missiles and Space Company, Inc., Independent Research Program and the Office of Naval Research, Contract #N00014-84-C-0032. The authors wish to adknowledge the contributions of R. M. Harrington of the Lockheed Palo Alto Research Laboratory for the mechanical property test results.

REFERENCES

[1] A. E. Vidoz, D. D. Crooks, R. E. Lewis, I. G. Palmer, and J. Wadsworth, ASTM STP on Rapidly Solidified Al Alloys, In Press, 1985.

[2] J. Wadsworth, A. Joshi, D. D. Crooks, and A. E Vidoz, Jour. Mater. Sci., submitted for publication, 1985.

[3] J. C Ekvall, J. E. Rhodes, and G. C. Wald, ASTM STP 871, Amer. Soc. for Testing and Materials, Philadelphia, PA, 1982, p. 328.

[4] A. R. Pelton, F. C. Laabs, and J. Wadsworth, 21st Annual Electron Microscopy Colloquium, Iowa State University, Ames, IA, 1984, p. 28.

[5] D. C. Van Aken and H. L. Fraser, Acta Metall., 33, 1985, p. 963.

[6] L. Tanner, Unpublished Research, Lawrence Livermore National Laboratories, 1984.

[7] I. G. Palmer, R. E. Lewis, and D. D. Crooks, Proc. 1982 AIME Conf. on Aluminum Powder Metall., Dallas, TX, February 1982, p. 369.

[8] E. A. Starke, Jr., T. A. Sanders, Jr., and I. G. Palmer, J. Metals, 33, (8), 1981, p. 24.

[9] R. P. Elliot, Constitution of Binary Alloys, 1st Suppl., McGraw Hill, 1965, p. 65.

[10] J. Wadsworth, A. R. Pelton, and A. E. Vidoz, Int. Jour. Mater. Sci. Eng., submitted for publication, 1985.

[11] A. R. Pelton, work in progress, Ames National Laboratory, 1985.

[12] L. E. Tanner, L. Jacobson and R. Gronsky, Proc. 43rd Annual Meeting of EMSA, p. 50, San Francisco Press, Inc., Box 6800, San Francisco, Ca 49101, (1985).

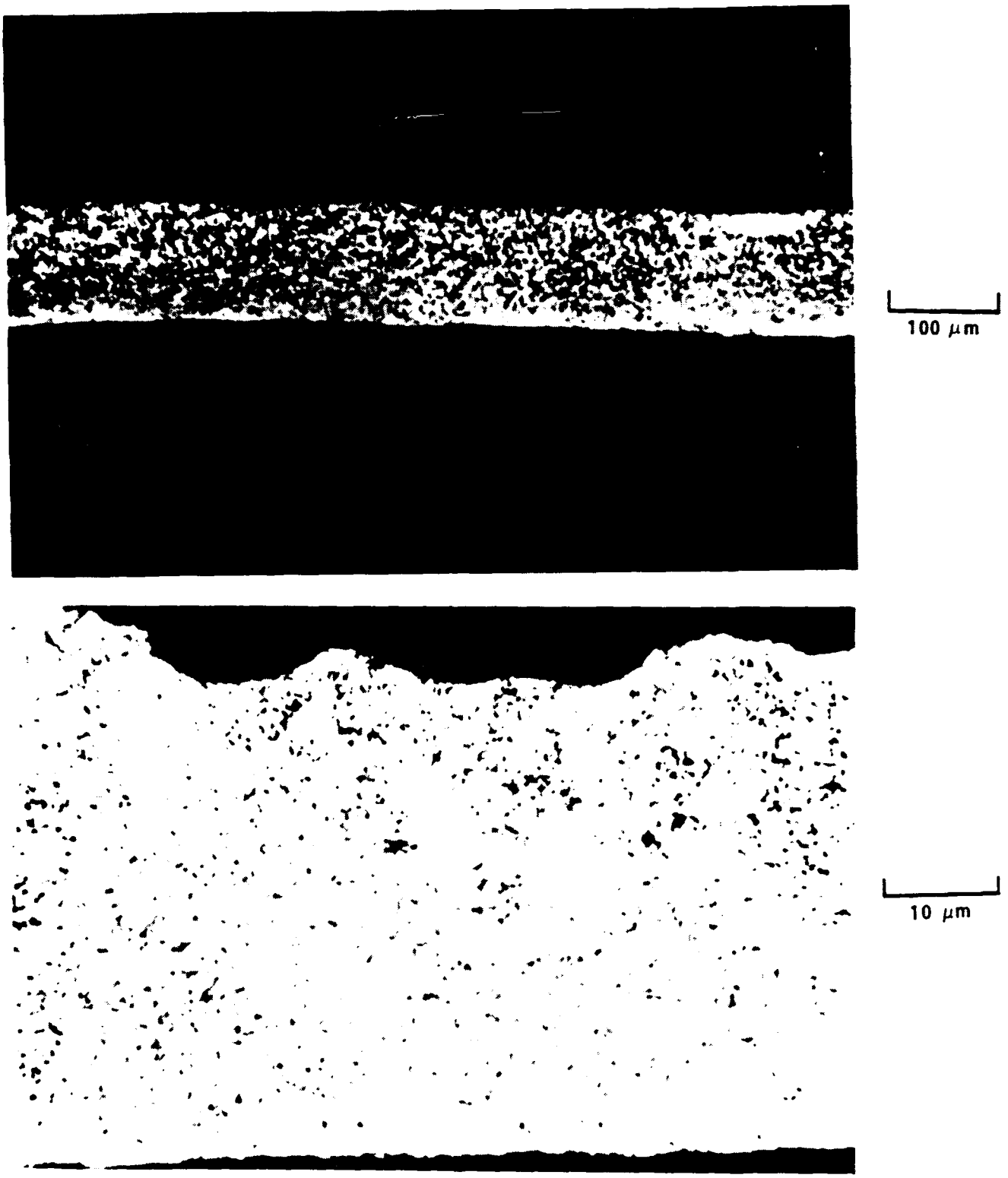

Fig. D1. Optical photomicrographs of the melt-spun Al-3Li-10Be alloy (contact surface is the lower surface in each case) at low (above) and high (below) magnifications in the etched condition.

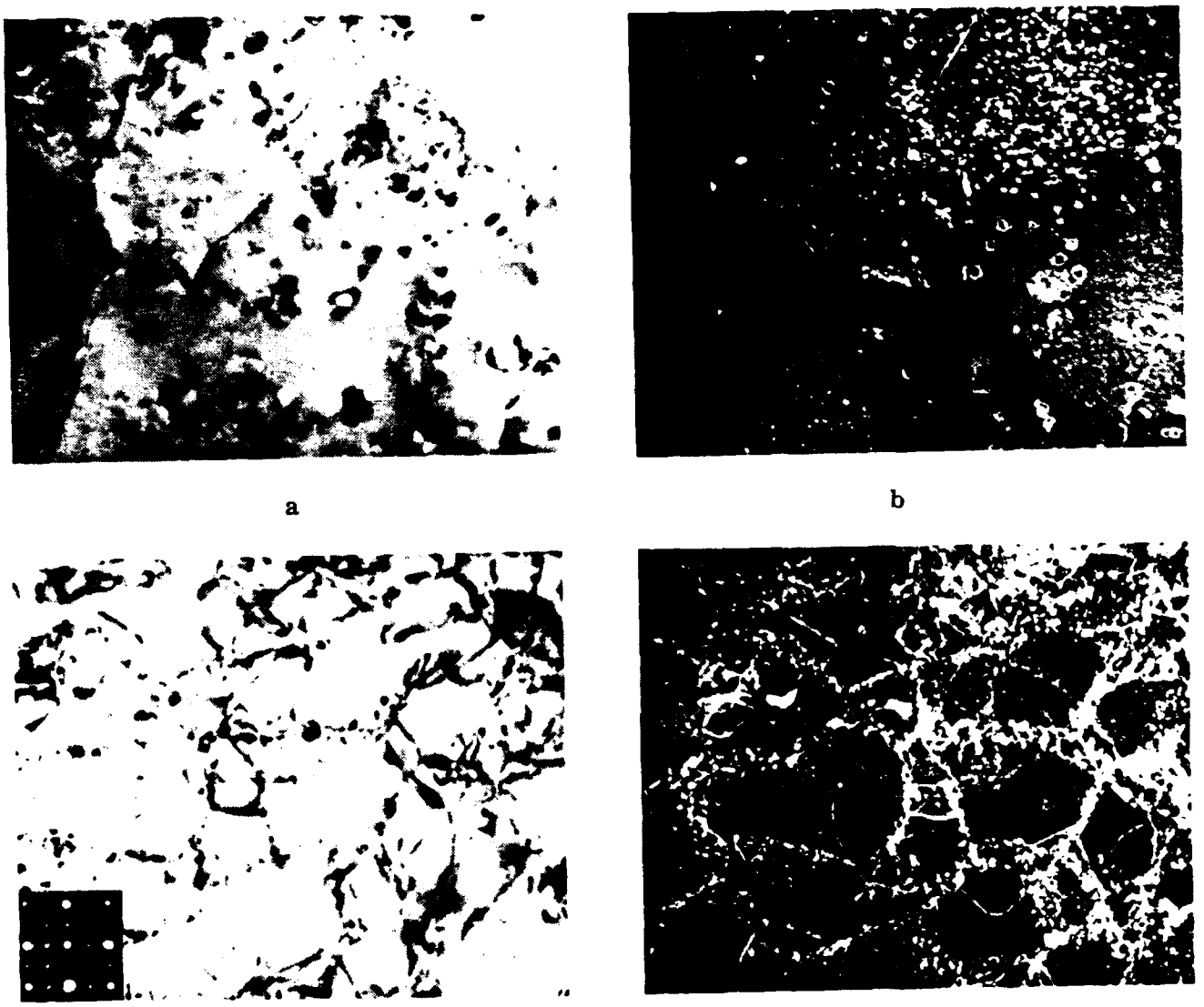

Fig. D2. I. (a) Bright field and (b) weak-beam dark field of Al-3Li-2Be ribbon.
II. (a) Bright field and 9b) weak-beam dark field of Al-3Li-10Be ribbon with inserted [001] diffraction pattern showing δ' reflection.

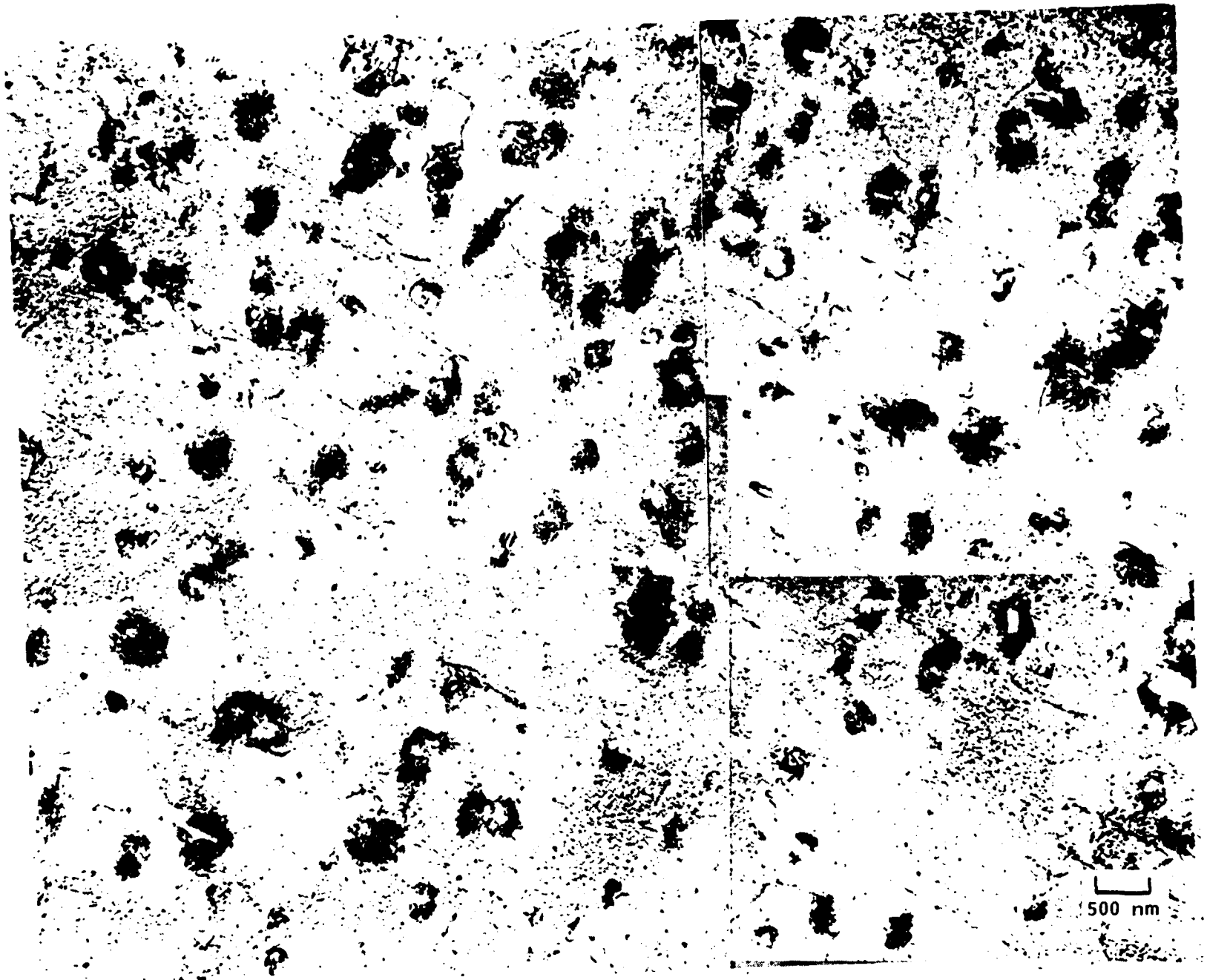

Fig. D3. Consolidated ribbon of Al-3Li-10Be alloy, extruded and heat treated to the T6 condition. This region shows a single crystal containing α-Be particles associated with intense deformation zones.

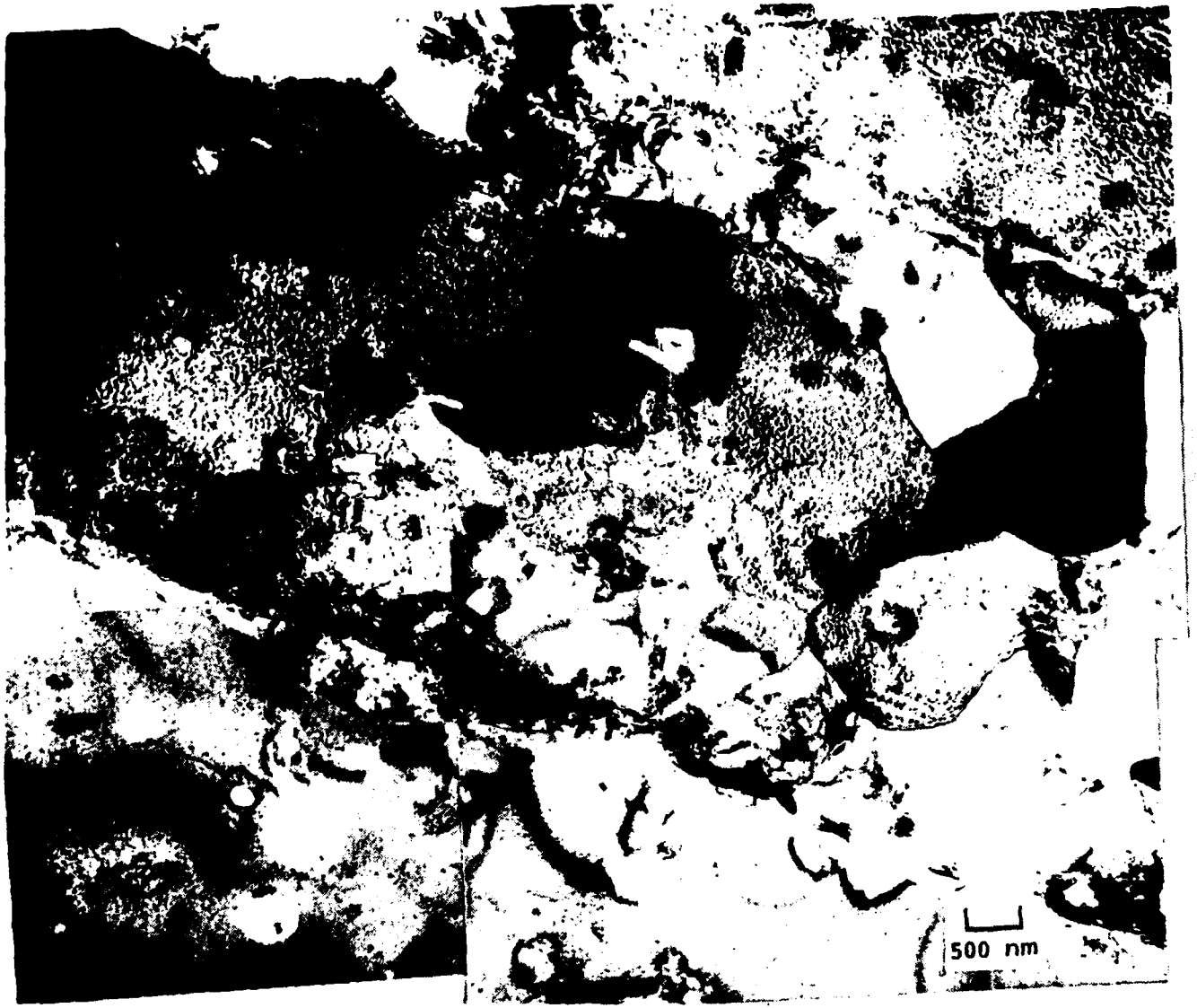

Fig. D4. Consolidated ribbon of Al-3Li-2Be alloy, extruded and heat trated to the T6 condition, but from a nearby region to that in Figure 3. In this case, elongated grains and subgrains are observed in addition to α-Be particles and deformation zones.

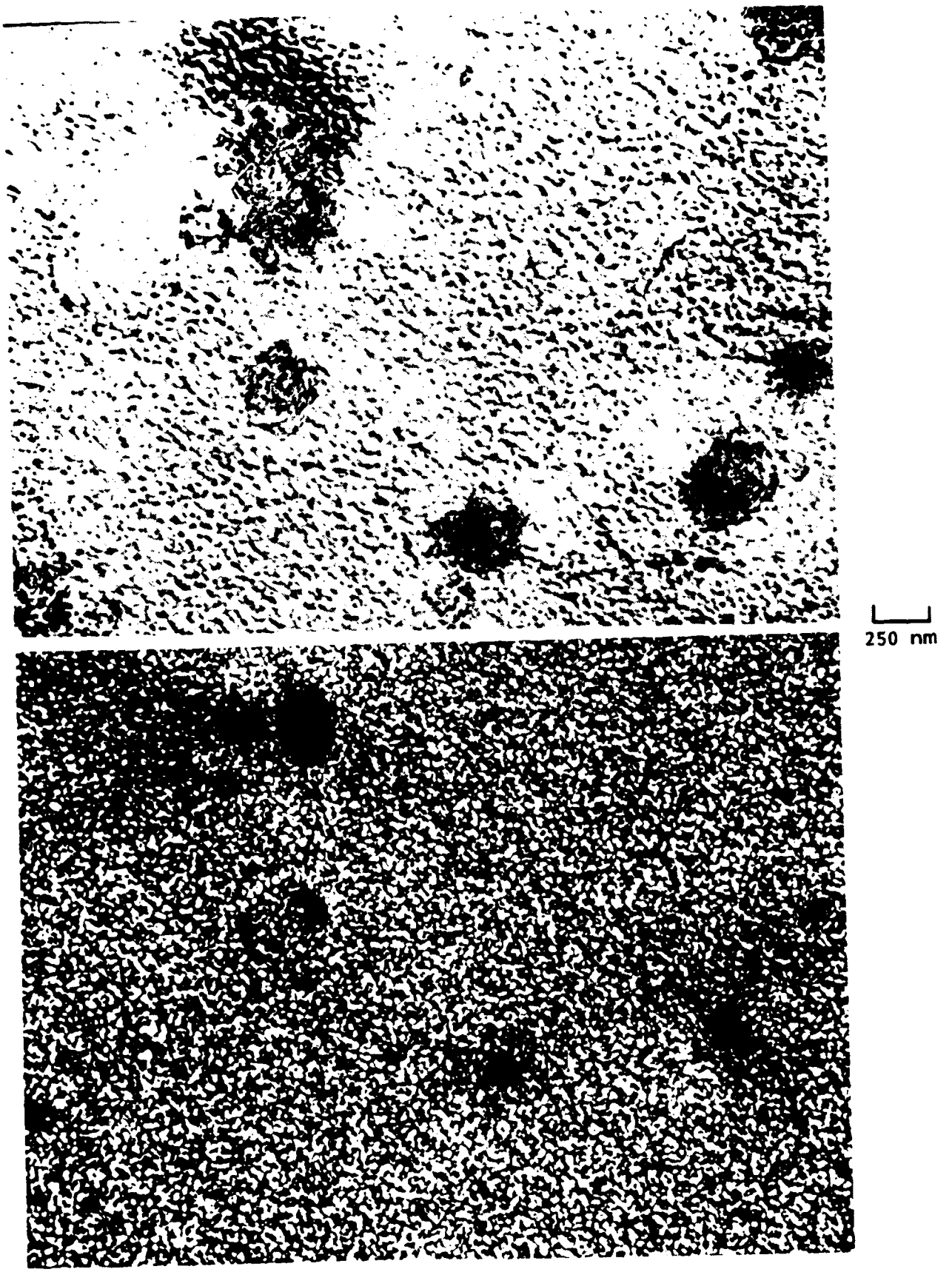

Fig. D5. BF/DF (δ′ reflection) pair of TEMs from the Al-3Li-2Be consolidated ribbon in both the extruded and heat treated to T6 conditions.

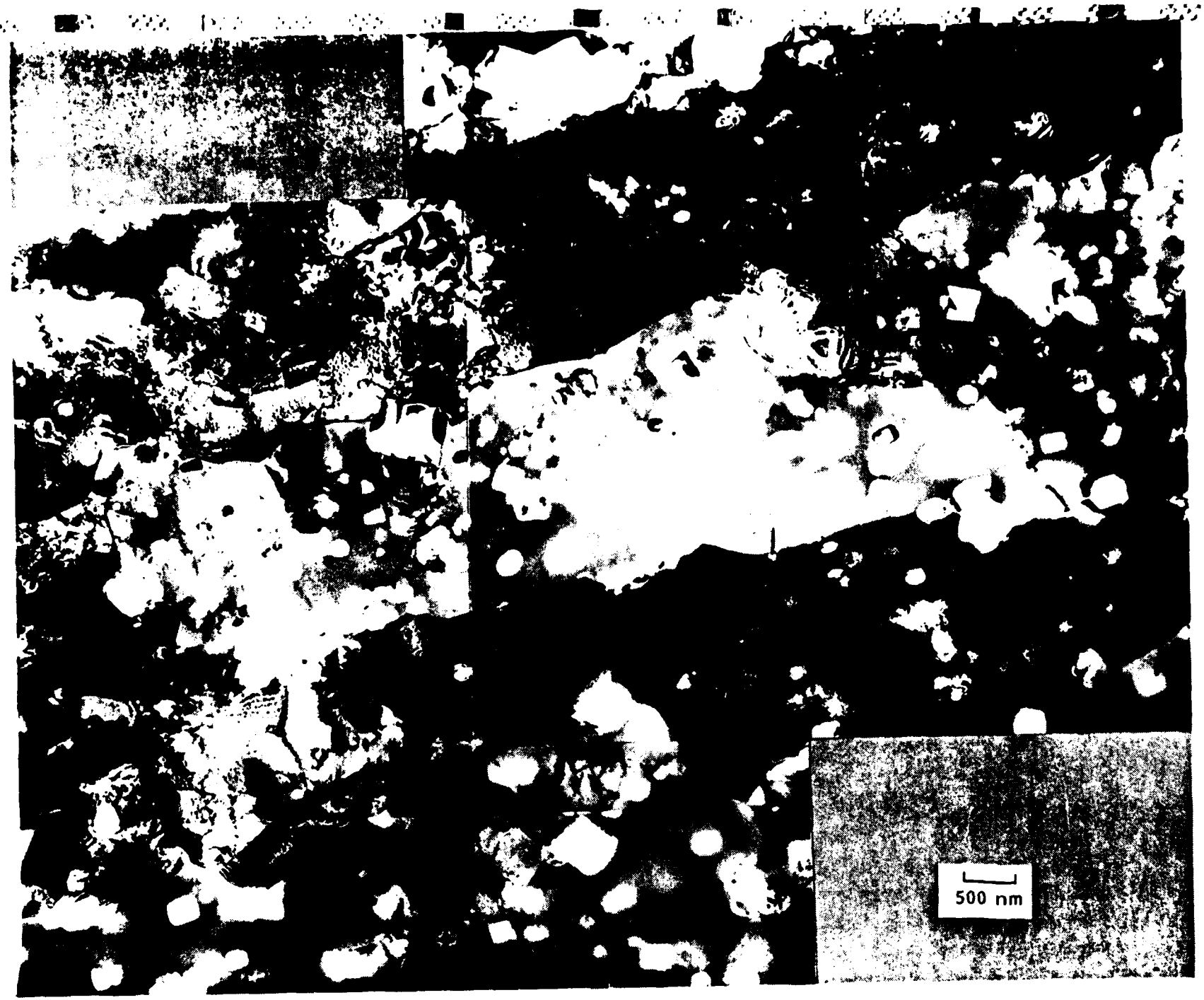

Fig. D6. TEM collage of the Al-3Li-10Be consolidated melt-spun ribbon in the extruded plus T6 heat treatment condition.

Fig. D7 Consolidated and heat treated Al-3Li-10Be alloy.

Fig. D8. Region from within Figure 7 showing agglomeration of small Be particles as a result of consolidation.

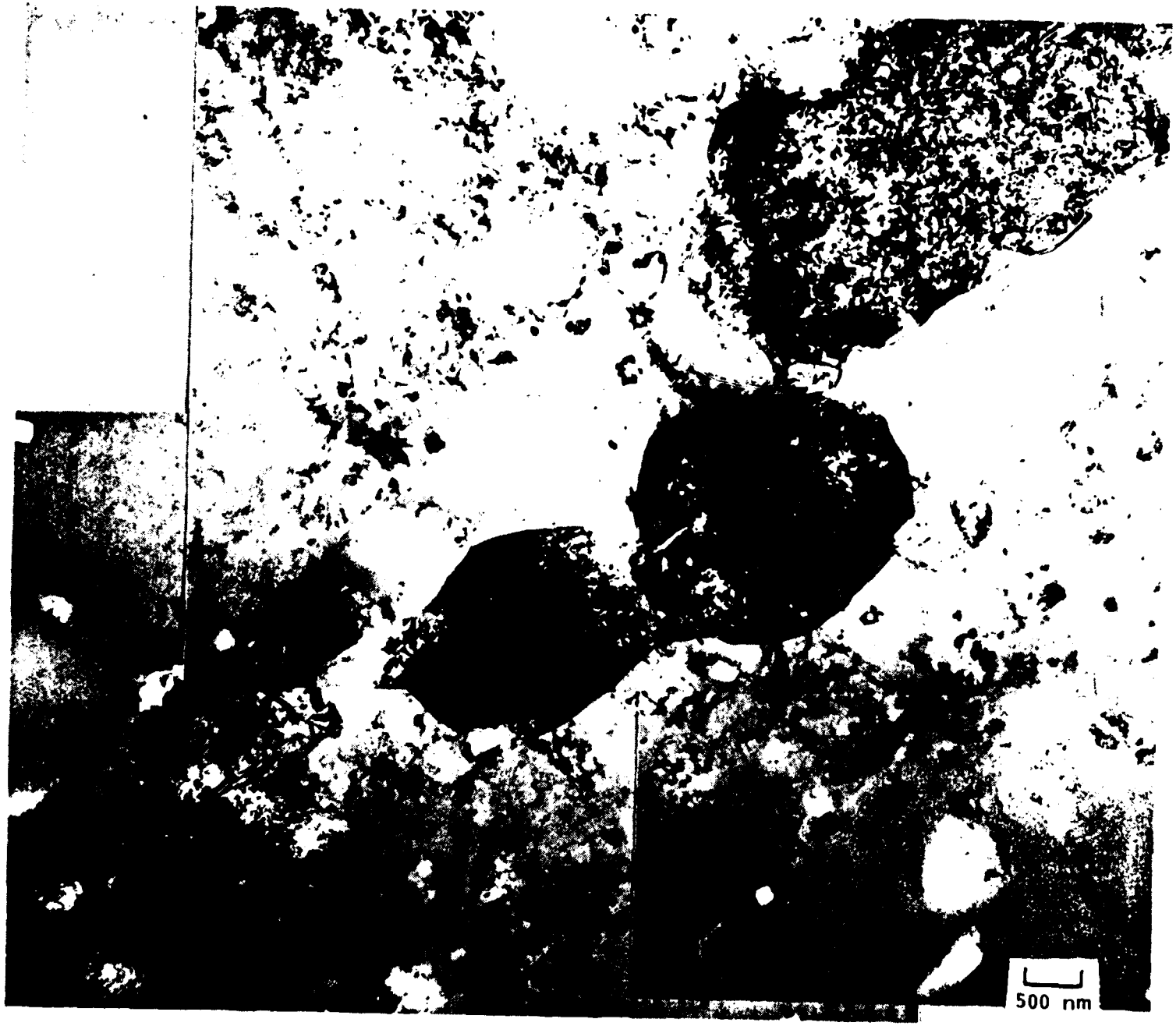

Fig. D9. Consolidated Al-3Li-2Be after tensile testing

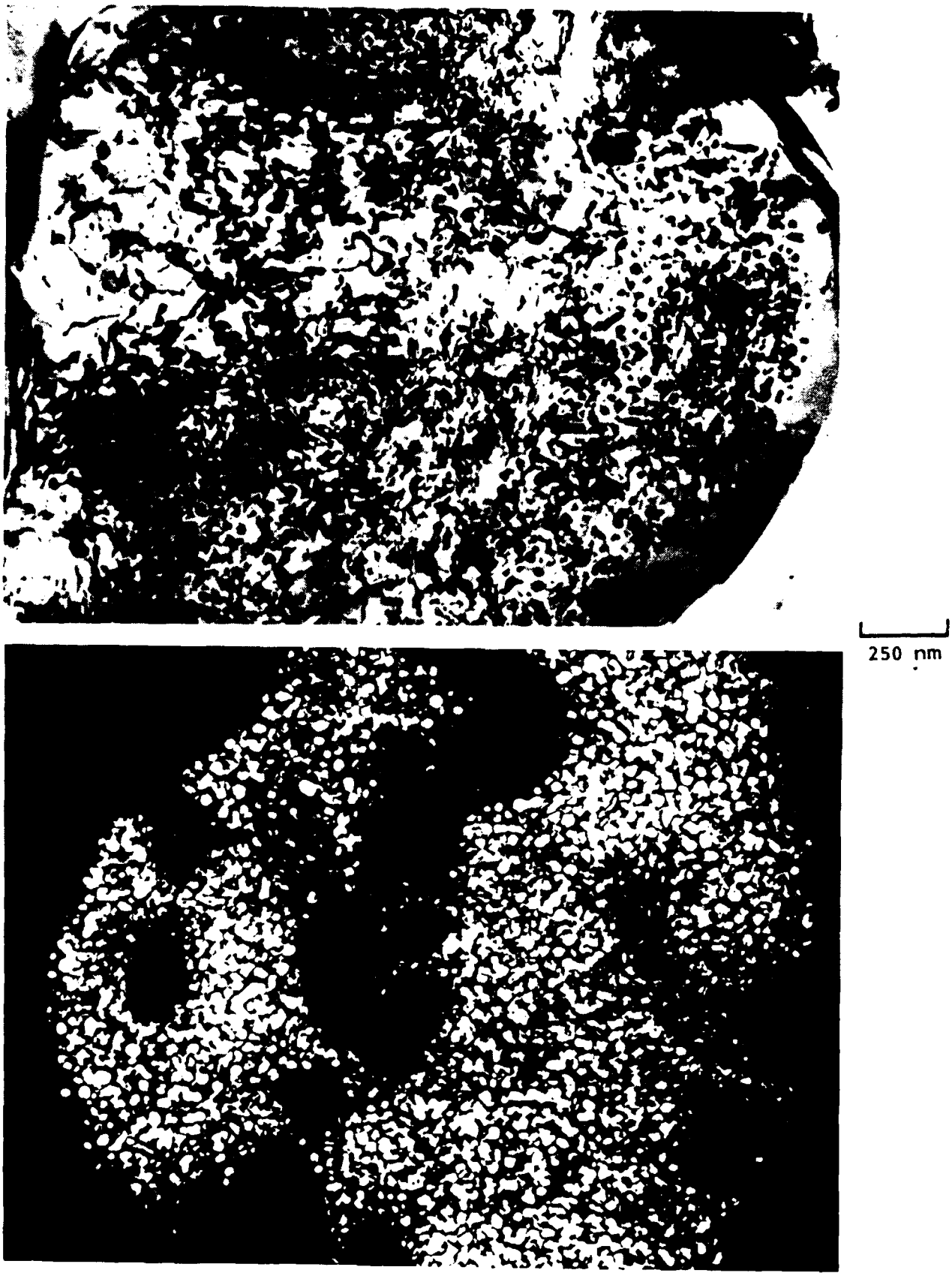

Fig. D10. BF/DF pair showing depleted region of δ' adjacent to grain boundaries and depleted regions within the grains of tensile tested Al-3Li-2Be alloy.

Fig. D11. Al-3Li-10Be consolidated alloy in the T6 condition after testing.

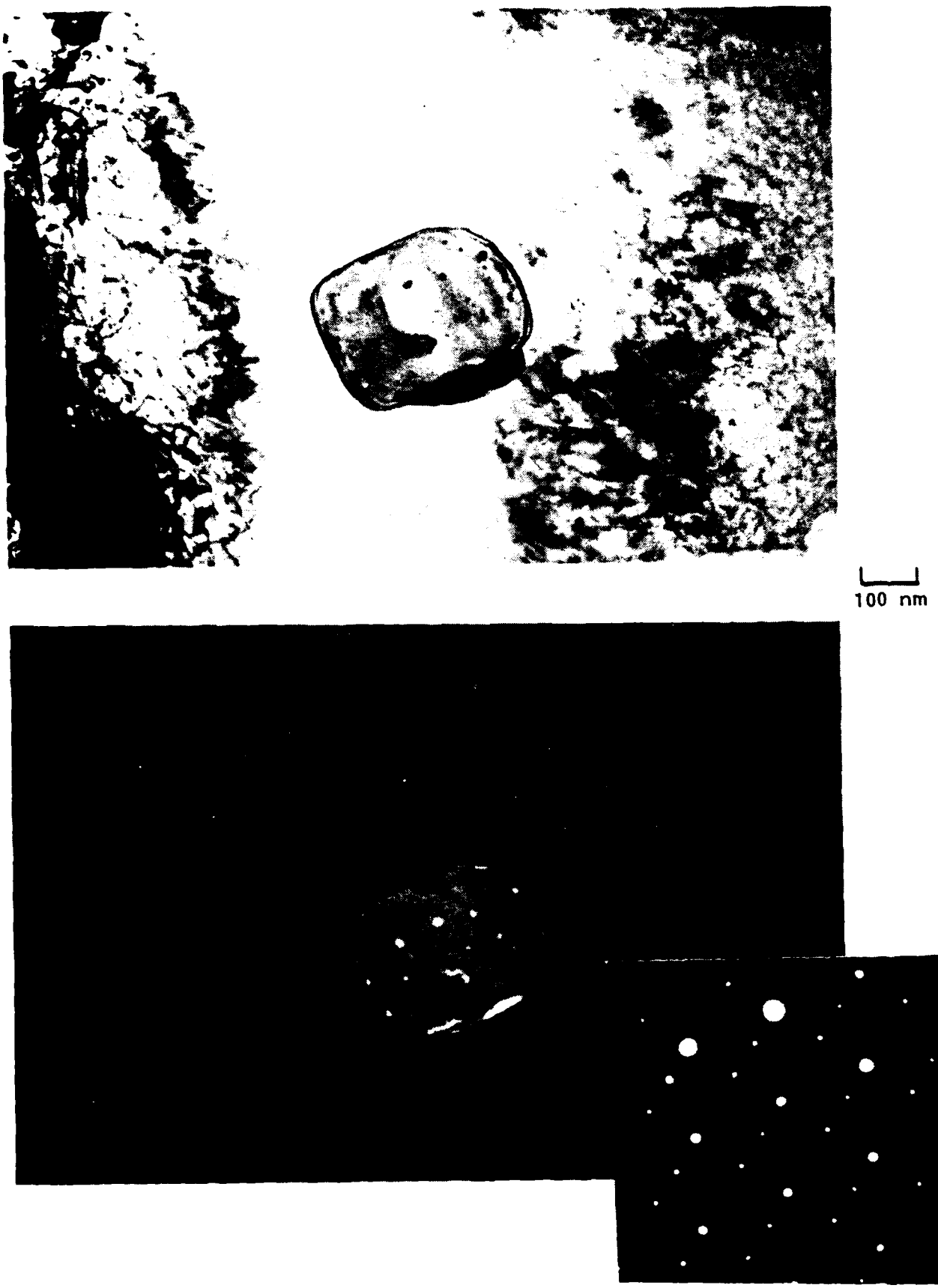

Fig. D12. BF/WBDF TEM pair showing small Be particles on an α-Be particle in the Al-3Li-10Be consolidated alloy. The convergent beam electron diffraction pattern is typical for this type of precipitation.

APPENDIX E

HIGH TEMPERATURE PROPERTIES OF RAPIDLY SOLIDIFIED Al-Be ALLOYS

T.G. Nieh, C.A. Henshall, and J. Wadsworth

Lockheed Palo Alto Research Laboratory
O/9310, B/204, 3251 Hanover Street
Palo Alto, CA 94304

Abstract

Rapidly solidified Al-Be binary alloys (10%, 20%,and 40% Be by weight) have been produced by melt spinning techniques. The microstructure, as well as the elevated temperature mechanical properties have been characterized over a range of strain rates. Despite the fact that the materials exhibited duplex microstructures, resulting from high-temperature processing, they showed behavior typical of dispersion strengthened alloys. The mechanical properties at elevated temperature can be accurately described by the equation $\dot{\varepsilon} = A (\sigma/E)^{12} \exp (- 126(kj/mol)/RT)$, where $\dot{\varepsilon}$ is the deformation rate, σ is the stress, E is the modulus, A is a material constant, and RT has is usual meaning. A direct comparison of the deformation properties was made between binary Al-Be composition and Al as baseline, as well as between Al-Be and some high temperature Al alloys. The Al-Be alloys do not exhibit good high temperature resistance, by comparison with other high-temperature Al alloys, e.g. Al-Fe-Ce alloy. This is a result of particle coarsening and agglomeration during processing and testing.

Introduction

Lithium and beryllium are the only two elemental additions to aluminum that can simultaneously increase the modulus and reduce the density. Aluminum-lithium alloys have been under extensive study recently because of their potential applications for

aerospace structures(1-3). In contrast, the Al-Be alloy system has not yet been thoroughly examined. This may be due, in part, to the difficult problems associated with the production of such compositions. However, the potential weight savings as a result of density deneure, and improvements in the elastic modulus, still make this alloy group worthwhile for evaluation.

A previous development known as Lockalloy(4), which had a composition of 38%Al-62%Be was once commmercially available; however, this is a Be-based alloy. Although aluminum-rich ternary alloys based on Al-Be-Mg have been evaluated by a number of researchers(5), the materials were either prepared by conventional powder metallurgy techniques or prepared by the chill casting technique. In this paper, Al-Be alloys prepared from melt spun ribbons are examined and their mechanical properties at elevated temperature are presented.

Experimental Procedure

Binary alloys of Al-Be were prepared by arc melting high purity ingot stock Al and electrolytic induction-melted Be stock. The arc-melted buttons were converted to melt-spun ribbon having the approximate dimensions of 1mm in width and less than 0.1 mm thickness. Melt spinning was carried out using an apparatus and techniques described elsewhere(6). The alloy ribbons were comminuted, hot pressed at 482C, and extruded at about 427C through a 20:1 reduction die with a 2:1 aspect ratio. The

extruded bar were further rolled down 70% to a sheet of final thickness 1.9 mm, from which the tensile coupons were machined.

Hardness measurements were carried out using either a conventional Rockwell machine or a Leitz miniload microhardness machine. Usually, five measurements were taken from each specimen. Elevated-temperature tensile tests were conducted with a conventional Instron machine controlled by a HP3497-based data acquisition system. A resistance heating furnace was used to bring the test specimen up to temperature. A preheat of approximately 45 min. was used to stablize the test temperature. All tests were carried out under conditions of constant true strain rate, ranging from $5x10^{-5}$ to 10^{-3} s^{-1}.

Microstructures and fracture surfaces were characterized using either optical metallography or scanning electron microscopy.

Results and Discussion

Microstructures of as-spun Al-Be ribbons are shown in Fig. 1. The microstructure of Al-10%Be is relatively fine and uniform and is similar to the microstructure observed in as-melt-spun Al-10%Be-3%Li (7). However, for both Al-20%Be and Al-40%Be alloys the microstructures can be clearly divided into two zones. The side which has a faster cooling rate has a much finer microstructure as compared to the other side. The dual microstructure observed in the materials with high Be content is

a result of the poorer thermal conductivities in those materials as compared to that in the 10%Be material. The contrast of the dual microstructure in the as-melt-spun ribbons becomes more apparent as the Be content of the alloy increases. In the case of Al-40%Be alloy, the Be particle size in the slow cooling zone in the ribbon is as coarse as 1-2 μm.

Differential scanning calorimetrical analyses from the as-melt-spun Al-Be ribbons do not show any exothermic or endothermic activity prior to the melting of the ribbon. This is consistent with the fact the there are no stable intermetallic compounds between Al and Be. It may further suggest that a metastable Al-Be compound either does not exist or the thermodynamic free energy of formation of such a compound is too low to be measured by the equipment used.

The microstructures of the Al-Be alloys after consolidation and extrusion are shown in Fig. 2. It is noticed that all of the compositions show irregular banded structures (coarse and fine) and Be particles are heterogeneously distributed. The band width for the coarse structure ranges from 20 to 100μm. Despite the fine dispersion of Be in the fine zone, in the coarse zone the Be particle size are nonuniform and sometimes as large as 10 μm. In the case of Al-40%(49.3vol.%)Be, because of the very large Be content, even continuous networks of Be form in the coarse zones. As mentioned earlier, the consolidation and extrusion temperatures are 482 and 427°C respectively. Apparently, the

consolidation temperature was sufficiently high to cause Be particles coarsened and the microstructure partially recrytallized. The recrystallized areas were subsequently elongated during extrusion. This resulted in the duplex microstructure. It should be noted that the size of the coarse zones in the extrudate is not related to the dimension of the coarse zone observed in the original as-spun ribbon. The microstructural coarsening during consolidation suggests that particles are not effective grain refiners for Al alloys. The coarsening is due to fast diffusion of Be in Al, as will be discussed later.

The mechanical properties of the two microstructural zones are also different, as expected. For example, the microhardness value (HV) for Al-10%Be in the fine zone is consistently about HV 66, however, for the coarse zone it ranges only from HV 30 to 50, depending on the exact Be distribution in that particular zone. For Al-40%Be, because of the higher Be content, hardness numbers are higher and are HV 160 and 80 for the fine and coarse zones, respectively.

Despite the prior high temperature thermal exposure, the microstructure of the extruded binary alloys still appears to be unstable in subsequent lower temperature exposure. Fig. 3 is the room temperature hardness measurements for both Al-10%Be and Al-20%Be that have been exposed to elevated temperatures for 1h. It is a general trend that the hardness for both materials decreases

continuously as the exposure temperature increases. The relative amount of reduction in hardness, especially for the Al-10%Be alloy, is difficult to account for by simply assuming that the softening can be attributed to dislocation annihilation during the thermal exposure. The softening behavior more likely may be a direct result of microstructural coarsening; in particular, the coarsening of Be particles at elevated temperatures. This is consistent with the fact that the relative amount of reduction in hardness is less for materials with a high Be content. In fact, for Al-40%Be, the hardness values for as-extruded and as-extruded-and-then-thermally-annealed materials are almost identical. For a material that has a higher Be content, the Be particle size is always coarser than for the Be contents. The particle coarsening rate is expected to be slower in such a material by comparison with an alloy that initially contains a finer particle dispersion. Because of the duplex nature of the microstructure, it is very difficult to directly measure the coarsening rate of the Be dispersion. However, microhardness measurements from an Al-10%Be sample show that the hardness values in the fine zone reduce from HV67 for the as-extruded condition to HV61 for the material that has been further exposed at 232°C for 30 min.

Although the room temperature mechanical properties for Al-Be alloys have been characterized elsewhere(8), their tensile properties at elevated temperatures have not been evaluated. A summary of the tensile data from 121 to 232°C is shown in Table 1

for both Al-10%Be and Al-20%Be alloys. Both alloys are ductile and have elongations to failure, typically, of 40 to 50%. The tensile stress-strain curves normally exhibit a steady-state type behavior near the end of the tensile test. The values of the flow stress are tabulated in Table 1. In general, the flow stress increases with the strain rate and decreases with the temperature. Also, the Al-20%Be alloy is stronger than Al-10%Be under the same test conditions. A log-log plot of the strain rate versus flow stress is shown in Fig. 4 for Al-20%Be. As shown in the figure, the stress exponent, n, in the equation $\dot{\varepsilon} = k\sigma^n$ where $\dot{\varepsilon}$ is the strain rate, σ is the flow stress, and k is a constant, is approximately equal to 12. Although it is not shown in the figure, the n value for Al-10%Be is also a constant and equal to 12. For pure Al, the n value is between 4 and 5 (9,10). The high stress exponent is a typical characteristic for dispersion strengthened materials (11,12) and some metal matrix composites(13). The stress exponent behavior in Al-Be is to be expected since Be is virtually insoluble in solid Al and the Be particles act as dispersoids in an Al matrix. In addition, the Be dispersoids are essentially non-deformable under the test conditions used in this study.

It was mentioned earlier that the alloys contain a duplex microstructure. However, when the material is subject to mechanical loading along the longitudinal direction, i.e., the direction which exhibits the elongated grain structure, both banded structures are under isostrain conditions. In this case,

the fine-zone area, which exhibits a higher mechanical strength than that of the coarse-zone area will dominate the deformation behavior of the material. This is particularly true in the present case, since the volume ratio for the coarse-zone volume fraction is estimated to be less than 20%.

The activation energy for the high temperature deformation for both Al-10%Be and Al-20%Be was calculated to be approximately 126kJ/mol, which is comparable to 138kJ/mol, the activation energy for self diffusion of Al(14,15). This result suggests that the deformation process is probably controlled by a dislocation-climb-like mechanism(16). Similar results have been reported in a number of other materials(17).

In summary, the deformation behavior of Al-Be alloys at elevated temperature can be well described by the equation

$$\dot{\varepsilon} = A\ (\sigma/E)^{12}\ \exp(-Q/RT)$$

where $\dot{\varepsilon}$ is the deformation rate, σ is the flow stress, Q is the activation energy for the deformation, and A is a material constant. The values of A are 2.5×10^{50} m^{-2} and 7×10^{47} m^{-2} for the Al-10%Be and Al-20%Be alloys, respectively. A summary of the normalized data plotted as $\log(\dot{\varepsilon}/D)$ versus $\log(\sigma/E)$ is shown in Fig. 5. The correlation between the data and the equation is reasonably good. In order to make a direct comparison, the creep data for pure Al(9,10) is also displayed in the same figure.

Although Al-Be alloys are much stronger than Al, it is misleading to consider Al-Be alloys as a high temperature alloy from the data of this figure. For example, the high temperature Al-8%Fe-4%Ce alloy exhibits a strength of 350 MPa at 230°C. For the Al-20%Be alloy the strength is only approximately 110 MPa under the same conditions(18). Even on a density-compensated basis, the strength for Al-Be is still far too low to compete with other high-temperature aluminum alloys(18).

The fracture surface of a detrated tensile tested sample, as shown in Fig. 6, in general, shows dimpled type features, indicating ductile fracture. This is consistent with the result that all test samples exhibited good tensile elongation-to-failure. It is interesting to note that the fracture surface also shows a duplex feature, as does the optical microstructure discussed earlier. The average dimple spacing for the fine zone is about 3 μm, while it is nearly 8 μm for the coarse zone. It is also noted that fracture of the samples almost invariably originated from a coarse zone or a coarse Be particle.

Conclusion

Rapidly solidified Al-Be binary alloys have been produced. A duplex microstructure has been observed in those alloys which was due to fast coarsening of Be particles during the consolidation and extrusion processes. The mechanical behavior of those alloys has also been characterized at temperatures between 121 and 232C.

The stress exponent was measured to be about 12 and the apparent activation energy for the tensile deformation was calculated to be 126 kJ/mol, which is close to the activation energy for self diffusion in Al. In general, the alloys behave like a conventional dispersion strengthened alloy. Although binary Al-Be alloys appear to be much stronger than Al itself, these alloys do not exhibit the high temperature resistance by comparison to with high-temperature Al alloys, e.g. Al-Fe-Ce. This is primarily due the relatively fast coarsening of Be in Al matrix at elevated temperature which leads to coarsening of the Be phase.

Acknowledgement

The authors would like to thank Mr. D.D. Crooks and Ms. W.C. Thomas for manufacturing the alloys and carrying out most of the mechanical tests. This work was supported by the Office of Naval Research under Contract N00014-84-C-0032.

References

1. T.H. Sanders, Jr., and E.A. Starke, Jr., eds., "Aluminum-Lithium Alloys," The Metallurgical Society of AIME, Wareendale, PA, (1981).

2. T.H. Sanders, Jr., and E.A. Starke, Jr., eds., "Aluminum-Lithium Alloys II," The Metallurgical Society of AIME, Wareendale, PA, (1984).

3. C. Baker, P.J. Gregson, S.J. Harris, and C.J. Peel, "Aluminum-Lithium Alloys III," The Institute of Metals, London, (1986).

4. R.W. Fenn, Jr., D.D. Crooks, W.C. Coons, and E.E. Underwood, Properties and Behavior of Beryllium-Aluminum Alloys in: "Beryllium Technology," Vol. 1, (L. McD. Schetky and H.A. Johnson, eds.), pp. 198-143, AIME Metallurgical Society Conf., Vol. 33, Gordon and Breach, New York (1966).

5. D.R. Floyd and J.N. Lowe, eds., "Beryllium Science and Technology," Vol. 2, p. 307, Plenum Press, New York, (1979).

6. A.E. Vidoz, D.D. Crooks, R.E. Lewis, I.G. Palmer, and J. Wadsworth, "Rapidly Solidified Powder Aluminum Alloys," M.E. Fine and E.A. Starke, eds., ASTM STP No. 890, Amer. Soc. for Testing of Materials, Philadelphia, PA, 1986.

7. J. Wadsworth, A.R. Pelton, D.D. Crooks, R.E. Lewis, and A.E. Vidoz, J. Mater. Sci. 1986, In Press.

8. R.E. Lewis, "Feasibility of Ultra-Low Density of Aluminum Alloy," Progress Report for June-September 1985, Naval Air Development Contract No. N62269-84-C-036.

9. I.S. Servi and N.J. Grant, Trans. AIME, Vol. 191, (1951), 909.

10. H. Luthy, A.K. Miller and O.D. Sherby, Trans. AIME, Vol. 233, (1965), 1116.

11. W.C. Oliver and W.D. Nix, Acta Metall., Vol. 30, (1982), pp 1335-1347.

12. A.H. Clauer and N. Hansen, Acta Metall., Vol. 32, (1984), pp. 269-278.

13. T.G. Nieh, Metall. trans., Vol. 15A, (1984), pp. 139-146.

14. T.S. Lundy and J.K. Murdock, J. Appl. Phys. 33, 1971 (1962).

15. M. Beyeler and Y. Adda, J. Phys. 29, 345 (1968).

16. G.S. Ansell and J. Weertman, Trans. AIME, Vol. 215, (1959), 838.

17. T.G. Nieh and W.D. Nix, Acta Metall., Vol. 28 (1980), 557.

18. C.M. Adam and R.E. Lewis, "Rapidly Solidified Crystalline Alloys," S.K. Das, B.H. Kear, and C.M. Adam, eds., pp. 157-183, The Metallurgical Soc. of AIME, Warrendale, PA, (1986).

TABLE I
STEADY-STATE DEFORMATION PROPERTIES
OF Al-10% Be and Al-20% Be

Alloy Composition	Temperature (°C)	Stress (MPa)	Strain Rate (s^{-1})	Elongation (%)	$\dot{\varepsilon}/D$ (m^{-2})	σ/E (10^3)
Al-20%Be	121	187.4	1×10^{-3}	32.4	3.03E18	2.93
Al-20%Be	177	148.1	1×10^{-3}	41.3	3.85E16	2.39
Al-20%Be	232	109.3	1×10^{-3}	39.7	1.35E15	1.84
Al-20%Be	288	69.0	1×10^{-3}	123.8	9.09E13	1.22
Al-20%Be	121	164.1	1×10^{-3}	36.3	3.03E17	2.56
Al-20%Be	149	143.8	1×10^{-4}	41.9	2.94E16	2.28
Al-20%Be	177	123.5	1×10^{-4}	57.3	3.85E15	1.99
Al-20%Be	232	80.3	1×10^{-4}	75.5	1.35E14	1.35
Al-20%Be	288	40.1	1×10^{-4}	102.8	9.09E12	0.71
Al-20%Be	121	154.7	5×10^{-5}	22.9	1.52E17	2.42
Al-20%Be	177	113.2	5×10^{-5}	42.6	1.92E15	1.83
Al-20%Be	232	69.3	5×10^{-5}	62.7	6.76E13	1.16
Al-10%Be	121	145.4	1×10^{-3}	31.5	3.03E18	2.27
Al-10%Be	177	93.6	1×10^{-3}	53.0	3.85E16	1.51
Al-10%Be	232	71.8	1×10^{-3}	69.1	1.35E15	1.21
Al-10%Be	177	70.3	1.3×10^{-4}	61.4	53E15	1.13
Al-10%Be	121	143.2	1×10^{-4}	37.2	3.03E17	2.24
Al-10%Be	129	109.3	1×10^{-4}	43.9	1.49E17	1.71
Al-10%Be	149	96.1	1×10^{-4}	47.9	2.24E16	1.52
Al-10%Be	177	85.5	1×10^{-4}	51.6	3.85E15	1.38
Al-10%Be	232	60.4	1×10^{-4}	73.8	1.35E14	1.01
Al-10%Be	121	110.2	5×10^{-5}	38.9	1.52E17	1.72
Al-10%Be	177	71.9	5×10^{-5}	64.9	1.92E15	1.16
Al-10%Be	232	50.1	5×10^{-5}	82.5	6.76E13	2.27

AD-A171 624 FUNDAMENTAL STUDIES ON THE ALUMINUM-LITHIUM-BERYLLIUM ALLOY SYSTEM(U) LOCKHEED MISSILES AND SPACE CO INC PALO ALTO CA RESEARCH AND D.. J WADSWORTH ET AL. AUG 86 2/2

UNCLASSIFIED LMSC-D067295 N00014-84-C-0032 F/G 11/6 NL

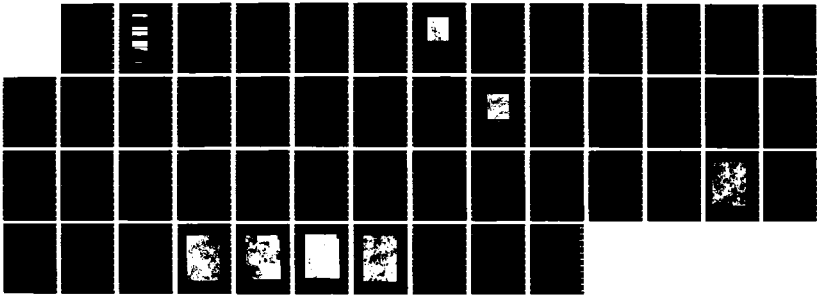

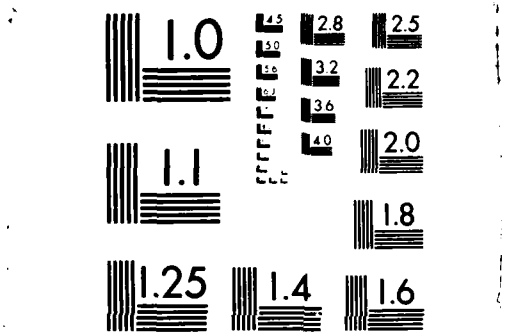
1.0
1.1
1.25
1.4
1.6
1.8
2.0
2.2
2.5
2.8
3.2
3.6
4.0

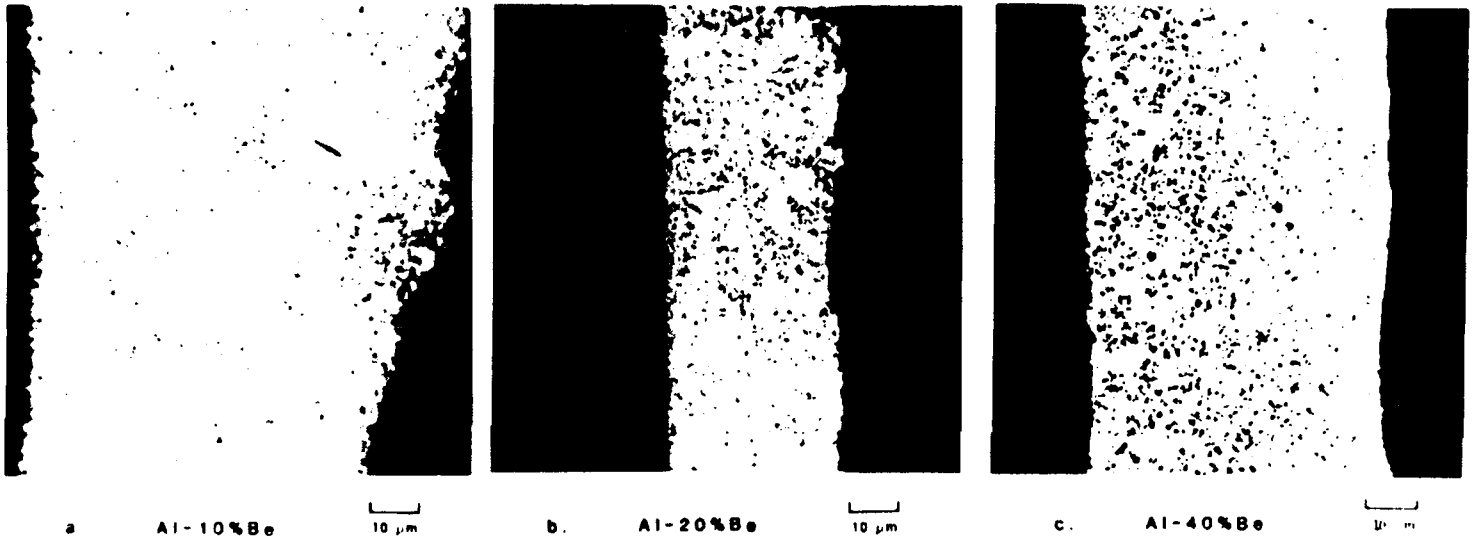

Fig. E1. Microstructures of as-spun Al-Be ribbons. Large α-Be particles are occasionally present in the Al-20%Be and Al-40%Be ribbons.

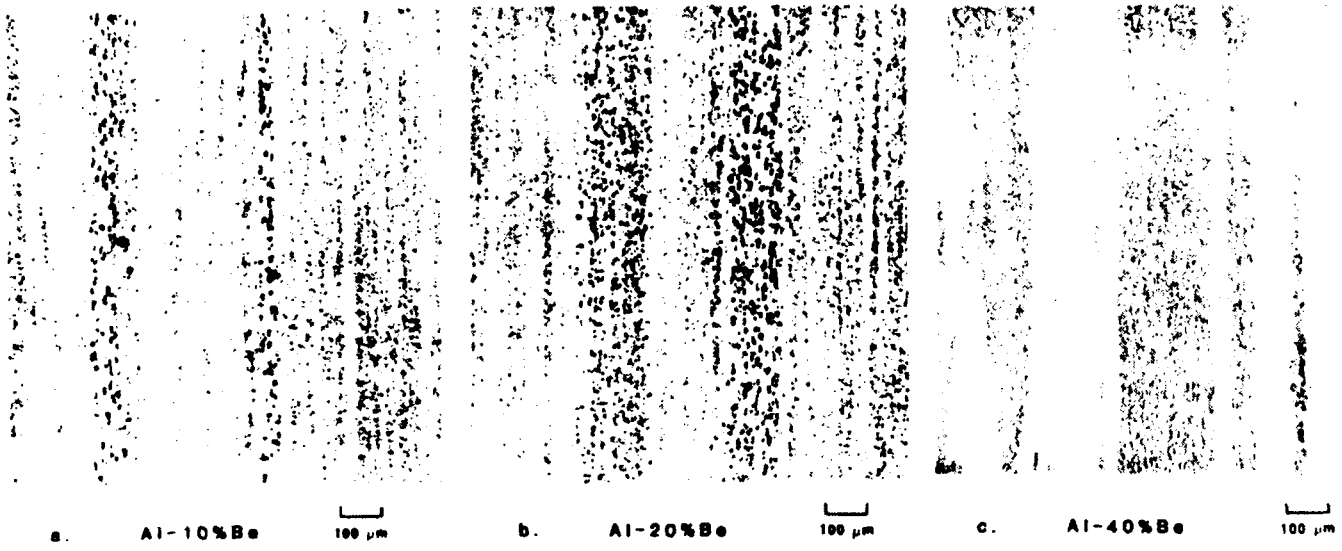

Fig. E2. Microstructures of as-extruded Al-Be alloys. The microstructures consist of a banded structure containing coarse and fine zones. The Be phase forms a continuous network in the coarse zone in the Al-40%Be slloy.

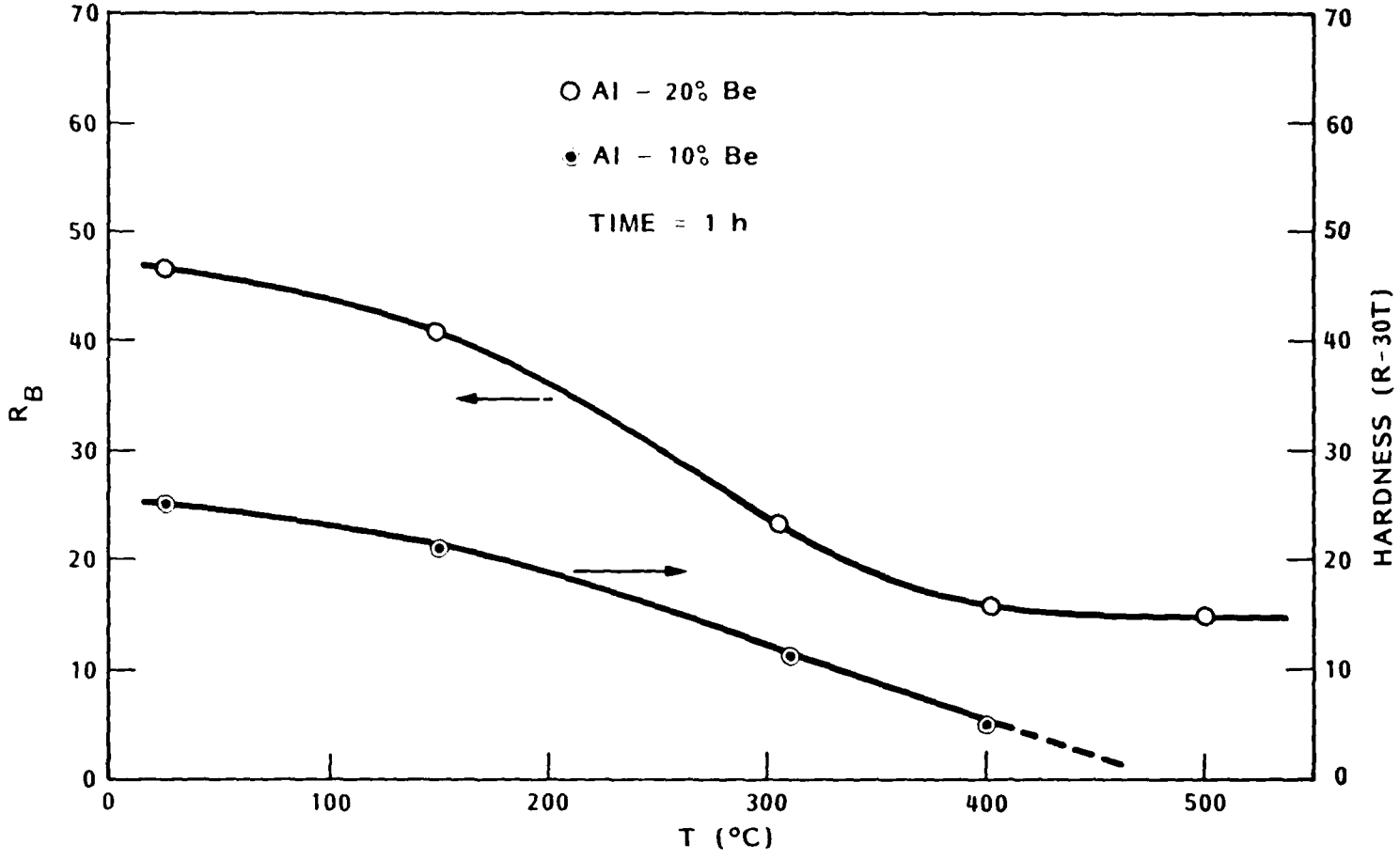

Fig. E3. Softening behavior of Al-10%Be and Al-20%Be alloys that have been annealed at elevated temperatures for 1h.

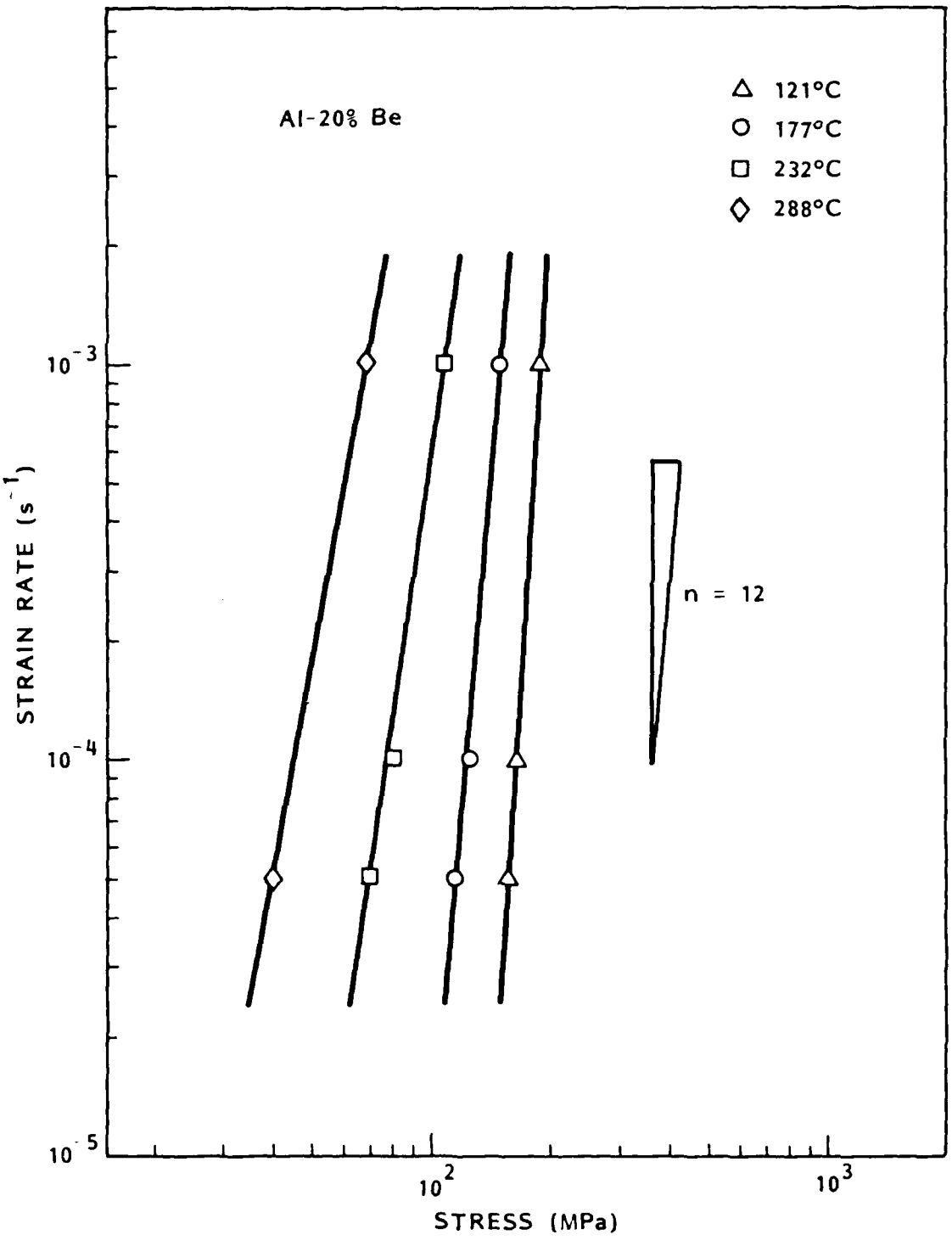

Fig. E4. Strain rate as a function of flow stress for Al-20%Be at elevated temperatures. The stress exponent, n, is approximately equal to 12.

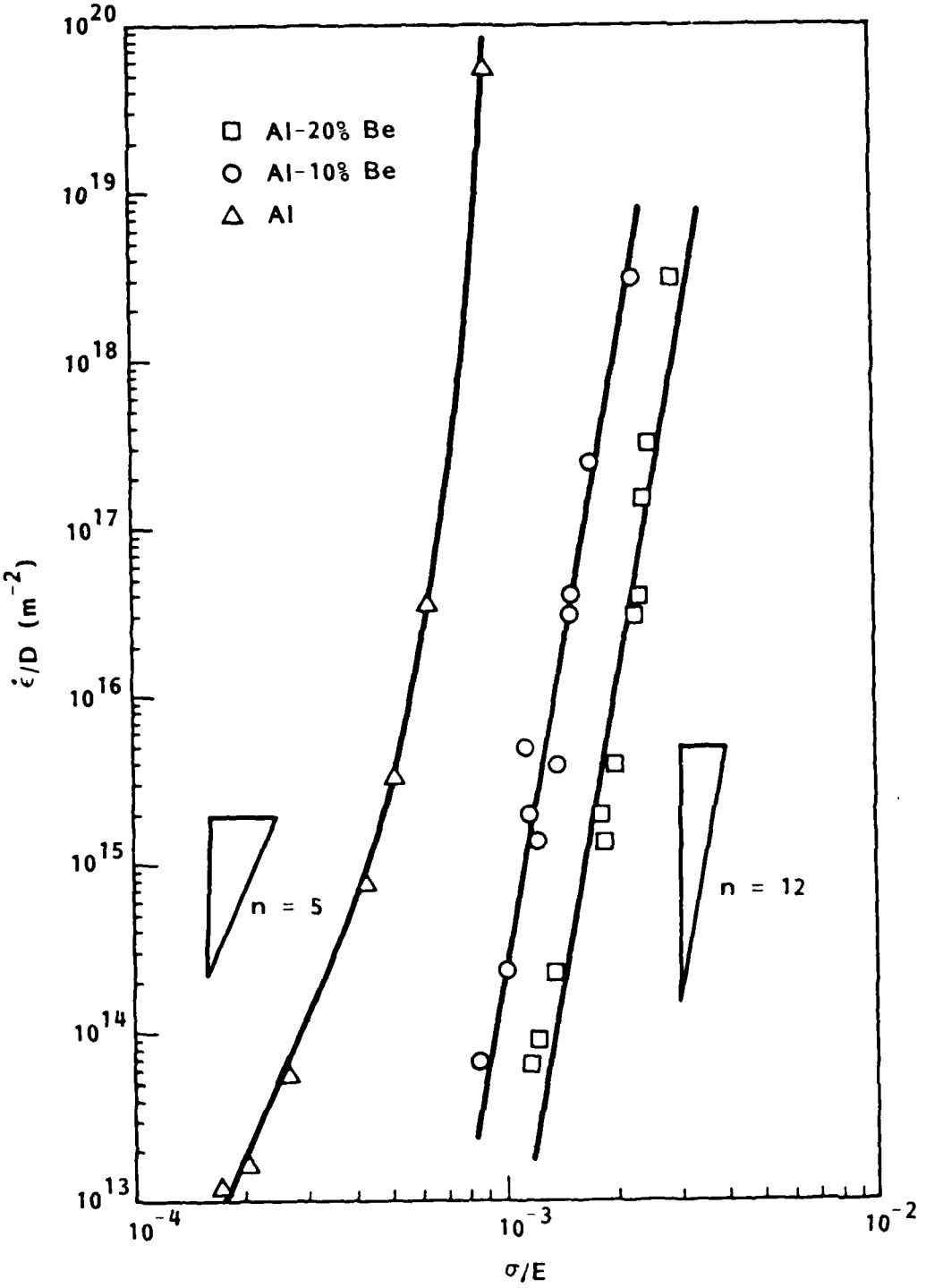

Fig. E5. Log ($\dot{\epsilon}/D$) vs. log (σ/E)plot for Al-10%Be, Al-20%Be. The data for pure Al (9,10) are also included in the figure for a direct comparison. Both Al-Be alloys are much stronger than pure Al. The high stress exponent at a high stress regime for pure Al represents power law breakdown.

Fig. E6. Typical dimpled, ductile fracture in Al-Be alloys.

APPENDIX F

MECHANICAL PROPERTIES OF A RAPIDLY SOLIDIFIED Al-10%Be-2%Li ALLOY AT ELEVATED TEMPERATURES

T. G. Nieh and J. Wadsworth

Lockheed Palo Alto Research Laboratory
Metallurgy Laboratory
3251 Hanover Street
Palo Alto, CA 94304

INTRODUCTION

Lithium and beryllium are the only two elemental additions to aluminum that can increase the modulus and reduce the density simultaneously. Lithium does so by forming the δ' phase with aluminum and beryllium does so by dispersion of α particles in the aluminum matrix, since beryllium has negligible amount of solid solubility in aluminum. Despite the fact that the multi-alloyed Al-Li system has been studied extensively(1-3), there is very limited study that has been carried out with the Al-Be-Li ternary system. It may be, in part, due to the toxic hazard associated with the handling of Be. Another reason is that the material has to be produced by rapid solidification in order to avoid segregation effect. It poses some technical difficulties in controlling the chemical composition in the melt while actually making such an alloy, since the melting point for Be is almost the same as the boiling point for Li. However, the potential weight saving and the improvement in the elastic modulus make such alloys very attractive for many aerospace structural applications.

Recently, rapidly solidified Al-Be-Li alloys have been produced and their room temperature properties have also been characterized(4). For example, Al-10% Be-3% Li(percentage by weight) shows nearly a 40% improvement in the specific modulus over conventional aluminum alloys, while still exhibits tensile strength of 520 Mpa and a tensile elongation of 4%. Such an alloy

is expected to show high temperature strengthening due to fine Be dispersion by rapid solidification. It is the purpose of this study to evaluate and characterize the high temperature properties of such an alloy.

EXPERIMENTAL PROCEDURE

Al-10%Be-2%Li(percentage by weight) were produced by arc melting high purity stock Al, high-purity, battery-grade Li and electrolytic induction melted Be stock. The arc melted buttons were converted to melt spun ribbon of approximate dimension 1 mm in width and less than 0.1 mm thickness. Melt spinning was carried out using an apparatus and techniques described elsewhere(4). The alloy ribbons were comminuted, vacuum hot pressed at 482C, and extruded at about 427C through a 20:1 reduction die with a 2:1 aspect ratio. The extruded bar were further cross-rolled down 70% to a sheet of final thickness 1.9 mm, from which the tensile coupons were machined.

Hardness measurements were carried out using either a conventional Rockwell hardness tester or a Leitz miniload microhardness machine. Five measurements were normally made for each specimen. Elevated-temperature tensile tests were conducted with a conventional Instron machine attached with an HP-3497A data aquisation system. A resistance heating furnace was used to heat up the test specimen. Normally, it took approximately 45 min. pre-heating time to stablize the test temperature. All tests

were carried out under the condition of constant strain rate, ranging from $5x10^{-5}$ to 10^{-3} s^{-1}.

Microstructure and fracture surface were characterized using either optical metallogragh or scanning electron microscope.

RESULTS AND DISCUSSION

The microstructure of the consolidated and extruded Al-Be-Li alloy is shown in Fig. 1. The microstructure is generally fine, but a coarse banded structure is also evident. The coarse banded zone contains relatively large α-Be particles (2-5 μm) which resulted from the consolidation and extrusion of the material; in this respect the microstructure is similar to that observed in an Al-Be binary alloy(5). However, the volume percentage of the coarse banded zones is estimated to be less than 5% in the ternary alloy; this is considerably less than that found in the binary system. The presence of a coarse or fully-recrystallized zone suggests that α-Be particles are not effective grain refiners for Al-Li alloys. The result also suggests that the diffusion rate of Be in Al is probably fast.

Hardness measurements from the Al-Be-Li alloy which had been heat treated to the T6 (4) condition and then further exposed to different temperatures for 1h are shown in Figure 2. It is observed that the hardness value remains virtually constant at aging temperatures below 200°C but decreases drastically as the

temperature increases above this value. Since 200°C is about the peak aging temperature for Al-Be-Li(4), the decrease in hardness at higher temperatures is mainly due to the δ′ coarsening and the δ′ to δ phase transformation. However, it may also, in part, be due to the coarsening of the Be particles.

Tensile tests have been carried out in air on the alloy at temperatures in the range from 121 to 232°C. In general, the values of elongation-to-failure are over 35% for this material and the tensile stress-strain curves exhibit steady-state type behavior prior to fracture of the test sample. The deformation rate is shown as a function of flow stress in Fig. 3 for Al-Be-Li alloy at 121 and 177°C. The stress exponent, n, in the equation $\dot{\varepsilon} = k\sigma^n$ where $\dot{\varepsilon}$ is the steady-state true strain rate, σ is the flow stress and k is a constant, is measured to be approximately 12, which is similar to that measured in a binary Al-Be alloy(5). The high stress exponent is expected, since it has been reported that the fine Be particles act as independent dispersoids in the Al-Li matrix(4). In addition, Be particles are essentially non-deformable at the test conditions in this study.

The apparent activation energy for the deformation is calculated to be approximately 126 kj/mol, which is close to the activation energy reported for self diffusion in Al(6,7). The combination of a high stress exponent and an activation energy for self diffusion are typical characteristics for the creep of oxide

dispersion strengthened Al alloys(8). A summary of the present data is plotted in as normalized strain rate ($\dot{\varepsilon}/D$) versus normalized stress(σ/E). In order to make a direct comparison of these data with other alloys , data from the binary Al-Be system is also included in the plot. It is apparent from the figure that the deformation behavior for Al-Be-Li alloy can be well-described by the equation

$$\dot{\varepsilon} = A\ (\sigma/E)^{12}\ \exp(-Q/RT)$$

where $\dot{\varepsilon}$ is the strain rate, σ is the flow stress and A is a material constant, which is approximately $2.4 \times 10^{47}\ m^{-2}$ for the Al-10% Be-2% Li.

Although the figure shows that the deformation resistance of the ternary alloy is about 100 times higher than the binary,this result only pertains to the test temperature of 177°C. At this temperature, the ternary alloy contains both α-Be and δ' dispersoids as the strengthening phases. At a higher temperature than 177°C, the deformation resistance of the ternary alloy is not much higher than the binary alloy. This is better illustrated in Fig 5, in which the flow stress is shown as a function of test temperature for a fixed strain rate. As shown in the figure, the difference in strength between the ternary and binary alloys decreases as the temperature increases above the peak aging temperature for the ternary alloy. This loss of strength is due therefore to changes in the effectiveness of the δ' phase in the ternary alloy, as a result of overaging.

A typical fracture surface for the Al-Be-Li alloy is shown in Fig. 6. It is observed that the material failed in a ductile fashion, consistent with the fact that the material normally exhibits good tensile elongations. The duplex feature manifested in the original microstructure, as shown in Fig. 1, is also noted on the fracture surface. The coarse Be zone, as marked by the arrow in Fig. 6, shows a much wider dimple spacing, roughly 6 μm, than the zones in the original microstructure. For the fine Be zone, the dimple spacing is estimated to be only 1-2 μm. The difference suggests that the Be particles, and specifically the Al/α-Be interface, acts as the void initiation site in the material.

It is worth commenting on the mechanical strength of Al-Be-Li alloy at elevated temperature as compared to some potential high-temperature Al alloys. Despite the fact that Al-Be-Li is stronger than Al and Al-Be binaries, the alloy is still much weaker than most of high-temperature Al alloys, e.g. Al-Fe-Ce, Al-Fe-Mo and, also, 2219 Al(9). Even on a density-compensated basis, the Al-Be-Li alloy is still not strong enough to compete with those high-temperature Al alloys.

CONCLUSIONS

A rapidly-solidified, Al-10%Be-2%Li alloy has been produced. The mechanical properties of the alloy at temperatures between 121

and 232°C have been characterized. In this temperature range, the material behaves like conventional oxide dispersion strengthened alloys, namely, it exhibits a high stress exponent (n=12) and thus an activation energy of 126kj/mol, which is close to the activation energy for self diffusion in Al. Despite the fact that the material is stronger than Al and Al-Be binary alloys, it is still much weaker, even on a density-compensated basis, than most of the high-temperature Al alloys.

ACKNOWLEDGEMENT

The authors would like to thank Ms. W.C. Thomas for conducting the mechanical tests, and Messrs. D.D. Crooks, R.E. Lewis and J. Allen for technical discussion and preparing the material used in this study. This work was supported by Office of Naval Research under Contract N00014-84-C-0032, monitored by Dr. D. Polk.

REFERENCES

1. T.H. Sanders, Jr., and E.A. Starke, Jr., eds., "Aluminum-Lithium Alloys," the Metallurgical Society of AIME, Warrendale, PA, (1984).

2. T.H. Sanders, Jr., and E.A. Starke, Jr., eds., "Aluminum-Lithium Alloys II," The Metallurgical Society of AIME, Warrendale, PA, (1984).

3. C. Baker, P.J. Gregson, S.J. Harris, and C.J. Peel, "Aluminum-Lithium Alloys III," The Institute of Metals, London, (1986).

4. A.E. Vidoz, D.D. Crooks, R.E. Lewis, I.G. Palmer and J. Wadsworth,"Ultralow-Density, High-Modulus, and High-Strength RSP Al-Li-Be Alloys", Rapidly Solidified Powder Aluminum Alloys, ASTM STP 890, M.E. Fine and E.A. Starke, Jr., Eds., American Society for Testing and Materials, Philadelphia, 1986, pp. 237-251.

5. T.G. Nieh and J. Wadsworth, unpublished work, 1986.

6. T.S. Lundy and J.K. Murdock,J. appl. Phys. 33, 1971(1962).

7. M. Beyeler and Y. Adda, J. Phys. 29, 345(1968)

8. W.C. Oliver and W.D. Nix, Acta Metall. vol. 30,pp. 1335 to 1347(1982).

9. C.M. Adam and R.E. Lewis, "Rapidly Solidified Crystalline Alloys," S.K. Das, B.H. Kear, and C.M. Adam, eds., pp. 157-183, The Metallurgical Society of AIME, Warrendale, PA, (1986).

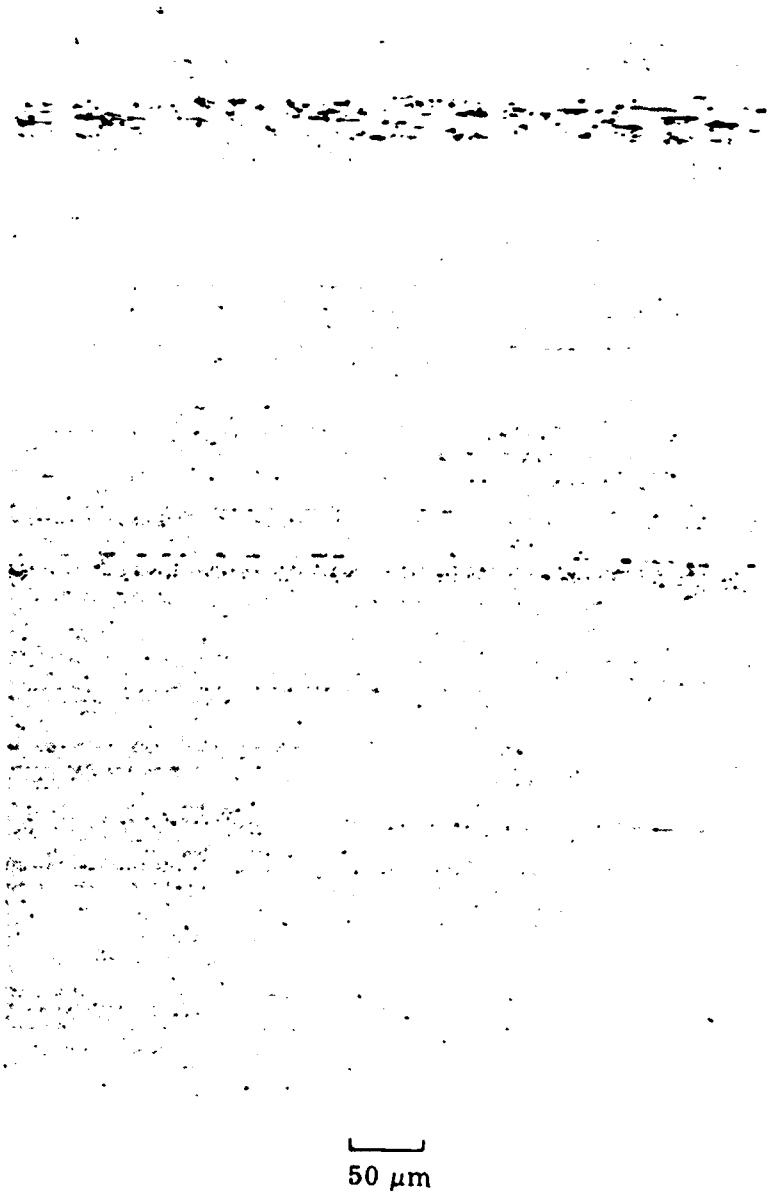

Fig. F1. Microstructure of the as-extruded Al-10%Be-2%Li alloy. Coarse bonded structure is evident.

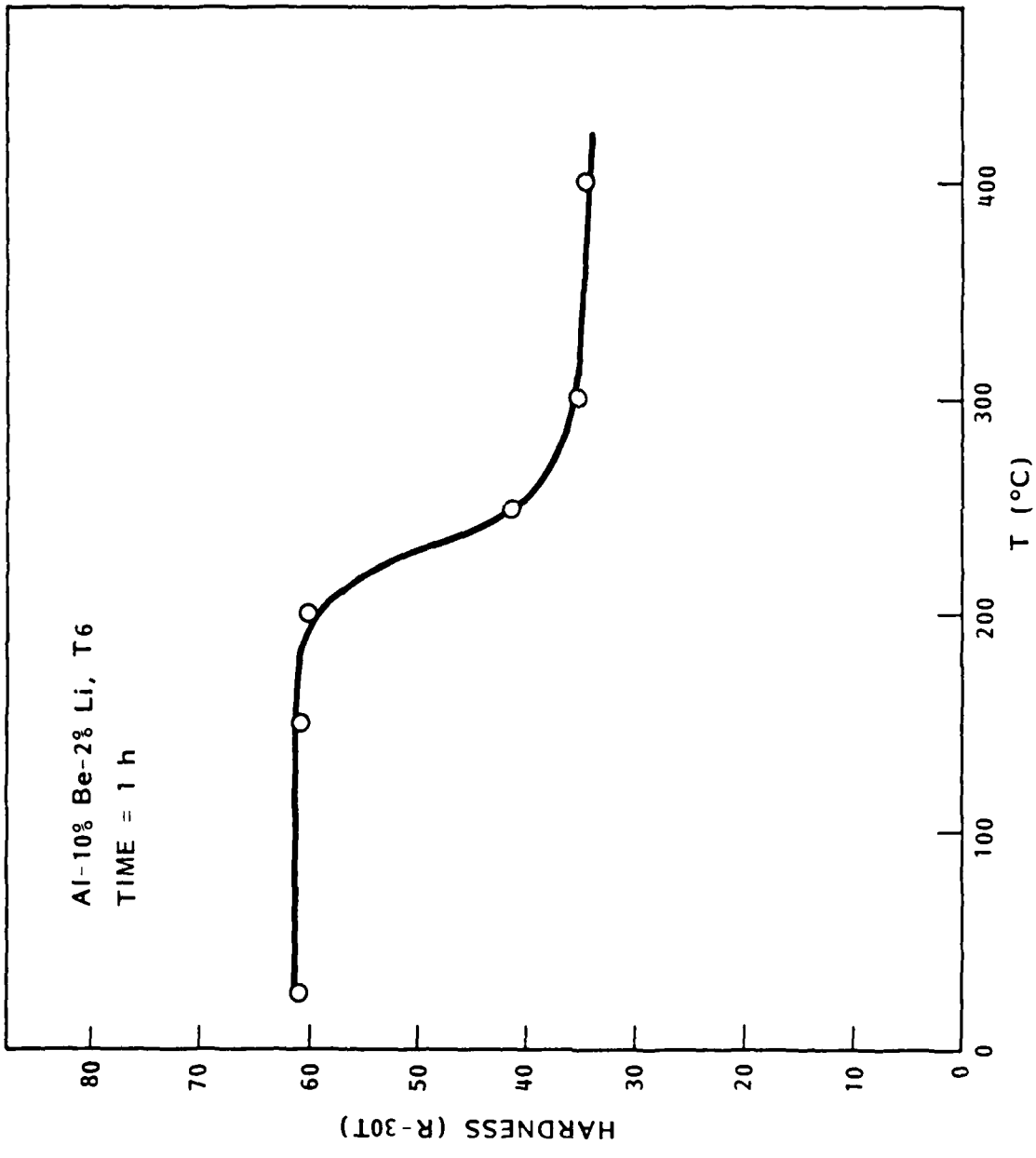

Fig. F2. Hardness measurements from Al-10%Be-2%Li (T6) exposed to elevated temperatures. The softening at temperatures higher than 200°C is due to overaging (δ′ to δ transformation).

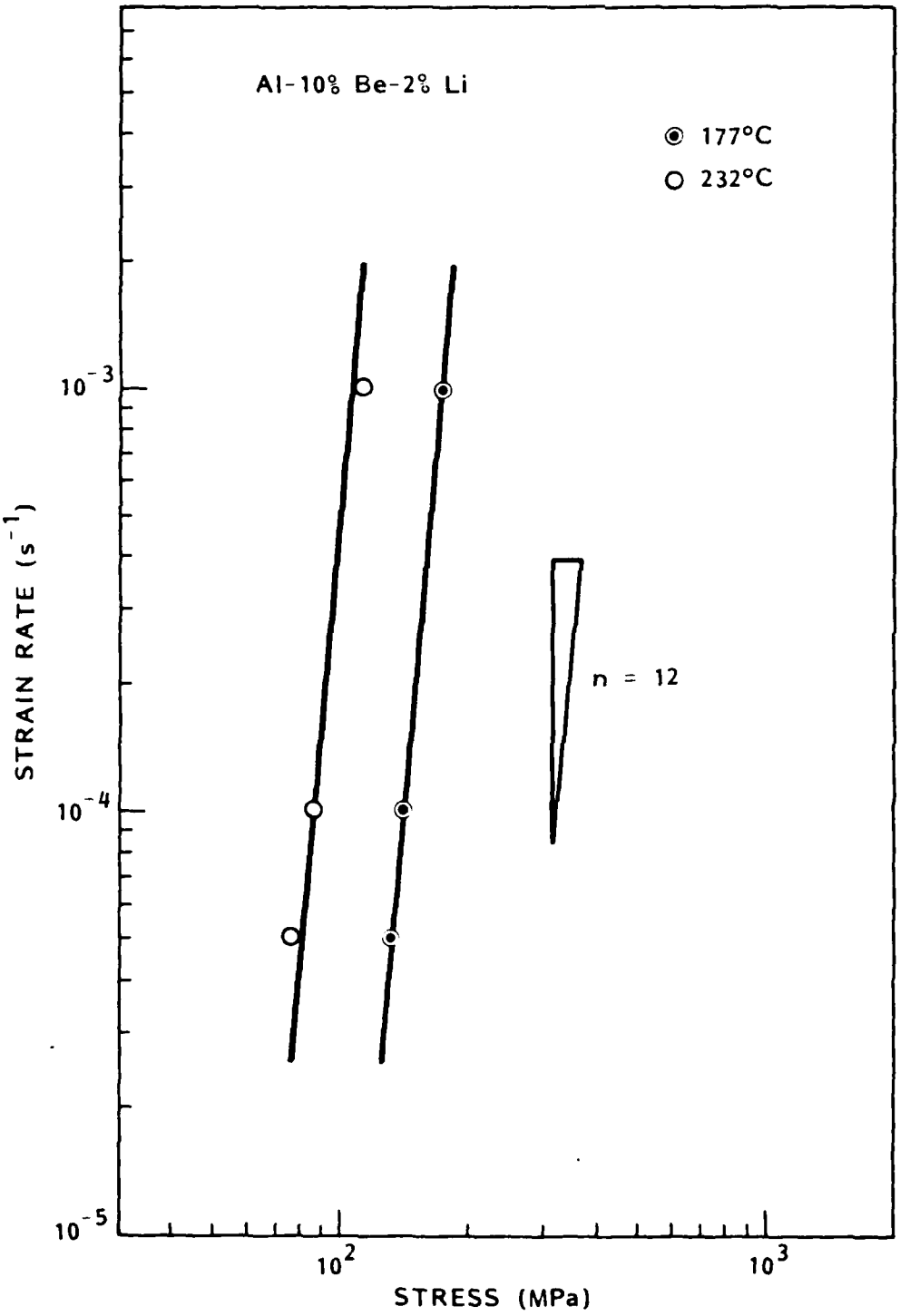

Fig. F3. Strain rate as a function of stress for AL-10%Be-2%Li at 177° and 232°C. The high stress exponent is typical for a dispersersion strengthened alloy.

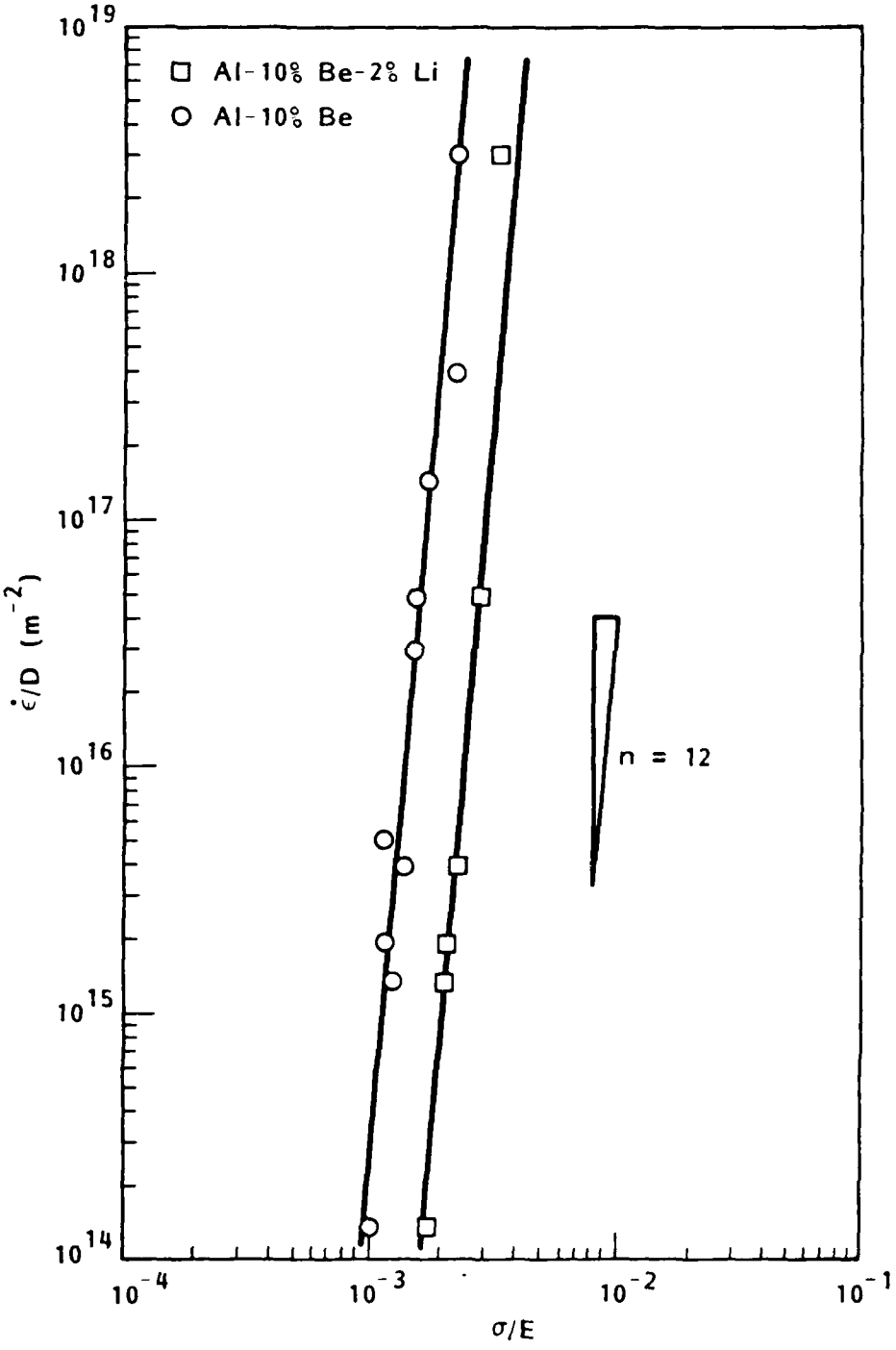

Fig. F4. Normalized strain rate, $\dot{\epsilon}/D$, versus normalized stress, σ/E, for Al-10%Be-2%Li. To make a direct comparison, the data for Al-10%Be binary alloy is also shown.

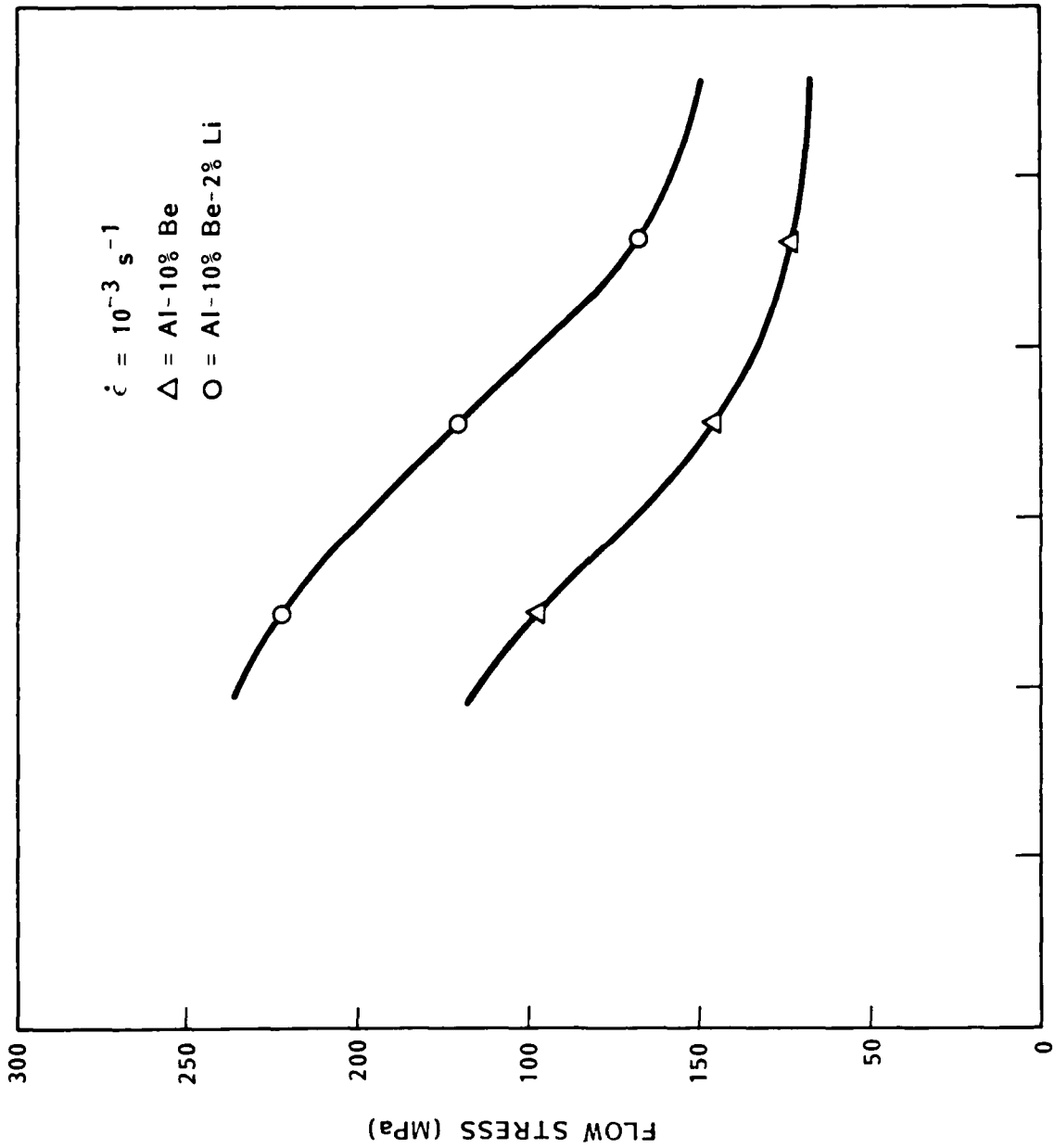

Fig. F5. Flow stress as a function of temperature for both Al-10%Be and AL-10%Be-2%Li alloys. The strengtheining effect that is due to Li gradually decreases at temperatures higher than approximately 200°C.

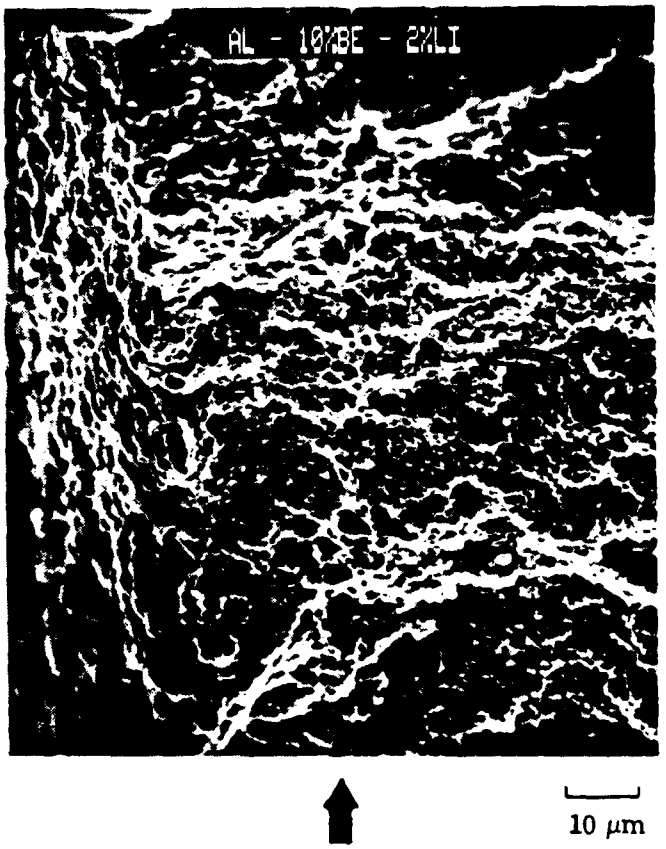

Fig. F6. Typical fracture surface for a Al-10%Be-2%Li tensile specimen. The coarse zone structure, shown in Fig. 1, is also manifested (indicated by the arrow) on the fracture surface.

APPENDIX G

CHARACTERIZATION OF THE AGING RESPONSE OF MELT-SPUN AL-BE-LI ALLOY RIBBON

T. G. Nieh, W. C. Oliver* and J. Wadsworth

Lockheed Palo Alto Research Laboratory
Metallurgy Laboratory
3251 Hanover Street
Palo Alto, CA 94304

*Oak Ridge National Laboratory
Metals and Ceramics Division
P. O. Box X
Oak Ridge, TN 37630

ABSTRACT

A rapidly solidified Al-10wt%Be-3wt%Li has been produced by a melt spinning technique. The aging behavior of the melt-spun ribbons has been characterized by a number of techniques, including differential scanning calorimetry, hardness measurements, and transmission electron microscopy. The results have shown that the aging responses of the ternary Al-Be-Li alloy are very similar to those of Al-Bi binary alloys. Specifically, δ' precipitates are formed at temperatures near 180°C and they transform to δ at temperatures around 300°C. Microstructural examination indicates that in the Al-Be-Li alloy no new phases are present in the matrix for specimens heat treated up to 400°C. The α-Be particles are present in the matrix as independent dispersoids and, apparently, have little effect on the aging behavior of the Al-Li matrix. The Be particles coarsen, however, above a temperature of approximately 300°C. The growth of Be particles follows the classical Ostwald coarsening type of mechanism.

INTRODUCTION

Lithium and beryllium are the only two elemental additions to aluminum that can simultaneously increase the elastic modulus and reduce the density in a significant manner. Al-Li alloys can be produced by powder metallurgy(PM), as well as ingot metallurgy(IM), without much difficulty because of the large

solid solubility of Li in Al. In contrast, fine-structured Al-Be based alloys containing high Be can only be produced by rapid solidification, because of the limited solid solubility(about 0.1% by weight maximum) of Be in Al. Although binary Al-Be alloys have been under investigation by many researchers for the last few years(1), ternary Al-Be-Li alloys have not yet been explored. In view of the potential weight saving, as well as improvement in the elastic modulus, the Al-Be-Li system is an extremely attractive one to study.

Recently, Wadsworth and co-workers have studied fine-structured Al-Be-Li alloys produced both by splat quenching and melt spinning techniques(2). They found that in the as-spun RSP Al ribbons containing both Li and Be, two different precipitates form independently, the δ' (Al_3Li) precipitates as coherent spheroids whereas the α-Be precipitates as dispersoids. In addition, they also found that Li- and Be-rich oxide layers are easily formed on the surfaces of the ribbons subjected to an oxidation environment(3).

The purpose of this study is to investigate the heat treat response of those RSP Al-Be-Li ribbons. Microstructural evolution in the heat-treated ribbons is analyzed with a number of supplementary techniques, including Differential Scanning Calorimetry(DSC), hardness measurements, and Transmission Electron Microscopy(TEM).

EXPERIMENTAL PROCEDURE

An Al-10% Be-3% Li (percentage by weight) ternary alloy was prepared by arc melting high purity ingot stock Al, high-purity, battery-grade Li and electrolytic induction melted Be stock. The arc melted button was converted to melt spun ribbon of approxmately 5 mm in width and less than 0.1 mm thickness. Melt spinning was carried out using an apparatus and techniques described elsewhwere(2).

DSC testing was conducted in high purity helium gas with approximately 8 mg of comminuted ribbons. The test was carried out from room temperature to 550°C and the controlled heating rate was about 20°C/min. The details of the test are described elsewhere(4). All test ribbons were encapsulated in a quartz tube and evacuated to approximately 1 Pa prior to heat treatment. This encapsulation was necessary to minimize the oxidation of the ribbon in order to prevent introduction of artificial effects on the microstructure and microhardness. Heat treatment was conducted using either a silicone oil bath or an air furnace, depending on the temperature. Each heat treated sample was sectioned into two samples, one for TEM examination and the second metallographically mounted for hardness measurement.

Specimens for TEM were hand ground to approximately 30 μm thick and then mounted on 3 mm mounting rings with epoxy. These samples were dual-ion milled with Ar^+ at 4 kV and a 30 μA specimen

current. This procedure, although time consuming, produced somewhat better specimens than those produced by electrochemical methods. In particular, electrothinning tends to etch out α-Be particles.

All metallographically mounted specimens were final polished with a 0.1 μm CeO compound prior to the hardness measurements. Two different techniques were used to obtain the hardness value from the specimens. One was using the conventional Leitz miniload microhardness machine but applying a much smaller load (4.0428 g). The instrument was calibrated immediately before the test. Another newly-invented method is the so-called Nanohardness Tester(5). The techique uses an extremely well-controlled diamond indent head to penetrate into a test specimen. The hardness value was calculated from the load versus depth curve. The actual area of contact between the indent and the test specimen was measured using either a high-resolution optical microscope or an electron microscope. The typical size of an indent is roughly 2 μm for a 500 nm penetration depth. Details of the test apparatus, as well as the test procedures have been given elsewhere(5).

RESULTS AND DISCUSSION

a.Thermal Analysis and Mass Spectroscopy (TA/MS)

An eifort was made to identify the degassing species from the as-spun ribbons using the TA/MS technique. The details of the

technique have been described elsewhere(2). The analysis indicates that the ribbons were relatively clean. The only significant degassed species was hydrogen, which evolves at approximately 350 to 470°C during the heating of the TA/MS anaysis. It is generally believed that hydrogen is one of the the major elements that is responsible for poor weldability of powder metallurgy materials, as hydrogen often generates voids or microporosities during fusion welding. While the effect of hydrogen on the embrittlement behavior in Al alloys is still controversial, there is considerable evidence to suggest that the presence of hydrogen in Al is detrimental to its ductility(6,7). In this case, the result obtained from the TA/MS analysis is useful information for incorporation into the Al-Be-Li alloy processing. For example, it demonstrates that a minimum temperature of about 400°C is needed for removing the residual hydrogen from the as-spun ribbons prior to their consolidation.

b.Differential Scanning Calorimetry

The as-spun ribbons were examined using DSC, employing techniques typical of current practice. A result is shown in Fig. 1, in which a DSC curve from the as-spun Al-Be-Li ribbon is plotted from room temperature to about 550°C. Three major events, occurring at approximately 180, 300, and 400°C, are readily observed from the DSC curve. Since the as-spun ribbon is metallurgically corresponding to a solution treated condition, the first exotherm at 170-180°C is believed to be due to $\delta'(Al_3Li)$ formation. The next exotherm, recorded at 290-300°C,

is believed to be due to the δ′ to δ(AlLi) transformation. The last exotherm, however, which takes place at a temperature around 400°C, is somewhat more difficult to explain. Subsequently, special efforts were made to understand this exotherm.

Figure 2 is a transmission electron micrographs obtained from an Al-Be-Li ribbon that had been thermally exposed at 405°C for 30 min. There are only three precipitate phases that can be identified in the microstructure, α-Be, δ′ and δ. It is noted in the figure that the average size of the α-Be particles is much larger than that found in the as-spun condition. The average particle sizes are 280 nm for the former and 140 nm for the latter. In fact, Be particles start to coarsen significantly at temperatures above 300°C (the details of coarsening will be discussed in a later section). Another important observation from the figure is that there is a significant amount of δ′ phase appearing in the matrix. The presence of δ′ is apparently due to re-precipitation after cooling from the heat treat temperature of 405°C. This result is similar to that found in Al-Li alloys by Baumann and Willams(8). Papazian et al.(9) have also reported that dissolution of δ may take place at temperatures near 400°C. It appears that coarsening of Be particles, re-precipitation of δ′ and dissolution of δ may take place simultaneously. Although the former two reactions are exothermic, the last one is endothermic. Therefore, the DSC curve for the portion higher than 400°C actually represents an summation of the above three concurrent events. Despite the fact that the TEM study has shown

evidence, at least qualitatively, for all of the processes, it is difficult to evaluate, quantitatively, the relative contribution of each process.

Since Al, Be and Li are all strong oxide formers (3), oxidation of the ribbons may still occur during the DSC experiment, even with the use of high purity helium. Oxidation of the ribbons is expected to have significant effect on the final DSC analysis. Therefore, a special effort was made to examine the surface chemistry, as well as the oxide thickness of ribbons that had been heat treated under a simulated condition for a DSC test. However, the experimental results failed to show any significant difference between ribbons that had been subjected to such a simulation and as-spun ribbons.

In summary, the DSC experiment suggests that the presence of Be has essentially little or no effect on aging behavior in the Al-Li alloy matrix. The aging characteristics for the Al-Be-Li ternary alloy were virtually identical to an Al-Li binary alloy. There is no chemical or metallurgical interaction between Al and Be, or between Li and Be.

c. Hardness Measurements

As mentioned in the experimental section, two techniques have been used to measure the hardnesses of the ribbons. The first one is the so-called Nanometer Hardness (NH) test in which the

hardness value of the sample was measured by continuously monitoring the load necessary to penetrate a fine diamond indentor into the sample to a well-controlled depth. The depth of penetration is normally, as the name of the technique implies, in the nanometer regime. In the present case the depth is 500 nm. Although the indent depth is only 500 nm, because of the large angle (65.3^{o}) between the face and the vertical axis, the projected area is actually of size near 4 μm on a side. Because of the extremely small size of the indentation, a number of factors must be taken into consideration. One example is that the ambient temperature must be controlled within a tenth of a degree during the test in order to avoid thermal expansion effects due to thermal fluctuations. Another example is the oxide film thickness on the test specimen; this may strongly influence the measurement as the indentation size decreases. This NH test is primarily a dynamic method. In contrast, the second method, which is static and more conventional, is to use a standard microhardness (MH) tester but applying a much smaller dead load. In this method, one calculates the hardness value by measuring the size of the indentation. Despite the differences in their operation principles, the results from those two methods are quite similar.

A typical load vs. depth data profile obtained from a NH test is shown in Fig. 3. The load, in general, represents a summation of both the elastic and plastic deformation, and increases as the depth increases due to a larger area of contact. The raw data can

be readily converted into the Meyer hardness (defined as load divided by the projected area of indent). The calculations are shown in Fig. 4. The bar represents the scatter band which is mainly due to the uncertainty in determining the size of the indent. It is noted from the figure that the hardness value is a function of indentation depth or size. The hardness, in general, increases as the indentation depth decreases. This is consistent with some of the classical observations(10). This also shows one of the major advantages of using the NH test, namely, it provides the hardness values at various indent depths simultaneously in one test.

Hardness data was measured from ribbons that had been heat treated at various temperatures for 1h. This data is summarized in Fig. 5; each data point in the figure represents an average of at least 5 measurements. It is noted that the hardness value remains essentially the same at temperatures below 150°C and then starts to decrease until about 180°C. In the temperature regime of 180 to 300°C, the hardness value reaches another plateau and, then, further decreases above 300°C. The first decrease in hardness is believed to be mainly due to dislocation annihilation in the as-spun ribbon. It has previously been shown that the as-spun material normally contains a large number of dislocations(11). The decrease of hardness may also be attributed, in part, to coarsening of the α-Be. At temperatures around 200°C, δ' precipitate forms rapidly which causes hardening of the material. However, this hardening effect is balanced by

the softening that results from dislocation annihilation and α-Be coarsening. At temperatures above 300°C, the δ′ precipitate transforms entirely into δ phase and, in addition, the α-Be particles also start to coarsen rapidly. Both events resulted in a decrease in hardness in the ribbon. The results are consistent with those obtained from DSC analysis shown in the previous section. The microstructural evidence for the δ to δ′ transformation, as well as the α-Be particle coarsening at 300°C are presented in the next section.

Microhardness measurements using the MH machine were also made with the metallograghically mounted specimens. Ten measurements were generally taken from each specimen. The hardness value is shown in Fig. 6 as a function of annealing temperature for the as-spun ribbons. As mentioned earlier, the results are quite similar to that obtained from the MH test, except the absolute hardness values from the MH test are generally less than that from the NH test. This is expected since the indent size is much larger (approximately 15μm) in a MH test, as compared to that in a MH test.

d. Microstructure Examination

Both the α-Be particles and δ′ precipitates are readily observed, as shown in Fig. 7 (in the as-spun ribbon). The Be particles, in general, exihibit a smooth morphology and do not show any preferential orientation with respect to the matrix. Although

the α-Be particles in this figure appear to be of uniform size, they in fact range in size from 65 to 120 nm. A large number of quenched-in dislocations are also noted in the microstructure.

However, the dislocation density is drastically reduced in the sample aged at 185°C as is also reflected by the hardness values. Fig. 8a is the microstructure of a ribbon aged at 185°C. The size of the α-Be particles is similar to that in the as-spun condition. The dark field microstructure (using the <100> δ′ reflection to demonstrate the δ′ precipitate distribution) from the area shown in Fig. 8a is illustrated in Fig. 8b. It is readily observed that the δ′ precipitates are uniformly distributed throughout the grain interior. In fact, 185°C is almost the peak aging temperature for both Al-Li and Al-Be-Li alloys (11,2). Heat treatment of the ribbon at higher temperatures results in overaging, and the δ′ precipitates gradually transform to δ precipitate. The microstructure of a ribbon heat treated at 300°C for 24 h is shown in Fig. 9. Selected area diffraction from such an ribbon failed to show any δ′ reflection. No δ′ precipitates were found in the microstructure. It is concluded that all δ′ precipitates present in the original ribbon have completely transformed into δ.

It is interesting to note that further heat treatment of the ribbon at higher temperature, e.g. 400°C, causes some δ precipitates to dissolve and δ′ to reprecipitate. It was discussed and shown earlier in Fig. 3. It is also worth noting

in Fig. 3 that the average size of α-Be particles is much coarser than those observed after annealing at a lower temperature.

An attempt has been made to measure the average sizes of the α-Be particles under different heat treatment conditions. The statistical measurements are shown in Fig. 10 for α-Be particle diameters as a function of heat treatment temperature. As indicated in the figure, the size distribution for Be is, in general, relatively nonuniform. Despite the large scatter in particle size, the data clearly indicate that Be particles start to coarsen in the temperature regime above 300°C. Below 300°C the average particle sizes are rather close and variations about the average size are within the scatter band.

Special efforts were made to carefully measure the coarsening rate of Be particles at 300°C. The results are shown in Fig. 11. In the figure, the average α-Be particle diameter is plotted in as a function of $t^{1/3}$, where t is the annealing time. Despite the large scatter, the particle size appears to be proportional to $t^{1/3}$, suggesting a lattice diffusion growth mechanism; i.e., particle growth by classical Ostwald coarsening phenomenon.

CONCLUSIONS

The aging behavior of rapidly solidified AL-10%Be-3%Li ribbon has been characterized. Several conclusions can be made from this study.

1. The general aging characteristics of the ternary Al-Be-Li alloys are very similar to binary Al-Li alloys.

2. Although δ' precipates are present in the as-spun ribbon, uniform δ' distribution was not observed until aging temperatures of about 180°C. Heat treatment of the ribbon at higher temperatures, e.g., 300°C, resulted in δ' to δ transformation.

3. In the Al-Be-Li ternary, the α-Be particles are present in the Al-Li matrix as independent dispersoids and have little effect on the aging response of the Al-Li matrix.

4. The size of the distribution of the α-Be particles is nonuniform. Upon heat treatment at temperatures higher than 300°C, α-Be particles tend to coarsen and the growth behavior of these particles follows a classical Ostwald coarsening mechanism.

Acknowledgements

The authors would like to thank Messrs. J. Allen, D.D. Crooks, and Ms. W.C. Thomas for manufacturing the alloys and carrying out some of the mechanical tests. This work was supported by Office of Naval Research under Contract N00014-84-C-0032.

References

1. R.E. Lewis, "Feasibility of Ultra-Low Density of Aluminum Alloy," Progress Report for June-September 1985, Naval Air Development Contract No. N62269-84-C-036.

2. A.E. Vidoz, D.D. Crooks, R.E. Lewis, I.G. Palmer, and J. Wadsworth, "Rapidly Solidified Powder Aluminum Alloys," M.E. Fine and E.A. Starke, eds., ASTM STP No. 890, Amer. Soc. for Testing of Materials, Philadelphia, PA, (1986).

3. A. Joshi, J. Wadsworth, and A.E. Vidoz, Scri. Metall., Vol. 20, (1986), p. 529.

4. J.G. Moncur, A.B. Campa, and P.C. Pinoli, J. High Resolution Chromotography, Vol. 5, (1982), pp. 322-324.

5. J.B. Pethica, R. Hutchings, and W.C. Oliver, Phil. Mag. Vol. 48A, No. 4, (1983), pp. 593-606.

6. RBJ. Gest and A.R. Troiano, "Corrosion," Vol. 30, No. 8, (1974), pp. 274-279.

7. D.P. Hill and D.N. Williams, "Relationship Between Hydrogen Content and Low Ductility in Al-Li Alloys," Final Report, Contract No. N00019-81-C-0433, October 1982.

8. S.F. Baumann and D.B. Williams, "Aluminum-Lithium II", E.A. Starke, Jr. and T.H. Sanders, Jr., eds., TMS-AIME, (1984), p. 17.

9. J.M. Papazian, C. Sigli and J.M. Sanchez, Scri. Metall., Vol. 20, (1986), pp. 201-206.

10. R.A. Oriani, Acta Metall., Vol. 12, (1964), pp. 1399-1409.

11. J. Wadsworth, A.R. Pelton, D.D. Crooks, R.E. Lewis and A.E. Vidoz, J. Mater. Sci., (1986), In Press.

12. D.B. Williams, "Aluminum-Lithium," T.H. Sanders, Jr. and E.A. Starke, Jr., eds., TMS-AIME, (1981), pp. 89-100.

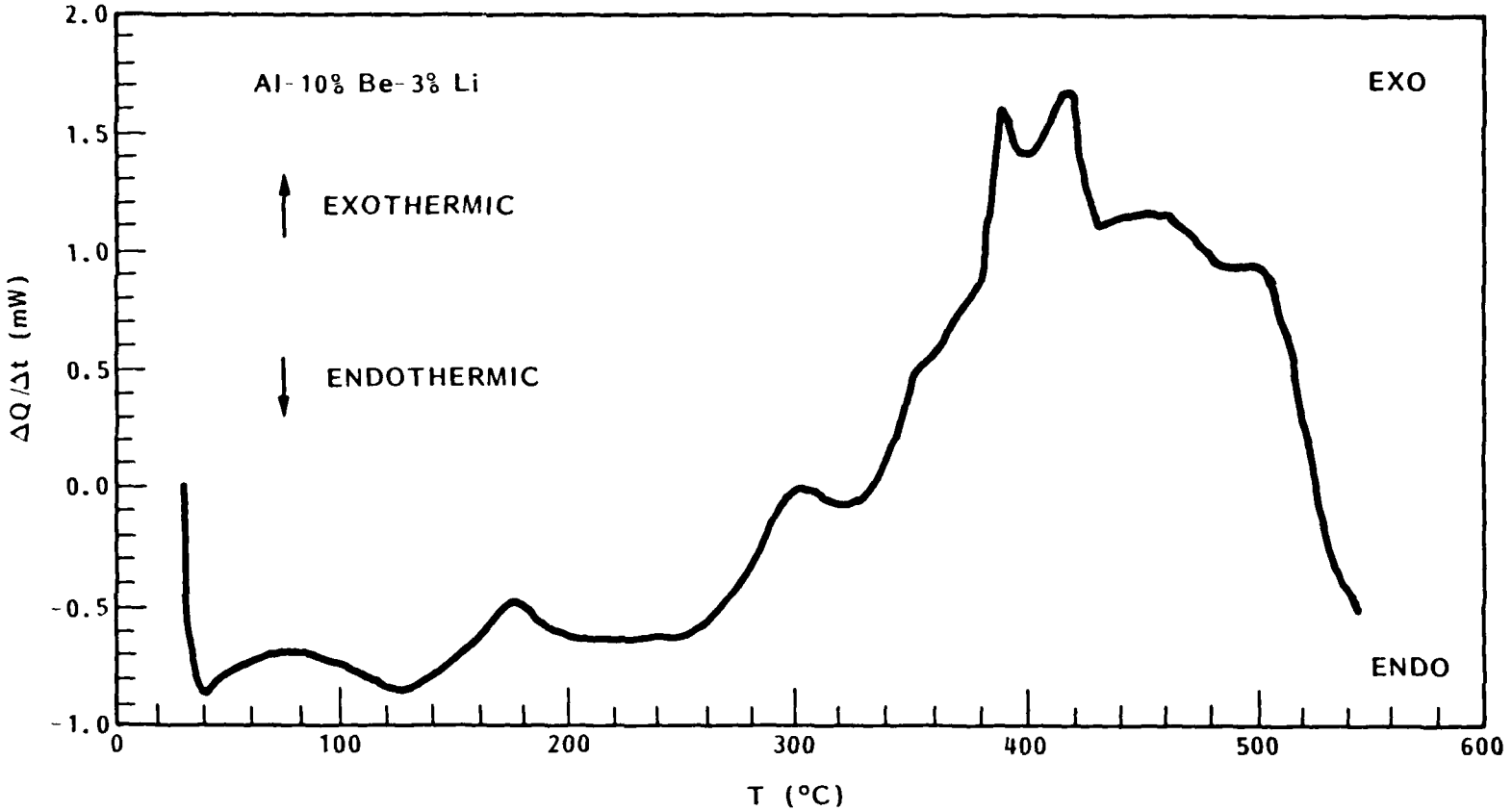

Fig. G1. Differential Scanning Calorimetry from the as-spun Al-10%Be-3%Li ribbon at 20K/min rate.

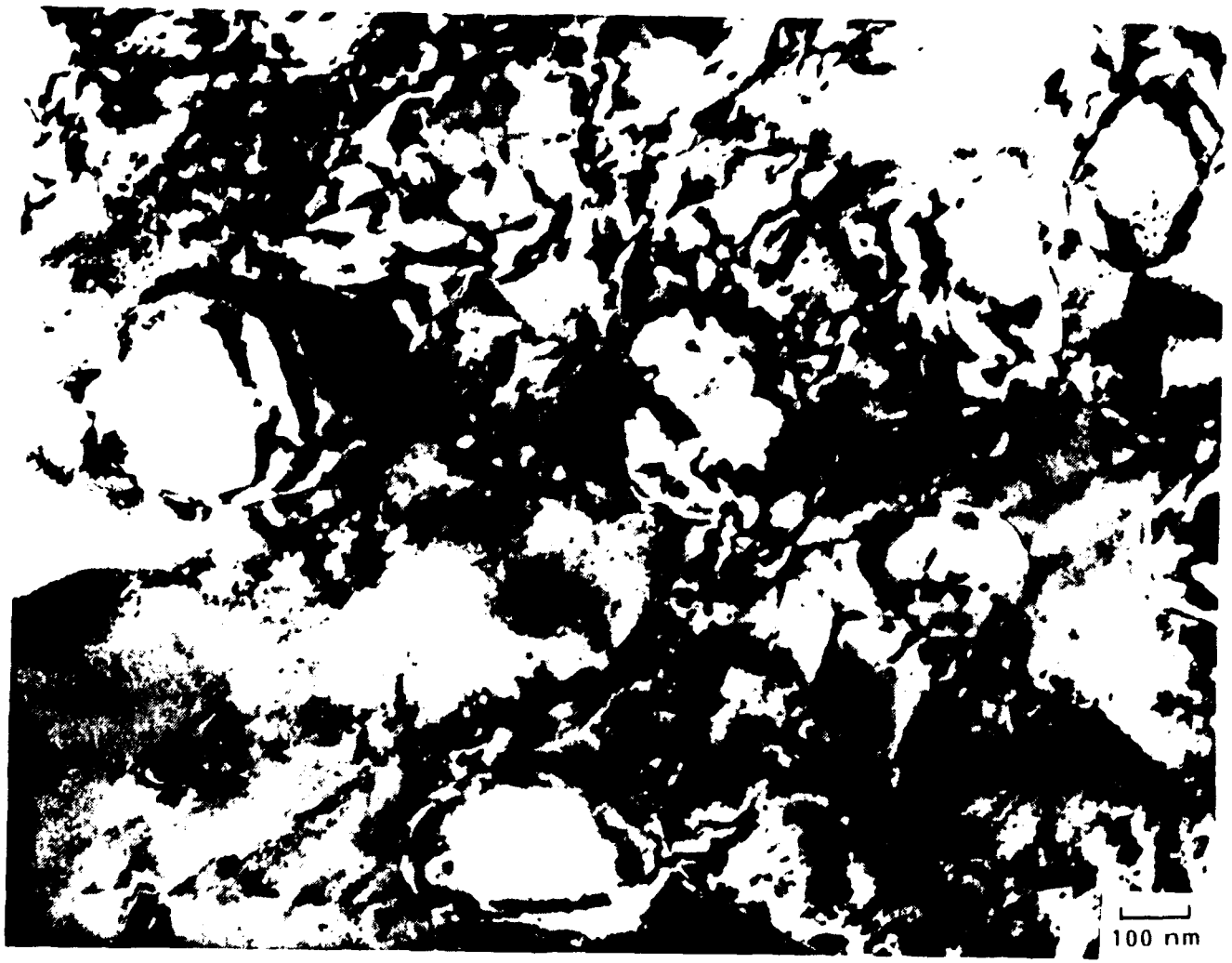

Fig. G2. Microstructure of an Al-10%Be-3%Li ribbon heat treated at 405°C for 0.5 h. There are three precipitate phases resent in the matrix, α-Be, δ' and δ.

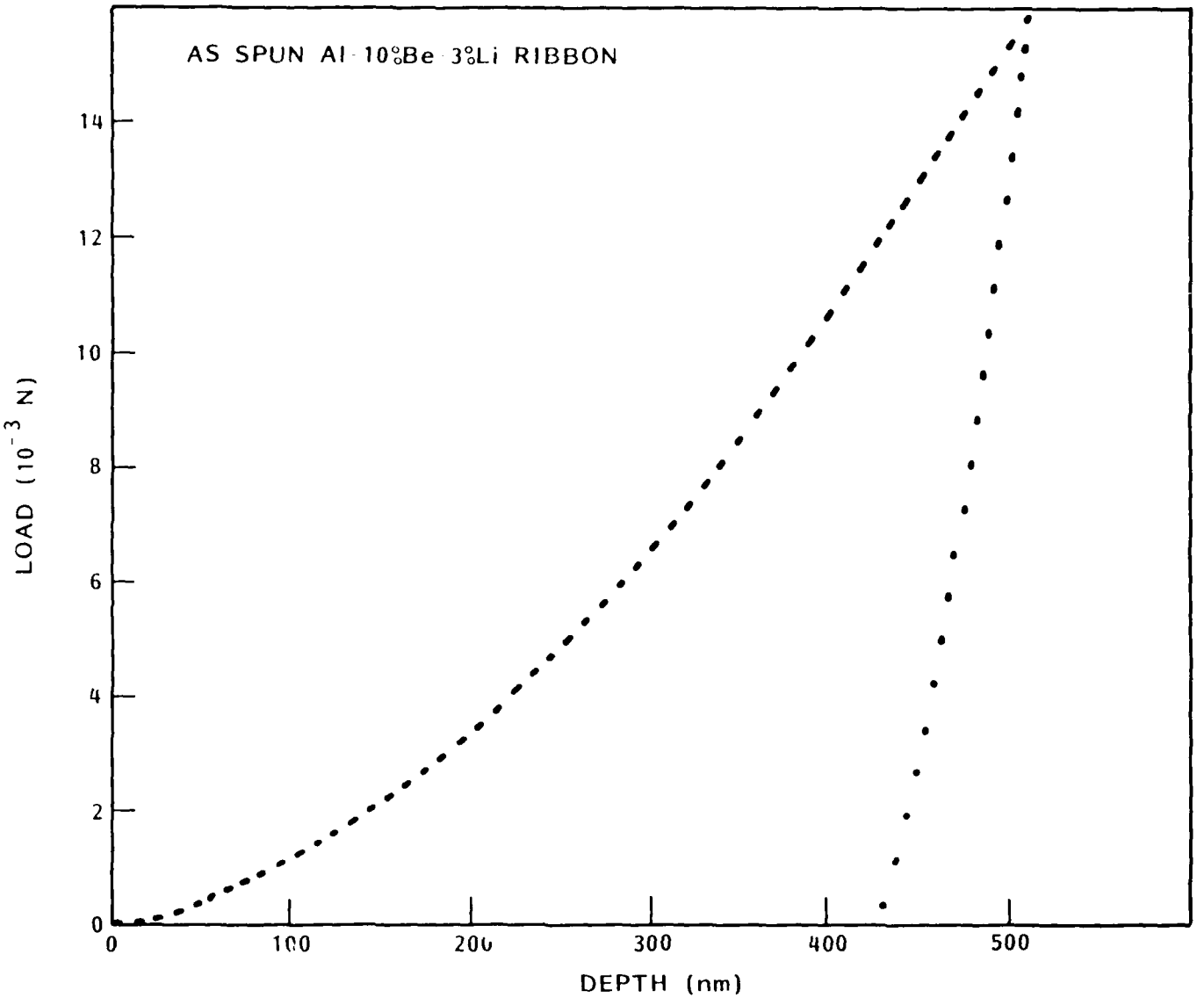

Fig. G3. Load vs. depth for the as-spun Al-10%Be-3%Li ribbon as obtained from a NH test.

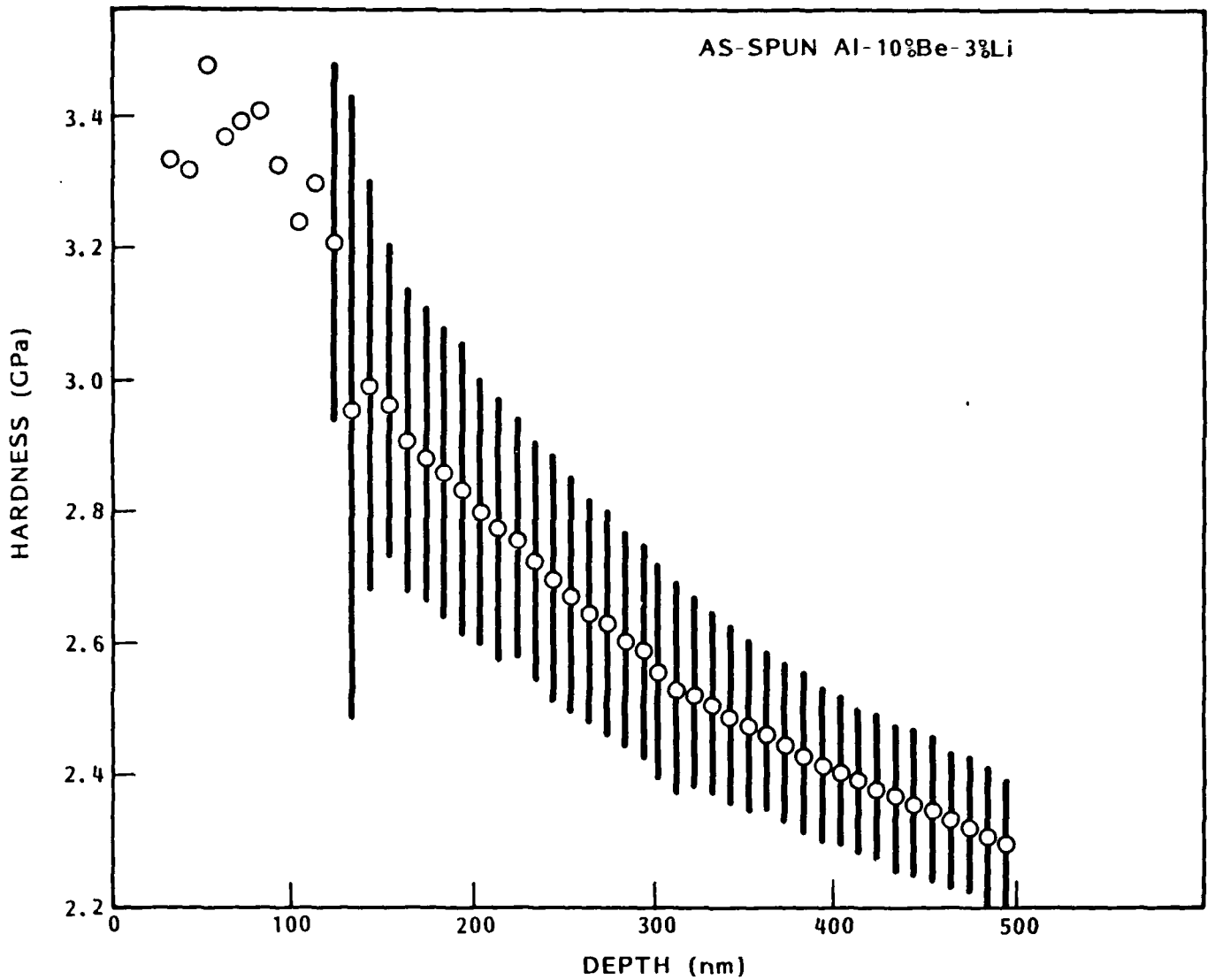

Fig. G4. Hardness as a function of indent depth calculated from Fig. 3. The hardness value decreases as the indent depth increases.

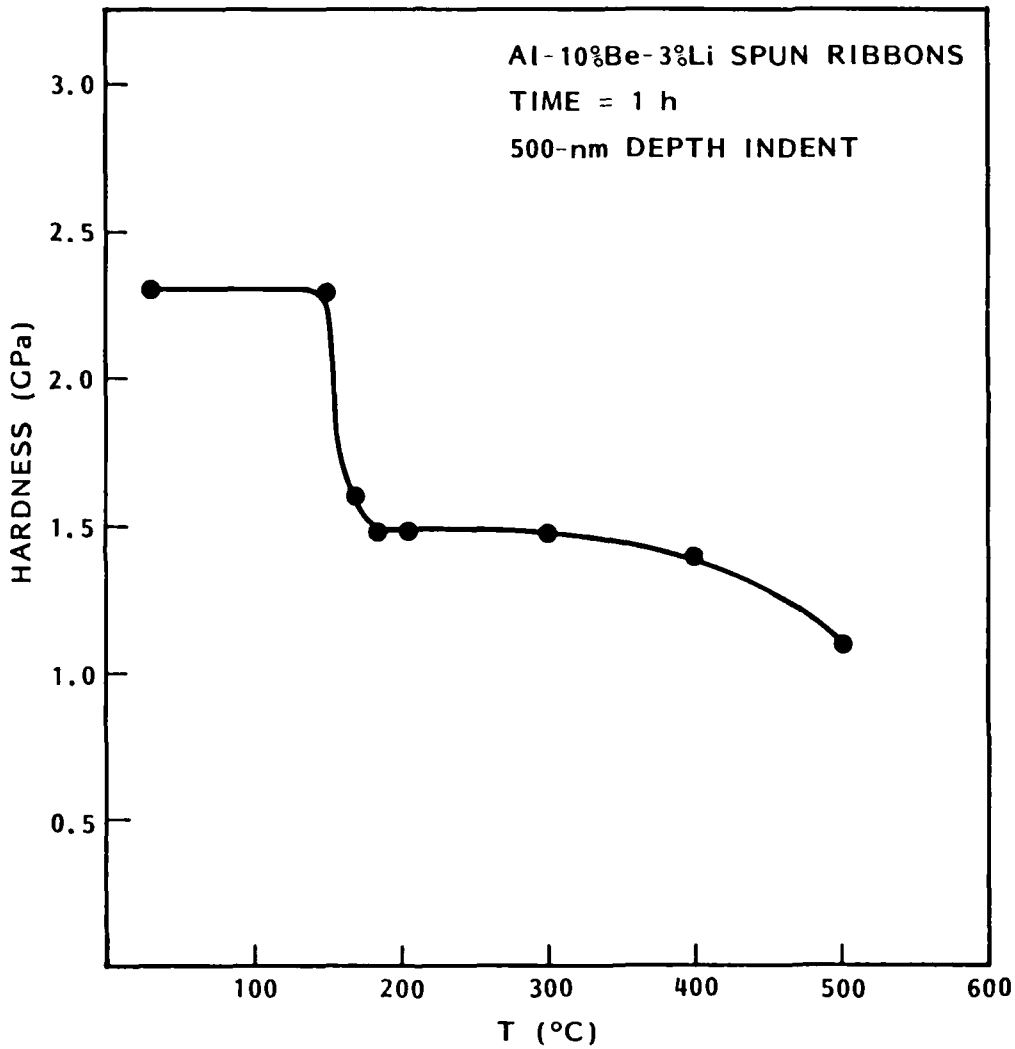

Fig. G5. Hardness value as a function of heat-treat temperature for Al-10%Be-3%Li ribbon. The hardness measurements were obtained from the NH test.

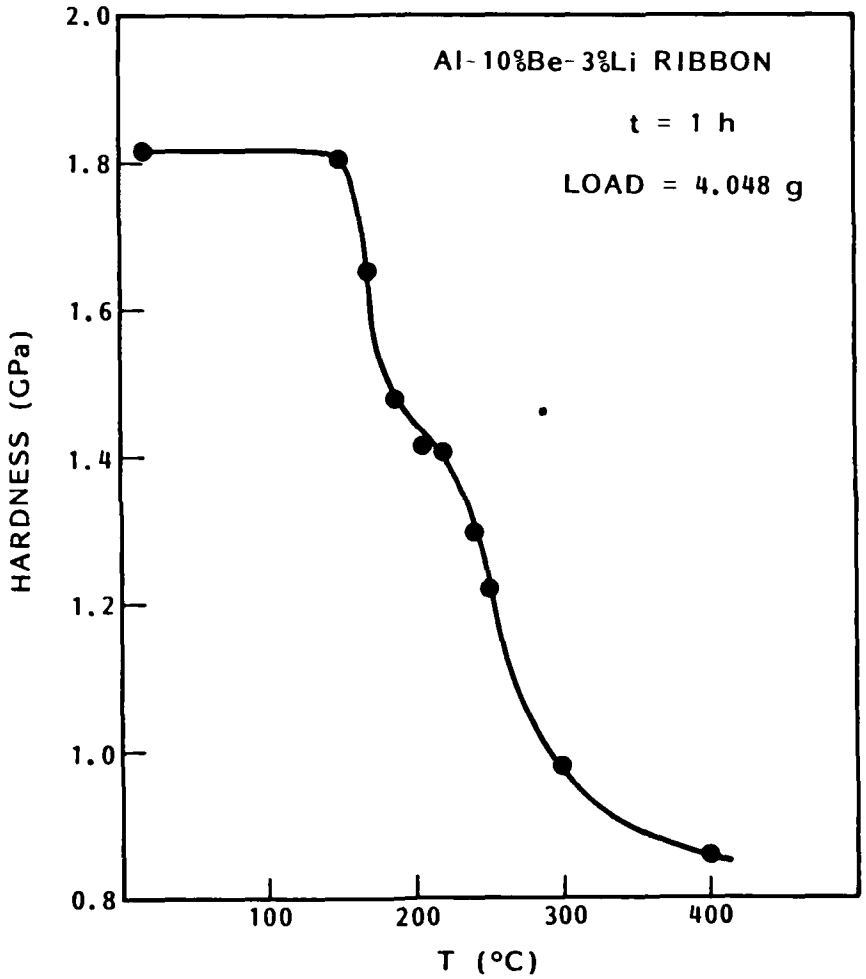

Fig. G6. Hardness as a function of heat-treatment temperature for Al-10%Be-3%Li ribbon. The hardness measurements were obtained from a standard microhardness test, but using a relatively small load, 4.048 g. The data are consistent with that shown in Fig. 5.

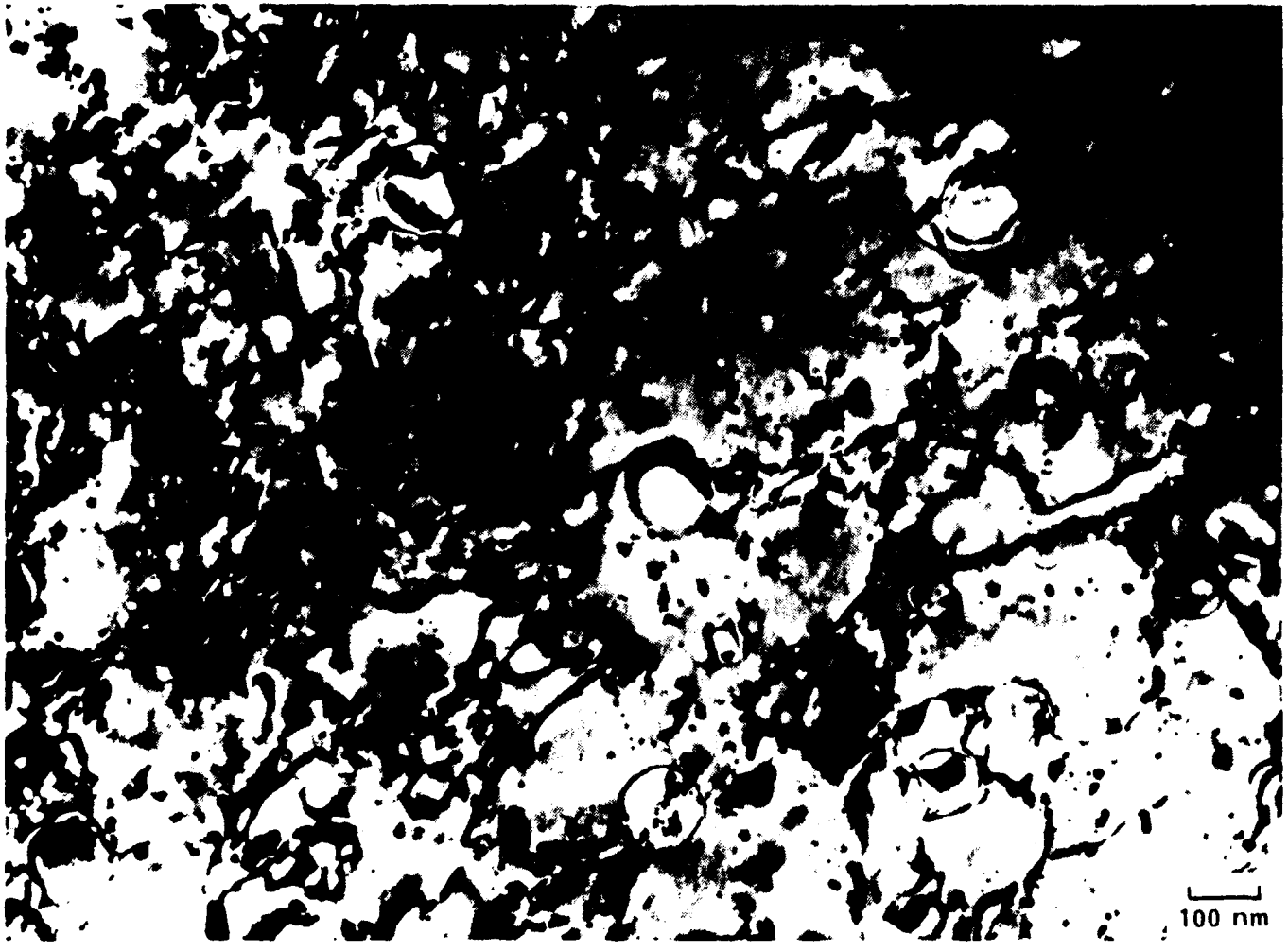

Fig. G7. Microstructure of an as-spun Al-10%Be-3%Li ribbon. Both the α-Be particles and δ′ precipitates are readily seen.

Fig. G8a. Microstructure of the AL-Be-Li ribbon heat-treated at 185°C for 1 h.

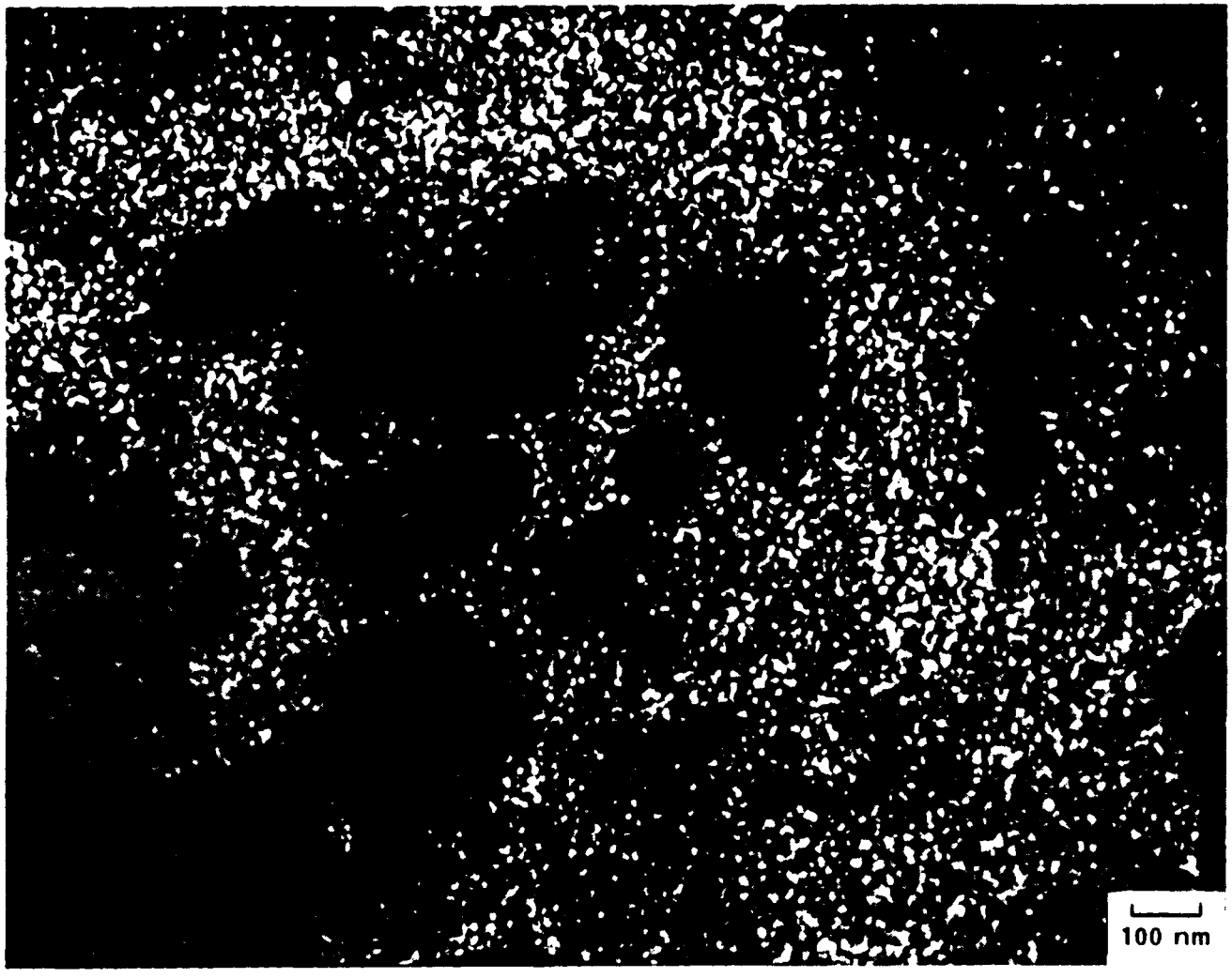

Fig. G8b. Dark field from the area in 8a, illustrating the uniform δ′ precipitate distribution.

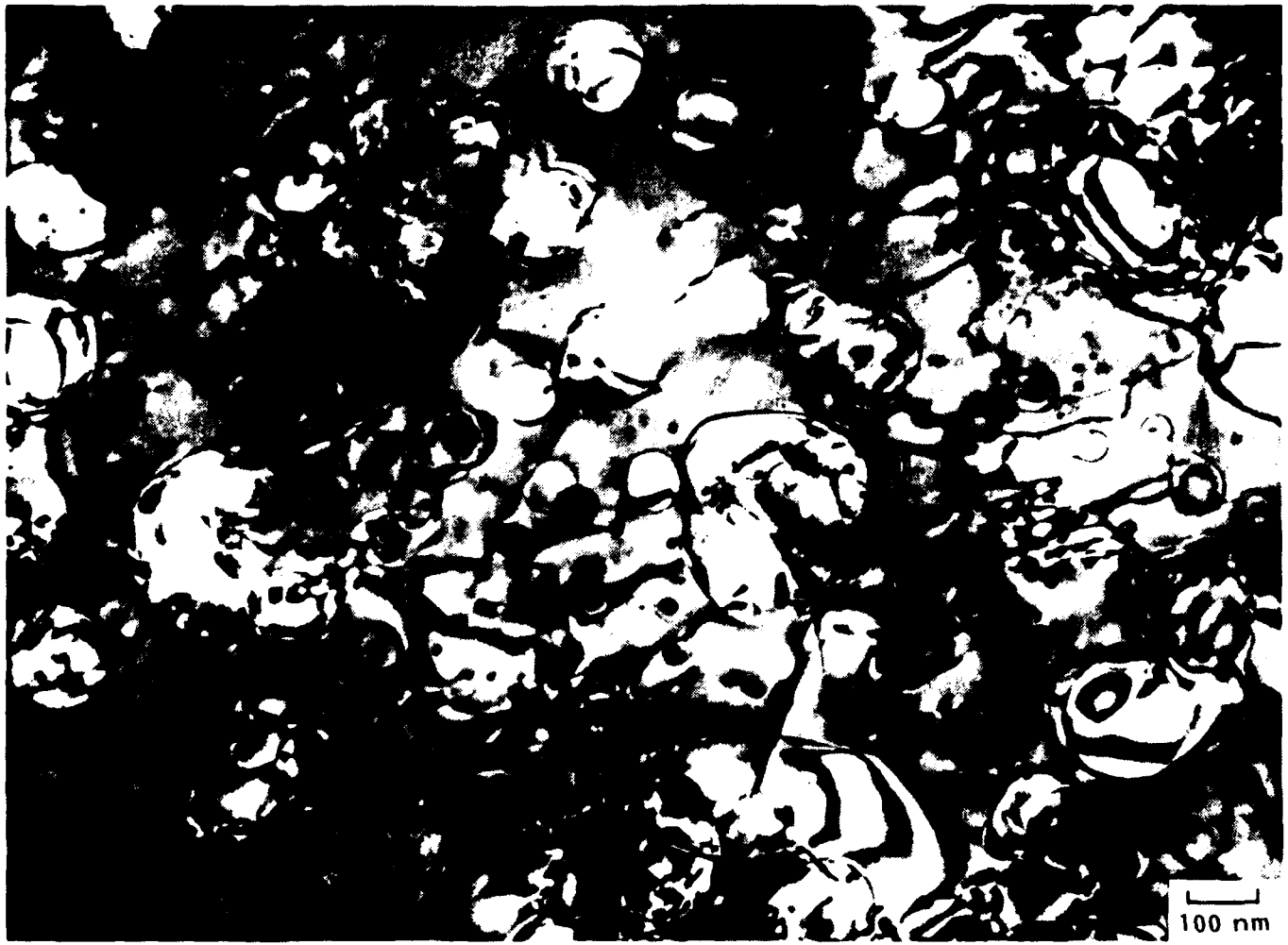

Fig. G9. Microstructure of a ribbon heat treated at 300°C for 24 h. SAD failed to show any δ′ precipitate in the matrix.

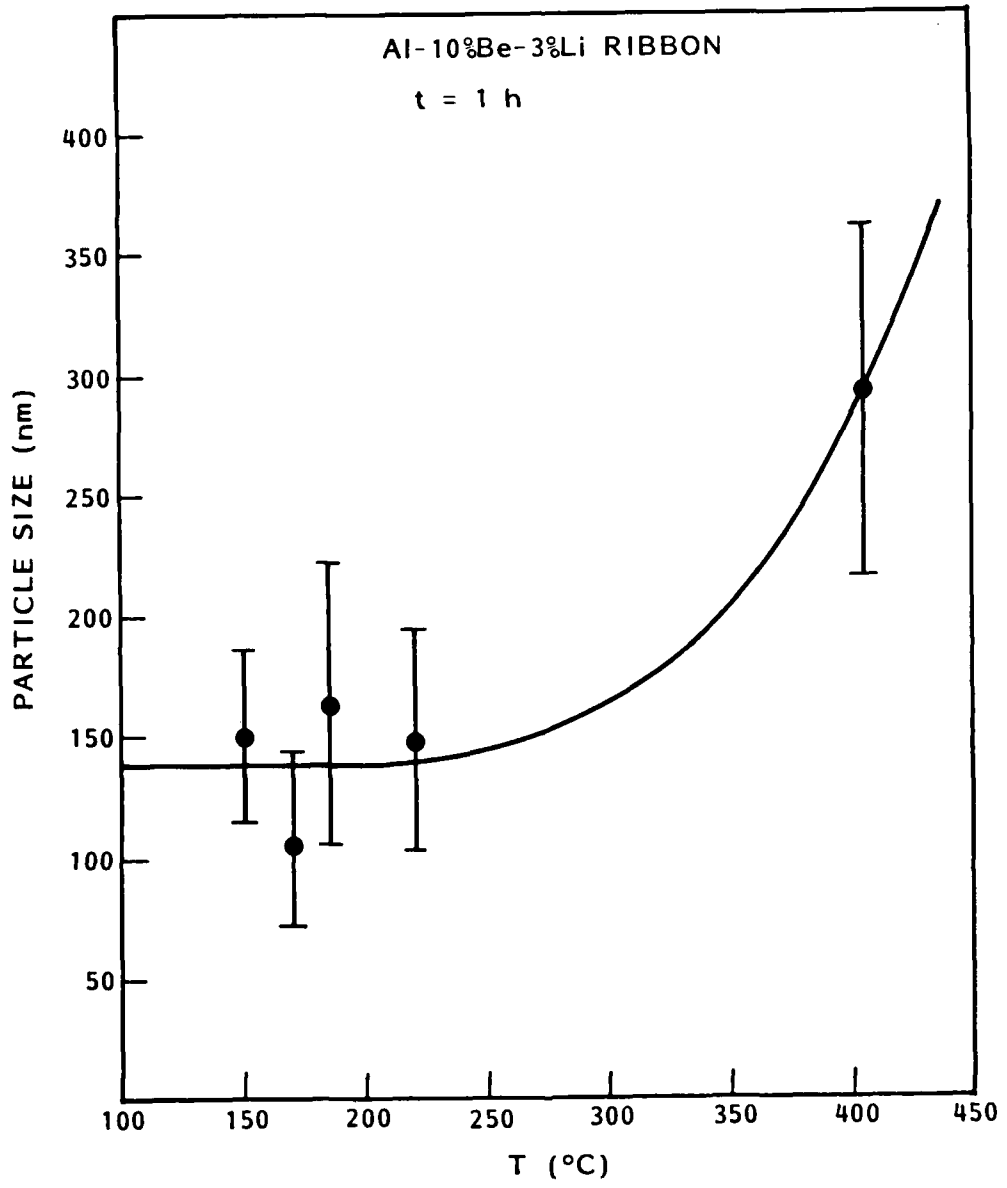

Fig. G10. α-Be particle size as a function of heat treatment temperature. Particle coarsening appears to take place at temperatures around 250 to 300°C.

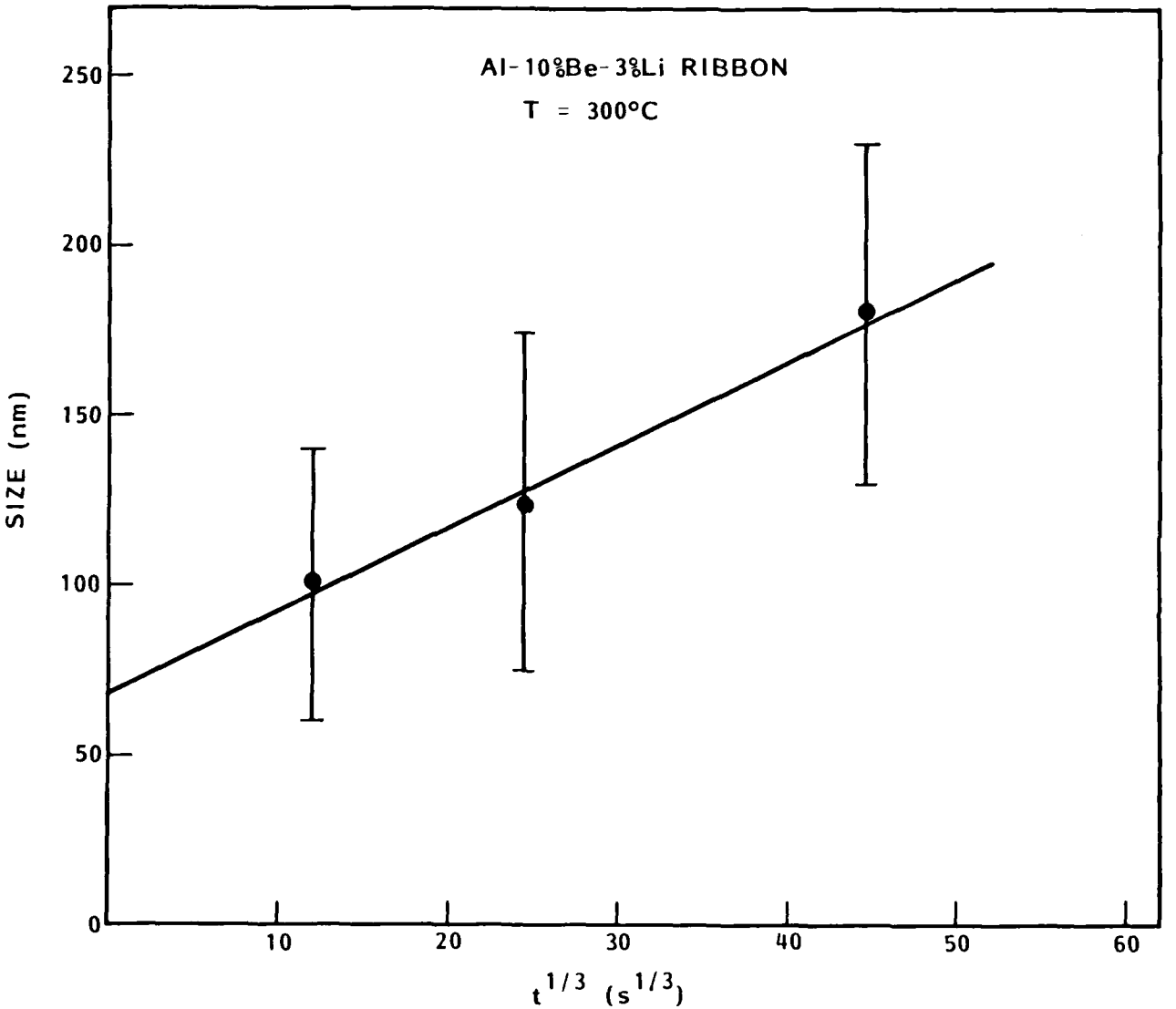

Fig. G11. α-Be particle diameter as a function of $t^{1/3}$, where t is the annealing time. The linearity of the plot suggests it is a classical Ostwald coarsening phenomenon.

END

10-86

DTIC